NASA CR-152,362

NASA-CR-152362
19830003802

A Reproduced Copy

OF

NASA CR-152,362

Reproduced for NASA

by the

NASA Scientific and Technical Information Facility

FFNo 672 Aug 65

NASA CONTRACTOR REPORT 152362

(NASA-CR-152362) APPLICATION OF ADVANCED TECHNOLOGIES TO SMALL, SHORT-HAUL TRANSPORT AIRCRAFT (STAT) Final Report (Cessna Aircraft Co.) 125 p HC A06/MF A01 CSCL 01C

N83-12072

Unclas

G3/05 01237

Application of Advanced Technologies to Small, Short-Haul Transport Aircraft (STAT)

E.F. Kraus
O.D. Mall
R.W. Awker
J.W. Scholl

CONTRACT NAS2-10263
November 1982

NASA

NASA CONTRACTOR REPORT 152362

Application of Advanced Technologies to Small, Short-Haul Transport Aircraft (STAT)

E.F. Kraus
O.D. Mall
R.W. Awker
J.W. Scholl
Advanced Design
Wichita, Kansas

Prepared for
Ames Research Center
under Contract NAS2-10263

National Aeronautics and
Space Administration

Ames Research Center
Moffett Field California 94035

PRECEDING PAGE BLANK NOT FILMED

TABLE OF CONTENTS

PAGE ii INTENTIONALLY BLANK

TABLE OF CONTENTS (Cont'd)

LIST OF FIGURES

LIST OF FIGURES (Cont'd)

LIST OF FIGURES (Cont'd)

LIST OF FIGURES (Cont'd)

FIGURE PAGE

LIST OF TABLES

LIST OF TABLES (Cont'd)

PREFACE

This report was prepared by the Cessna Aircraft Company, Wallace Aircraft Division under NASA contract NAS2-10263 for "A Study of the Application of Advanced Technologies to Small, Short-Haul Transport Aircraft". This study, hereafter referred to as the STAT (Small Transport Aircraft Technology) study, was performed from June 1, 1979 to August 31, 1980.

The NASA Technical Monitor for the Cessna STAT study was Thomas L. Galloway, Aeronautical Systems Branch, Ames Research Center, Moffett Field, California.

The Cessna Study team consisted of Emmett F. Kraus, Study Manager; Randal W. Awker, Technical Manager and responsible for aircraft performance, sizing and optimization; Jerry W. Scholl, responsible for aircraft configuration design; and Ozzie D. Mall, responsible for technology applications.

The authors wish to acknowledge the contribution of J. Siemens in performance analyses; V. Re[illegible]au and J. Bair in advanced materials applications; C. Gonzalez in advanced engine applications; and G. Schmidt in configuration design.

1.0 SUMMARY

This study addresses the benefits of advanced technology applications for 19 and 30 passenger, short-haul aircraft. Configuration sensitivities are also reviewed in order to show the design tradeoffs associated with passenger capacity, cabin comfort level and design field length. Besides providing guidelines for commuter aircraft, the study results are generally valid for large, twin-engine, turboprop business airplanes.

The study was divided into four parts:

1. Definition of four baseline airplanes and two design missions.

2. Review and application of advanced technologies to the baseline airplanes.

3. Evaluation of the benefits of advanced technology applications.

4. Recommendations for further research and technology efforts.

Table 1 shows the 32 study airplanes examined in this study, including 4 current technology baselines and 28 advanced technology aircraft. The engine size, wing area, and wing geometry of each of these configurations was optimized for minimum direct operating cost (DOC) using the technologies noted.

The four baseline airplanes provided the opportunity for assessing the sensitivity of DOC and fuel efficiency to configuration differences. Three baselines were sized for a 4000 ft takeoff field length (TOFL), while one short-field version was designed for a 3,000 ft TOFL. The longer-field 19 passenger airplane could off-load 8 passengers to permit operations from a 3000 ft field, but the penalty was a 73% increase in DOC per available seat. The baseline designed for short field operations incurs a much lower 5.8% DOC penalty, relative to designing for a 4000 ft field length.

Two cabin cross-section designs were studied, 2-abreast and 3-abreast. The 2-abreast cross-section was based on the Cessna Citation II fuselage and is similar in size to the Swearingen Metro. This cross section was used only for 19 passenger designs. The 3-abreast cross section has a 6 ft aisle height, flat floor, overhead and underseat storage, and room for hanging baggage, galley provisions, and lavatory. Both 19 and 30 passenger airplanes were designed with this cross section.

Comparison of the 2- vs 3-abreast 19 passenger baselines shows that the costs associated with providing excellent cabin comfort are small. In fact, the breakeven passenger load for the 3-abreast design is only 9 passengers, just 1 more than the breakeven load for the 2-abreast airplane.

The 19 and 30 passenger, 3-abreast baselines were compared to show the efficiencies of larger airplanes. The 30 seat airplane has 16% lower seat-mile DOC's and 18% lower fuel use per seat.

Table 1. STAT Aircraft Designs

OPTIMIZED CONFIGURATIONS	PASSENGERS			
	19			30
	2-ABREAST		3-ABREAST	
	4000 ft TOFL	3000 ft TOFL		
CURRENT TECHNOLOGY BASELINES:				
• BASELINE 1	X			
• BASELINE 2 (SHORT FIELD)		X		
• BASELINE 3			X	
• BASELINE 4				X
ADVANCED TECHNOLOGY AIRCRAFT WITH:				
• LEVEL 1 ADVANCED AERODYNAMICS	X		X	X
• LEVEL 2 ADVANCED AERODYNAMICS	X		X	X
• LEVEL 1 ADVANCED PROPULSION	X		X	X
• LEVEL 2 ADVANCED PROPULSION	X		X	X
• LEVEL 1 ADVANCED STRUCTURES	X		X	X
• LEVEL 2 ADVANCED STRUCTURES	X		X	X
• LEVEL 1 RIDE CONTROL	X			
• LEVEL 2 RIDE CONTROL	X			
• LEVEL 1 COMBINED TECHNOLOGIES	X	X	X	X
• LEVEL 2 COMBINED TECHNOLOGIES	X	X	X	X

Technical sensitivities were also conducted. The study shows DOC to be most sensitive to weight, followed in order by SFC, drag, maximum takeoff lift coefficient, and aircraft price. Fuel efficiency is most affected by engine SFC, followed by drag, weight, and maximum takeoff lift coefficient.

Advanced technologies were studied in four areas: aerodynamics, propulsion, structures, and ride quality. Two levels of technology were studied in each of these four areas: Level 1, representing near-term, low-risk applications; and Level 2, moderate risk applications for the post-1990 time period. The combined aerodynamic, propulsion, and structural technologies provide the following benefits:

	Level 1	Level 2
Reduction in DOC	13%	21%
Reduction in Block Fuel	24%	39%

Each technology provided important reductions in DOC and block fuel, particularly for these Level 2 applications:

- Advanced airfoils and high lift systems.

  Tailored airfoils were studied along with flap systems designed for high takeoff lift coefficient. Airplane cruise drag coefficients were reduced 3% and maximum takeoff lift coefficients were increased up to 35%. These result in DOC savings of about 6% and a block fuel reduction of 11%.

- Advanced propulsion systems.

  Analyses for improved engines and propellers were based on STAT propulsion studies conducted under NASA-Lewis sponsorship by Detroit Diesel Allison, Garrett AiResearch, General Electric, and Hamilton Standard. Improvements selected for this report provide up to 20% better SFC values and 5% higher propeller efficiencies, resulting in about 13% lower DOC's and 29% lower fuel use.

- Advanced materials and structures.

  Low drag airfoils, advanced flap systems, and higher efficiency propellers all rely on new materials and structural arrangements for achieving maximum benefits. In addition, airframe weight savings of up to 20% for bonded metals and 35% for composites are predicted. These airframe weight savings result in 5% better DOC's and block fuel savings of about 4%.

- Ride quality improvements.

  An active ride control system, along with higher wing loadings, can provide significant improvements in passenger ride comfort. Gust response can be reduced up to 70% in cruise.

ORIGINAL PAGE IS
OF POOR QUALITY

2.0 INTRODUCTION

The commuter airlines have become a major factor in the U.S. air transportation system, providing over one-third of all scheduled airline flights. The rapid growth in commuter airline activity in the past ten years has created strong interest in new aircraft for this market. This study recommends appropriate new technologies for these aircraft.

The commuter airlines were initially defined as a class of exempt scheduled air carriers by the Civil Aeronautics Board (CAB) in 1969. As a condition for being exempt from many of the reporting requirements of CAB regulations, the commuter aircraft were limited in size to 5670 kg (12,500 lb) gross takeoff weight. This effectively limited the aircraft to a capacity of 19 passengers. The CAB later increased the size of commuter aircraft to a passenger limit of 30 and a weight limit of 3400 kg (7500 lb) payload, effective September 17, 1972.

The Airline Deregulation Act of 1978 increased the size limits to 55 seats and 8165 kg (18,000 lb) payload. Effective May 17, 1979, the CAB permitted the exempt commuter carriers to operate aircraft having up to 60 seats and 8165 kg (18,000 lb) payload.

To provide another means for the commuter carriers to use larger aircraft, the Airline Deregulation Act allows commuter airlines to receive Certificates of Public Convenience and Necessity from the CAB under Section 401 of the Federal Aviation Act. Over 30 commuter carriers have been granted these certificates. They may fly any size aircraft, but they must also comply with the additional regulations for certificated airlines.

The exempt all-cargo commuters may fly aircraft with an 8165 kg (18,000 lb) payload capacity. Those which have received All Cargo Certificates under Section 418 may use any size aircraft in all-cargo service. Over 20 commuters hold All Cargo Certificates.

Commuter airline traffic has grown from 4.3 million passengers and 39.5 billion kg (43.5 million tons) of cargo in 1970 to an estimated 15.5 million passengers and 454 billion kg (500 million tons) of cargo in 1980. The average annual growth in passengers emplaned was 14% for this period, and average annual cargo growth was 28%.

Trunk and local service carriers began withdrawing from short-haul routes after passage of the Airline Deregulation Act of 1978, which introduced easier market entry and exit rules. High fuel costs made it unprofitable to operate their large jet-powered aircraft on short-haul routes. The commuter air carriers experienced record growth in 1979, the first year after deregulation, as they expanded into short-haul markets abandoned by the trunk and local service carriers.

During 1979, commuter passenger traffic increased 27% and the commuter air carriers added a record number of new aircraft to their fleets. The number of commuter airplanes having 10 or more passenger seats grew 22% during the year. There were 1606 aircraft in commuter service by July, 1980. Of these, 267 were used exclusively for cargo.

This growth in the commuter fleet is expected to continue. A study by the Aerospace Corporation projects U.S. sales of aircraft with 15-60 seats to be 2373 units for the years 1980-2000. Total worldwide sales of these aircraft are projected to be some 5400 units for the same period (Reference 1).

The expanding international market for short-haul aircraft has resulted in a number of new and modified aircraft development programs for the 15-60 seat airplane market. Few of these programs involve domestic manufacturers. Furthermore, the domestic programs are either modifications of existing aircraft or joint programs with an overseas partner.

In 1978, anticipating the need for additional domestic research and development for commuter aircraft, the U.S. Senate Committee on Commerce, Science, and Transportation requested that NASA report on commuter aircraft technologies that could increase their acceptance and use, and also on whether NASA research and development efforts could assist manufacturers in providing these technologies. The Small Transport Aircraft Technology (STAT) research activity at the NASA - Ames Research Center was initiated in response to this request.

NASA had already been investigating operational requirements and advanced technologies for small, short-haul aircraft (Reference 2 and 3). These studies provided an understanding of the low and medium density markets associated with commuter and regional airlines. They also highlighted the importance of having low operating costs along with high passenger and community acceptance.

These and other studies (such as Reference 4) additionally show a clear economic advantage for turboprop aircraft in commuter service because of the small aircraft size, high frequencies, short stage lengths, low cruise altitudes, and short runways common to this market.

As part of the STAT effort, NASA has issued technology application study contracts to 4 airframe, 3 engine, and 2 propeller manufacturers. These include the Cessna Aircraft Co. Wallace Aircraft Division, Beech Aircraft Co., the General Dynamics Convair Division, Lockheed California, Garrett AiResearch, the General Electric Aircraft Engine Group, the General Motors Detroit Diesel Allison Division, Cessna Aircraft Co. McCauley Accessory Division, and United Technologies Hamilton Standard Division. Results of these contracts are summarized in Reference 5.

The objectives of this study were to:

- Identify promising advanced technologies for 19 and 30 passenger short-haul aircraft.
- Define the fuel efficiency and operating cost benefits of each study technology.
- Outline the research and development necessary to ensure the confident use of promising technologies in new aircraft.

The Cessna STAT study consisted of the following tasks:

- Task 1 - Baseline Aircraft and Mission Definition
  Baseline airplane configurations were designed to represent current technology commuter aircraft. The design mission definition was based on short-haul operational requirements.

- Task 2 - Application of Advanced Technology
  Several candidate advanced technologies were analyzed to determine their appropriate application in small, short-haul aircraft. They were then applied individually and in combination to each of the baseline aircraft.

- Task 3 - Evaluation of Advanced Technology
  The cost and benefits of each advanced technology were evaluated for each size of study aircraft in terms of fuel efficiency, operating cost, and passenger acceptance.

- Task 4 - Recommendations for Future Research
  Specific areas requiring further research were identified. The recommended research efforts are needed to achieve and verify the readiness of the promising advanced technologies.

3.0 SYMBOLS AND ABBREVIATIONS

ABR	abreast
AF	blade activity factor
AR	aspect ratio
B	overhead burden factor
BFL	balanced field length
c	cents
C	Celsius
CAB	Civil Aeronautics Board
CAST	Cessna Aircraft Sizing Technique
C_a	airframe price
C_{ae}	price of typical optional avionics and equipment
C_{AL}	airframe maintenance labor costs (\$/flight).
C_{AM}	airframe maintenance material costs (\$/flight)
C_c	crew costs (\$/flight)
C_D	depreciation costs (\$/flight)
C_e	price per engine
C_f	price of fuel (\$/gallon)
C_{FC}	fuel cost (\$/flight)
C_I	insurance costs (\$/flight)
C_L	lift coefficient
$C_{L\ MAX}$	maximum lift coefficient
C_p	propulsion system price - engine and propeller
C_{PM}	engine and propeller maintenance costs (\$/flight)
C_t	total aircraft first price

cm	centimeter
D	propeller diameter
deg	degrees
D_p	depreciation period (yr)
DOC	direct operating cost
F	Fahrenheit
$(F_a)_i$	cost complexity factor for the i^{th} airframe component
F_b	block fuel
F_p	cost complexity factor for propulsion
ft	feet
hr	hour
I	annual insurance rate
in	inch
K_1	airframe labor hourly rate
K_2	airframe labor cyclic factor
K_3	airframe material hourly factor
K_4	airframe material cyclic factor
K_5	constant factor for hourly maintenance costs
K_6	price factor for hourly maintenance costs
K_7	engine and propeller cyclic cost factor
K_a	average airframe price factor
K_p	engine and propeller price factor
K_s	airframe and engine spares ratio
kg	kilogram

KIAS	knots indicated airspeed
km	kilometer
kPa	kilopascal
kt	knot
KTAS	knots true airspeed
kW	kilowatt
lb	pound
lbm	pounds mass
L/D	lift-drag ratio
LDG	landing
LR	labor rate ($/hr)
m	meter
M	maximum cruise Mach number
N	maximum propeller speed (rpm)
N_e	number of engines
N_s	number of passenger seats
NLF	natural laminar flow
nm	nautical mile
P	engine power
P_t	total maximum rated sea level static power
PAX	passengers
psi	pounds per square inch
R	residual value ratio
rad	radians

RCS	ride control system
R/C	ride control
RMS	root mean square
rpm	revolutions per minute
Sw	wing area
SFC	specific fuel consumption
shp	shaft horsepower
skm	seat kilometer
snm	seat nautical mile
STAT	Small Transport Aircraft Technology
t_b	block time (hr)
t_f	flight time (hr)
t_g	ground maneuver time
T.O.	takeoff
TOFL	takeoff field length
TOGW	takeoff gross weight
U	annual utilization
VAPP	minimum approach speed
VCR	maximum cruise speed
W_a	operators' empty weight less engines and propellers
$(W_a)_i$	weight of the i^{th} airframe component
W_T	propeller weight, less spinner, deice, and governor
λ	taper ratio

4.0 DESIGN APPROACH

Each of the 32 study aircraft was sized to satisfy the design mission and optimized for minimum direct operating cost (DOC). This section describes the sizing and optimization procedures, the DOC method, and the pricing formula used for these analyses.

4.1 Sizing and Optimization

The Cessna Aircraft Sizing Technique (CAST) was used to size and optimize the wing, engine, fuel load, and weight of each study airplane. The aircraft geometries were optimized by means of a multiple carpet plot procedure.

4.1.1 Carpet Plots

The basic approach to sizing and optimizing each aircraft involved carpet plots, as presented in Figure 1. The basic carpet is a 4 x 4 grid of wing area (Sw) and engine power (P). Each intersection of two grid lines represents an individual airplane (point design) that meets the payload-range requirements of the sizing mission. Complete performance and DOC information was calculated for each point design. The left hand scale shows the design takeoff weight associated with grid locations.

The performance requirements (or design constraints) were applied on the carpet plot, as shown in Figure 2. The design constraints shown include balanced field length, cruise speed at maximum cruise power and approach speed. Takeoff and balked landing climb gradient constraints were also checked, but none of the study designs were constrained by the climb gradient requirements because the cruise speed requirement was more demanding.

Since the performance of each point design is known, these lines of constant performance levels can be located by interpolation and drawn on the carpet plot. The performance constraints are indicated by crosshatching. Aircraft on the crosshatched side of the line do not meet the constraints. Additional parameter lines can be drawn to determine the sensitivity of airplane size and weight to the design constraints. For example, BFL_1 represents the balanced field length constraint, and BFL_2 represents a shorter field length. This shorter field length is shown to require a larger wing and/or larger engines, resulting in a heavier airplane.

Figure 2 shows a large design region where aircraft meet the constraints, as well as the mission requirements. To find the optimum design point in this region, lines of constant direct operating cost are overlayed, as in Figure 3. These DOC lines represent the dollar cost of flying an airplane on an average 185 km (100 nm) stage length. The minimum DOC design point in the design region is indicated by point A. This point represents the lowest DOC, or optimum airplane on the plot that meets all the design requirements. The CAST program employs an automatic routine to check the DOC gradient and the constraints to find this optimum design point.

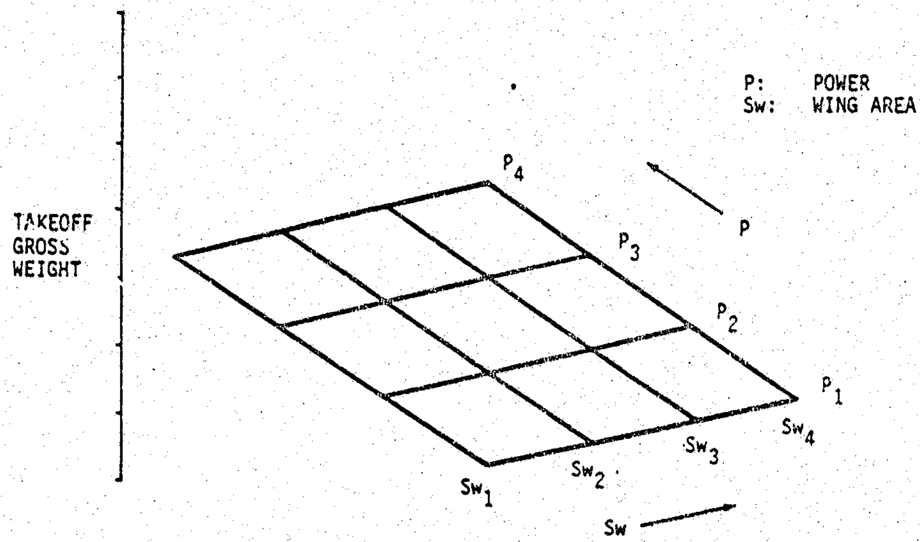

Figure 1. Carpet Plot

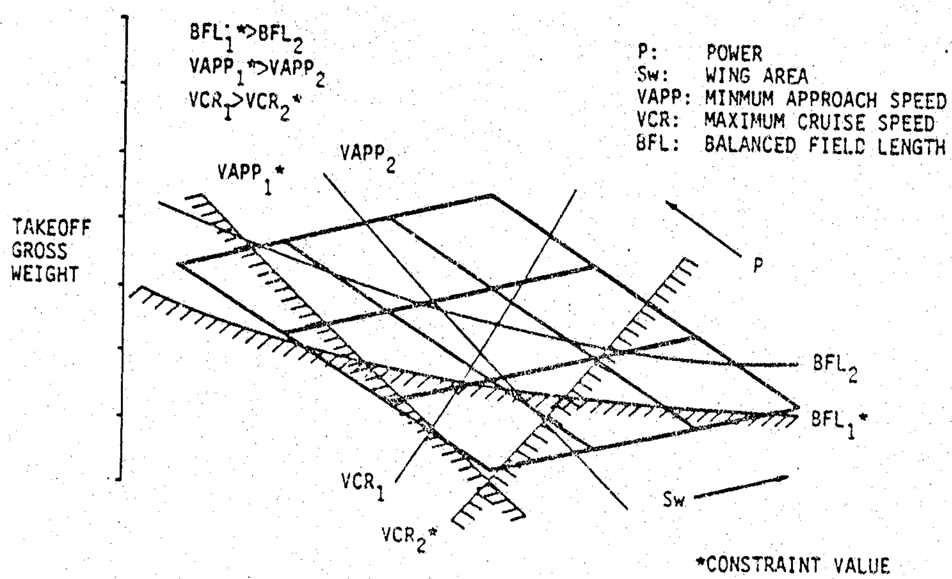

Figure 2. Carpet Plot Sizing

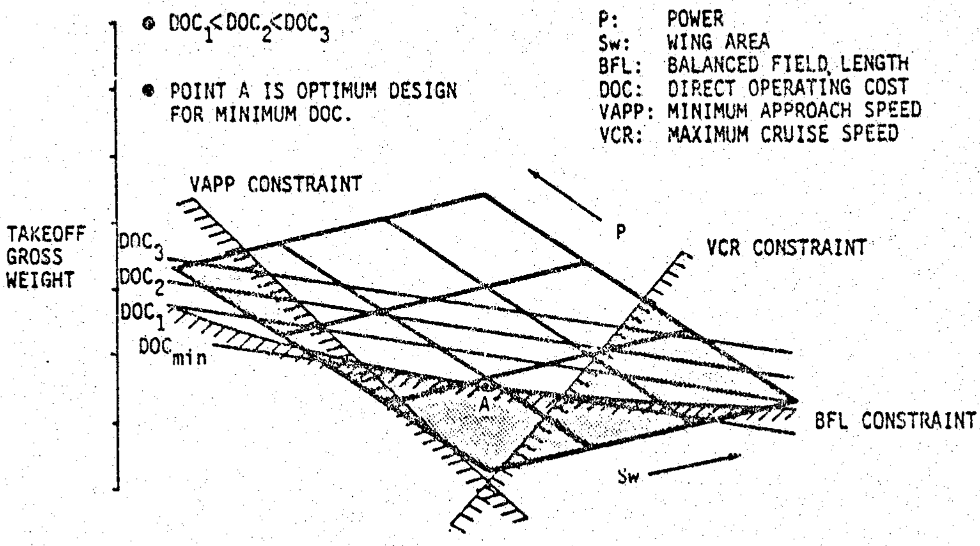

Figure 3. Carpet Plot Optimization

4.1.2 Geometry Optimization

Each of the 16 airplanes that comprise a particular sizing grid has the same wing and propeller geometry (wing sweep, thickness ratio, taper ratio, aspect ratio, and propeller diameter). Consequently, the optimum point on a carpet plot represents the minimum DOC combination of wing and engine size only for that particular airplane geometry.

The optimization of airplane geometry requires a number of carpet plots. Three geometry parameters were optimized: wing aspect ratio, wing taper ratio, and propeller diameter. Since the aircraft are subsonic, the sweep and thickness ratio values did not require optimization. These were fixed at 0° sweep and 15% average wing thickness.

Figure 4 illustrates the geometry optimization procedure. This example uses four grids to find the optimum value of taper ratio (λ), while holding aspect ratio (AR) and propeller diameter (D) constant. Four values of aspect ratio and taper ratio, and five values of propeller diameter were analyzed (Table 2). Consequently, a total of 20 DOC curves of the type shown in Figure 4 could be plotted, requiring 80 carpet plots to optimize the geometry of each study airplane.

In this study, 4 baseline airplanes and 28 advanced technology airplanes were sized and optimized, which could require a total of 32 aircraft x 80 grids per aircraft x 16 points per grid = 40,960 point designs. This large number of designs represents a considerable demand for computer use. However, excellent computational productivity was achieved by checking design sensitivities throughout the optimization process in order to reduce the number of point designs needed.

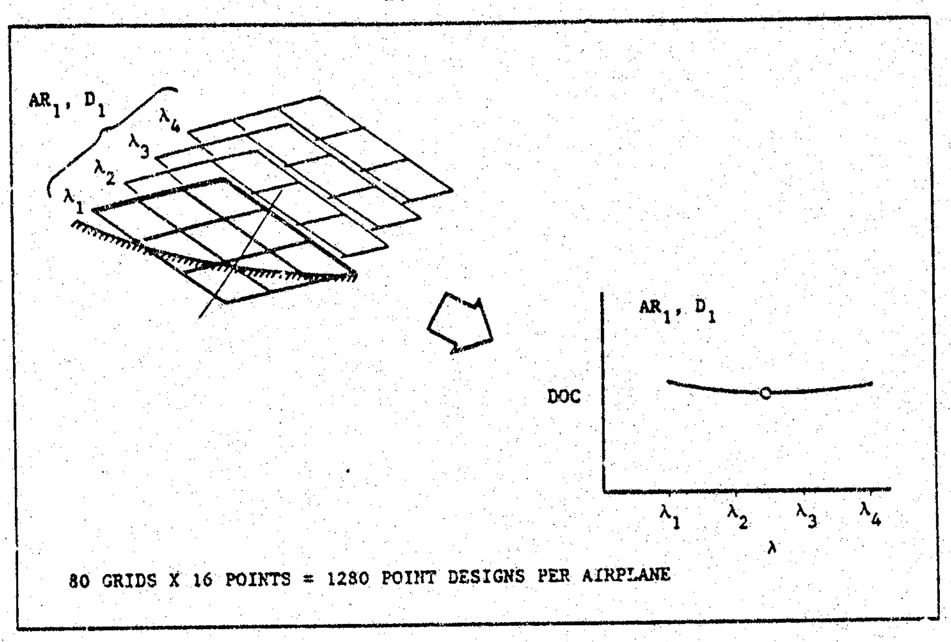

Figure 4. Geometry Optimization

Table 2. Geometry Values Analyzed

TAPER RATIO, λ	ASPECT RATIO, AR	PROPELLER DIAMETER, D
λ_1 = .2	AR_1 = 7	D_1 = 254 cm (100 in)
λ_2 = .3	AR_2 = 9	D_2 = 279 cm (110 in)
λ_3 = .4	AR_3 = 11	D_3 = 305 cm (120 in)
λ_4 = .5	AR_4 = 13	D_4 = 330 cm (130 in)
--	--	D_5 = 356 cm (140 in)

ORIGINAL PAGE IS
OF POOR QUALITY

4.1.3 CAST Description

The carpet plots were generated by the Cessna Aircraft Sizing Technique (CAST), shown in Figure 5. The CAST design process begins with the preparation of an initial 3-view configuration drawing. Parametric lift, drag, and weight data are generated for this initial configuration. This parametric data is part of the input to CAST. The remaining input data includes the mission definition, engine data and installation effects, and tail sizing criteria.

The innermost loop determines the fuel load needed to complete the mission. The gross weight is adjusted in this loop in order to reflect the design effects of changes in the fuel load. The drag polar adjustment in the fuel sizing loop is used when there are external fuel stores. After each aircraft is sized on this innermost loop, a full set of performance and operating cost data is calculated.

The outer loops adjust wing area, engine power, wing geometry, and propeller geometry. Basic lift, drag and weight data are modified accordingly. Upon completion of each 4 x 4 array of wing area and power, the sizing information is automatically plotted for analysis.

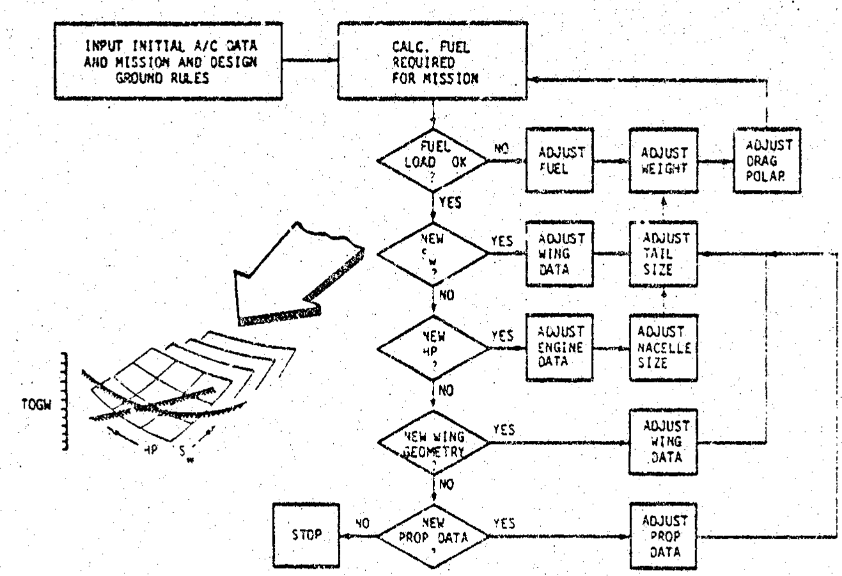

Figure 5. CAST Flow Chart

4.2 Direct Operating Cost Model

Several direct operating cost methods have been developed under NASA funding for use in the design of small, short-haul aircraft (References 3,6,7,8 and 9). The Aerospace Corporation Model (Reference 9) includes a comparison with the Boeing and Douglas models. Additionally, the Civil Aeronautics Board has developed it's own small aircraft costing method (Reference 10) in order to provide profit-loss estimates for particular aircraft in specific route segments. The CAB model costing inputs are updated quarterly (e.g., References 11 and 12).

The Cessna DOC method follows the general format of the 1967 ATA DOC method (Reference 13), with modifications necessary to represent commuter and regional aircraft operating costs in 1979.

4.2.1 DOC Ground Rules

NASA established the following ground rules for the DOC calculations:

- All costs to be presented in 1979 dollars.
- Crew costs ($/block hr) to be 2.7 x passenger seats, with a minimum of $30.24/block hr.
- Maintenance labor rate to be $10/hr.
- Maintenance burden to be 80%.
- Utilization to be 2800 hr/yr for all calculations.
- Annual insurance rate to be 1.5% of the total aircraft price.
- Spares requirement to be 6% of the aircraft price for 19 passenger aircraft and 8% for 30 passenger aircraft.
- Depreciation on aircraft and spares to be straight line over a 12 year period to a 15% residual value.
- Non-productive aircraft maneuvering time (including air and ground maneuvers) to be 10 minutes for all flight distances.
- Fuel cost to be $1.00/gallon.

4.2.2 DOC Cost Estimating Relationships

The operating cost elements include the crew, insurance, depreciation, airframe labor and material (broken down into hourly and cyclic costs), propulsion system hourly and cyclic costs, and fuel.

Airframe maintenance cost factors were derived from Cessna airframe cost data for 1975-1978. Powerplant maintenance cost factors were derived from Pratt & Whitney PT6 engine maintenance and overhaul cost data.

<u>Crew</u>:

$$C_c = 2.7\ (N_s)\ t_b$$

where:

C_c = crew costs ($/flight)

N_s = number of passenger seats

t_b = block time (hr)

<u>Insurance</u>:

$C_I = [I\ (C_t)\ t_b]/U$

where:

C_I = insurance costs ($/flight)

I = annual insurance rate = 0.015

C_t = total aircraft first price (1979$)

U = annual utilization = 2800 hr/yr

<u>Depreciation</u>:

$C_D = [(1 - R + K_s)\ C_t\ t_b]/[(D_p)(U)]$

where:

C_D = depreciation costs ($/flight)

R = residual value ratio = 0.15

K_s = airframe and engine spares ratio

K_s = 0.06 for 19 passenger aircraft

K_s = 0.08 for 30 passenger aircraft

D_p = depreciation period (yr) = 12

<u>Maintenance</u>

Airframe Labor:

$C_{AL} = [K_1 t_f + K_2][(W_a)(LR)(B)]$

where:

C_{AL} = airframe maintenance labor costs ($/flight)

K_1 = airframe labor hourly factor

t_f = flight time (hr) = $t_b - t_g$

K_2 = airframe labor cyclic factor

t_g = ground maneuver time = .0667 hr

(ground manuever time = 4 min

air maneuver time = 6 min)

W_a = operator's empty weight less engines and propellers (lb)

LR = labor rate = 10.00 \$/hr

B = overhead burden factor = 1.8

Airframe Material:

$$C_{AM} = [K_3 t_f + K_4]W_a$$

where:

C_{AM} = airframe maintenance material costs (\$/flight)

K_3 = airframe material hourly factor

K_4 = airframe material cyclic factor

Engine & Propellers:

$$C_{PM} = N_e[(K_5 + K_6 C_p)(LR)(B)(t_b) + K_7 C_p]$$

where:

C_{PM} = engine and propeller maintenance costs (\$/flight)

N_e = number of engines

K_5 = constant factor for hourly maintenance costs

K_6 = price factor for hourly maintenance costs

C_p = propulsion system price for engine and propeller (1979\$)

K_7 = engine and propeller cyclic cost factor

<u>Fuel</u>:

$$C_{FC} = C_f F_b / 6.7$$

where:

C_{FC} = fuel cost (\$/flight)

C_f = price of fuel = \$1.00/gallon

F_b = block fuel (lb)

4.3 Aircraft Pricing

Aircraft prices in 1979 dollars were estimated on the basis of airframe weight, engine rated power, and typical avionics and equipment:

$$C_t = C_a + C_p + C_{ae}$$

where:

C_t = total aircraft first price (1979$)

C_a = airframe price $= (K_a) \sum \left[(F_a)_i (W_a)_i \right]$

K_a = average airframe price factor = $251/kg ($114/lb)

$(F_a)_i$ = cost complexity factor for the i^{th} airframe component

$(W_a)_i$ = weight of the i^{th} airframe component

C_p = propulsion system price $= (K_p)(F_p)(P_t)$

K_p = engine and propeller price factor = $295/kw ($220/hp)

F_p = cost complexity factor for propulsion

P_t = total maximum rated sea level static power

C_{ae} = price of typical optional avionics and equipment = $125,000

The cost complexity factors were used to account for the different cost per pound or cost per horsepower of the various advanced technologies discussed in Section 6.0. If, for example, the cost per pound of an advanced technology airframe component was 50% higher than for the current technology item it replaced, the cost complexity factor for pricing the advanced technology component was 1.5. For current technology items, these factors are 1.0.

The airframe weight items used for pricing in the above formula include everything in the basic empty weight except engines, propellers, and optional avionics and equipment. This definition of airframe weight is different from that used in Section 4.2.2 for calculating airframe maintenance costs because of the different way the operating costs are incurred.

The airframe average price factor of $251/kg ($114/lb) was derived from published price and weight data for Cessna, Swearingen, Shorts, and De Havilland turboprop aircraft. The engine and propeller price factor was derived from data submitted by the manufacturers. The price of optional avionics and equipment represents an average options price for commuter aircraft delivered in 1979.

5.0 BASELINE AIRCRAFT AND DESIGN MISSION

The baseline aircraft and design missions are described in this section. Four current technology baseline airplanes were designed, three 19 passenger aircraft and one 30 passenger airplane (Table 3). These baselines represent a current technology reference for comparison with the advanced technology airplanes described in Section 7.0. In addition, the baselines were compared among themselves to indicate their design sensitivities to the balanced field length requirement, passenger cabin comfort, and number of seats. These airplanes were sized to meet the operational requirements of the short-haul environment, and each airplane design was optimized for minimum direct operating cost.

5.1 Design Background

5.1.1 Choice of Passenger Seating Capacities

Both 19 and 30 passenger airplanes have become standard sizes in the commuter airline industry. Originally, these seating capacities were a result of the regulatory constraints. In particular, commuter carriers operating under FAR Part 135 are permitted to carry up to 19 passengers without incurring the additional expense of a cabin attendant. The Swearingen Metro and the DeHavilland DHC-6 Twin Otter are the existing 19 pasenger, short-haul airplanes in service. Development programs for this size aircraft include the Beech 1900, BAe Jetstream 31, Dornier 228-200, and the upgraded Embraer EMB-110P3 Bandierante.

The 30 passenger size resulted when FAR Part 135, "Air Taxi Operators and Commercial Operators of Small Aircraft", was revised in 1972. Operators using aircraft carrying more than 30 passengers had to comply with the additional maintenance, personnel, training, and flight dispatch requirements of FAR Part 121. The Shorts 330 is the only existing 30 passenger, short-haul aircraft. Two additional 30 passenger aircraft are in development; the Embraer EMB-120 Brasilia and the Ahrens 404.

5.1.2 Baseline Aircraft Design Philosophy

The baseline airplanes were designed using the airframe, propulsion, aerodynamic, and systems technologies that are found in the existing commuter fleet. The 2-abreast aircraft were derived from the Cessna Citation II fuselage and empennage. The wing, powerplants, undercarriage, and systems are all new. This approach provided a 2-abreast baseline that is similar in size and overall configuration to the Swearingen Metro.

The 3-abreast, 19 passenger airplane is an all new design. It was designed for increased passenger acceptance. The larger cabin allows easy entry and exit with carry-on baggage, space for hanging baggage, underseat and overhead storage, a flat floor, a standup aisle, and a lavatory. The costs associated with providing these additional conveniences in the 19 passenger airplane were examined later in the study.

The 30 passenger airplane was conceived as a stretched version of the 3-abreast, 19 passenger baseline. This allowed a joint-program pricing structure for major fuselage and system elements. The wing and propulsion system were resized and optimized for the higher payload.

The study aircraft were not constrained by an external or internal noise goal; however, some allowances for noise control were incorporated, consistent with current design practice. A propeller speed of 1700 rpm was chosen, which is identical to PT6A-45 and -65 propeller speeds. The clearance between propeller tips and the fuselage was set at 0.61 m (24 in) and a weight allowance for moderate cabin sidewall treatment was included. On each of the designs, the empennage arrangement is intended to reduce structural-borne noise by removing the horizontal tail from the propeller wake.

The study aircraft were all low wing configurations. High wing aircraft can have advantages where service vehicle or ground obstruction clearances are critical. However, it was judged that passengers would prefer the cleaner, airline look of a low wing configuration. Furthermore, with low wing airplanes, there is less chance of passengers being disturbed by flap and landing gear operation.

Table 3. Baseline Technology Aircraft

AIRCRAFT	PASSENGER SEATS	SEATS ABREAST	BALANCED FIELD LENGTH m (ft)
BASELINE 1	19	2	1219 (4000)
BASELINE 2	19	2	914 (3000)
BASELINE 3	19	3	1219 (4000)
BASELINE 4	30	3	1219 (4000)

5.2 Aircraft Design Ground Rules

The certification and operation requirements of FAR parts 25 and 135 were followed in the study aircraft designs. Additional requirements were included as a result of previous NASA and Cessna short-haul aircraft studies. The design ground rules listed in this section incorporate these requirements, as well as many of the recommendations made to NASA during it's survey of commuter and local service carriers in 1978.

5.2.1 Configuration Ground Rules

The aircraft configurations were designed to the following requirements:

- A 90.7 kg (200 lb) allowance per passenger including baggage.
- Provision for at least 0.14 m^3 (5 ft^3) of preloaded baggage per passenger.
- Provisions for at least 2.0 cm (0.80 in) of cabin hanging garment space per passenger.
- Provisions for at least 0.07 m^3 (2.55 ft^3) of underseat plus overhead storage per passenger for carry-on baggage in the 3-abreast airplanes. A 23 x 41 x 51 cm (9 x 16 x 20 in) maximum underseat bag dimension was used in the 3-abreast cabins, in order to match the underseat limits of most large transports. The 2-abreast airplane underseat bag size requirement was 13 x 36 x 46 cm (5 x 14 x 18 in).
- A 1.83 m (72 in) minimum interior aisle height for the 3-abreast configurations, and a 1.45 m (57 in) aisle height for the 2-abreast aircraft.
- An 81.3 cm (32 in) minimum seat pitch for the 3-abreast airplanes, and a 76.2 cm (30 in) seat pitch for the 2-abreast aircraft.
- A 45.7 cm (18 in) minimum seat width.
- A 45.7 cm (18 in) minimum aisle width for the 3-abreast configurations, and a 35.6 cm (14 in) minimum aisle width for the 2-abreast aircraft.
- Air-stair passenger door.
- Lavatory provisions in the 3-abreast airplanes.
- Beverage service provisions in the 30 passenger aircraft.
- Cabin pressurization to 42 kPa (6 psi).
- Air conditioning.

- Provision for 1 cabin attendant in the 30 passenger aircraft.
- 2 pilot cockpit.
- An airframe design life of 30,000 hours and 60,000 cycles.
- Dual wheel gear.
- All fuel tanks in wing outer panels.
- High horizontal tail for unobstructed access to aft cargo/baggage door.

5.2.2 Performance Ground Rules

The study aircraft were designed to meet the following performance requirements:

- Full design payload to be carried over a range of 1111 km (600 nm) with reserves for a 185 km (100 nm) alternate plus 45 minutes at maximum cruise power at the enroute cruise altitude.
- Field length to not exceed 1219 m (4000 ft) for a 32.2°C (90°F) day at sea level.
- Cruise speed capability to be at least 463 km/hr (250 kt) indicated airspeed at 3048m (10,000 ft) altitude in standard day conditions. This represents a 536 km/hr (289 kt) true airspeed at 3048 m (10,000 ft).
- Terminal area speed capability to be at least 333 km/hr (180 kt) indicated airspeed with gear and flaps extended in order to interface with jet traffic.
- Approach speed to not exceed 222 km/hr (120 kt) indicated airspeed in the landing configuration at maximum landing weight in order to qualify for operations in Category B of the instrument approach procedures, as defined in FAR Part 97. This corresponds to a stall speed in the landing configuration of 171 km/hr (92 kt).

5.3 Design Missions

A sizing mission was defined to incorporate the payload-range requirement and the additional operational requirements of the short-haul environment. All aircraft were sized to meet the capabilities of the sizing mission. A shorter mission, representative of the average commuter stage length, was used to optimize the aircraft.

5.3.1 Sizing Mission

The sizing mission is shown in Figure 6. This mission includes takeoff with seats full at takeoff gross weight, climb at maximum climb speed, cruise at 4572 m (15,000 ft) altitude at maximum cruise power to a 1111 km (600 nm) destination, maneuver for 6 minutes, descent, missed approach, and flight to a 185 km (100 nm) alternate with 45 minutes reserves. The 4572 m (15,000 ft) cruise altitude was chosen to assure a reasonable low altitude range capability, since these aircraft would be typically operated on a series of short, low altitude flights.

The sizing mission primarily defines the sequence of operating procedures used to determine the fuel quantity required for each point design. The only performance items specified in the mission are the range, alternate distance, and reserve endurance requirements. The remaining performance ground rules (speed and field length requirements) are applied as constraints in the carpet plot procedure described in Section 4.1.1.

5.3.2 Optimization Mission

All study aircraft were optimized for minimum DOC on a 185 km (100 nm) stage length. The optimization mission is identical to the sizing mission, except for the shorter stage length. Takeoff was at the design takeoff gross weight (full fuel, seats full), the cruise altitude was 4572 m (15,000 ft), and maximum cruise power was used (Figure 7).

5.4 Baseline Aircraft Description

The baseline designs represent optimized current technology aircraft. These are compared to advanced technology aircraft in Section 7.0. The configuration descriptions, aerodynamics, operating costs, and design sensitivities are presented in this section. The baseline airplanes are identified by number in Table 3, and Table 4 provides a summary of the baseline aircraft characteristics.

5.4.1 Configuration Description

5.4.1.1 General

The baseline aircraft were designed with technologies representative of today's 19 and 30 passenger short-haul airplanes. The wing designs have NACA 230XX airfoils and partial span, single-slotted flaps. The airframe designs are of riveted aluminum construction. Basic engine installation data and scaling factors were derived from the Pratt & Whitney PT6 engine series. Systems weights were based on the Citation II mechanical, hydraulic, electric, environmental, instrumentation, and avionics systems.

ORIGINAL PAGE IS
OF POOR QUALITY

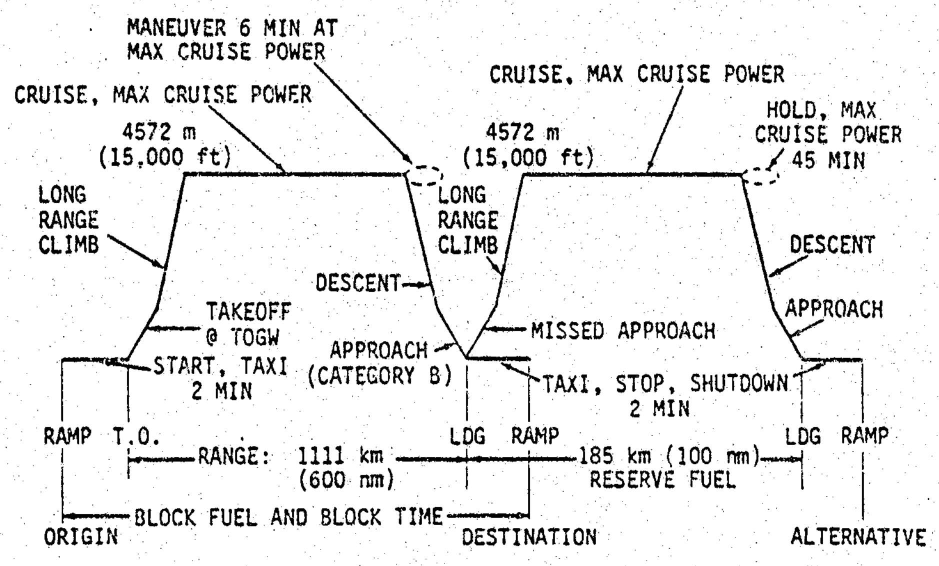

Figure 6. Sizing Mission

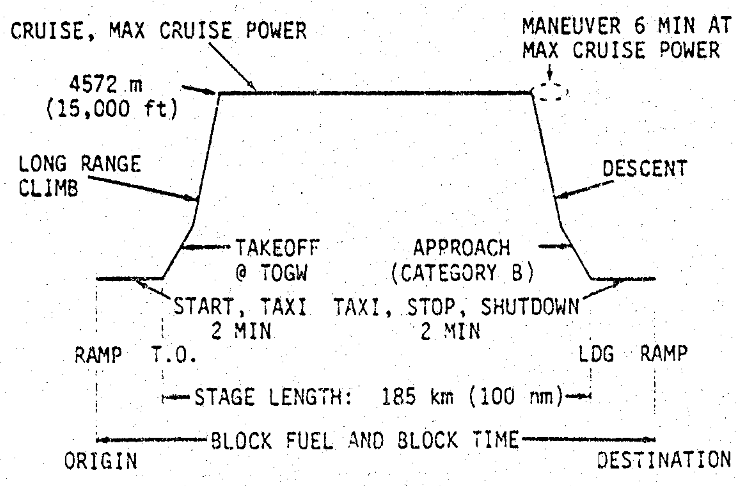

Figure 7. Optimization Mission

ORIGINAL PAGE IS
OF POOR QUALITY

Table 4. Baseline Aircraft Characteristics

CHARACTERISTICS		19 PASSENGER # 1 2 ABR	19 PASSENGER # 2 SHORT FIELD 2 ABR	19 PASSENGER # 3 3 ABR	30 PASSENGER # 4 3 ABR
TAKEOFF GROSS WEIGHT	kg	7239	7468	8140	10981
	(lb)	(15960)	(16465)	(17945)	(24210)
EMPTY WEIGHT	kg	3983	4057	4679	5897
	(lb)	(8780)	(8945)	(10315)	(13000)
SEA LEVEL POWER[1]/ENGINE	kW	928	1040	1070	1439
	(SHP)	(1245)	(1395)	(1435)	(1930)
WING LOADING	kg/m^2	240	215	251	259
	(lb/ft^2)	(49.1)	(44.1)	(51.3)	(53.1)
POWER LOADING	kg/kW	3.9	4.0	3.8	3.8
	(lb/HP)	(6.4)	(6.6)	(6.3)	(6.3)
WING:					
AREA	m^2	30.2	34.7	32.5	42.4
	(ft^2)	(325)	(373)	(350)	(456)
SPAN	m	17.6	17.9	17.8	20.0
	(ft)	(57.7)	(58.7)	(58.4)	(65.8)
ASPECT RATIO		10.25	9.25	9.75	9.50
PERFORMANCE:					
TAKEOFF FIELD LENGTH	m	1219	914	1219	1219
(FAR 25)	(ft)	(4000)	(3000)	(4000)	(4000)
TAKEOFF DISTANCE	m	716	564	721	744
(FAR 23)	(ft)	(2350)	(1850)	(2365)	(2440)
RATE OF CLIMB	m/min	1024	1123	1050	1039
@ SEA LEVEL	(ft/m)	(3360)	(3685)	(3445)	(3410)
APPROACH SPEED	km/HR	206	194	209	213
@ SEA LEVEL	(KTAS)	(111)	(105)	(113)	(115)
MAX. CRUISE SPEED	km/HR	463	463	463	463
@ 3048m (10000 ft)	KIAS)	(250)	(250)	(250)	(250)
RANGE[2] @ 4572m	km	1111	1111	1111	1111
(15000 ft)	(nm)	(600)	(600)	(600)	(600)
BLOCK FUEL					
185 km (100 nm)	kg	249	272	281	363
	(lb)	(550)	(600)	(620)	(800)
1111 km (600 nm)	kg	934	1039	1073	1427
	(lb)	(2060)	(2290)	(2365)	(3145)
AIRCRAFT INITIAL PRICE	$MIL	1.49	1.56	1.74	2.23
DOC[3]	¢/SEAT-km	5.936	6.278	6.712	5.657
	(¢/SEAT/nm)	(10.993)	(11.627)	(12.430)	(10.476)
RELATIVE DOC		1.000	1.058	1.131	0.953

1. THERMODYNAMIC POWER
2. WITH RESERVES
3. 185 km (100 nm) STAGE LENGTH

5.4.1.2 Interior Configurations

The configuration designs began with the layout of cabin interiors to meet the study ground rules. Figure 8 shows the interior of the 2-abreast aircraft. The fuselage outside diameter is 1.63 m (64 in). The 1.45 m (57 in) aisle height includes a 13 cm (5 in) dropped aisle. Seat pitch is 0.76 m (30 in). Armrests are provided only on the outboard side of the seats because of FAR 25 aisle width rules. There are no hanging or overhead baggage provisions because of the small cross section, but underseat space is provided for a soft bag or a 13 x 36 x 46 cm (5 x 14 x 18 in) briefcase. The aft baggage hold provides 0.164 m^3 (5.8 ft^3)of volume per passenger. The 2-abreast interior cross section is compared to the 3-abreast arrangement in Figure 9. Both configurations use air-stair doors for passenger entry/exit.

The outside diameter of the larger cabin is 2.44 m (96 in). This permits a 1.83 m (72 in) aisle height with a flat floor. Aisle width is 0.46 m (18 in) and the seats are more substantial than for the 2-abreast interior. Overhead storage is provided along one side of the larger cabin, and underseat storage space is more generous and useable, especially under the double seat.

Figure 10 shows the 3-abreast, 19 passenger interior arrangement. Seat pitch is 0.81 m (32 in). A lavatory is provided in the aft cabin, and a 0.91 m (36 in) hanging baggage closet is near the entry door. Overhead storage volume is 0.026 m^3 (0.91 ft^3) per passenger. The underseat space provides clearance for luggage with dimensions up to 23 x 41 x 51 cm (9 x 16 x 20). The aft baggage hold provides 0.37 m^3 (13.2 ft^3) of volume per passenger.

The 30 passenger interior is shown in Figure 11. This is based on a stretched 3-abreast, 19 passenger fuselage. A cabin attendant seat is located near the entry door. The lavatory, beverage service area, and a .61 m (24 in) hanging baggage closet are in the forward cabin. Overhead storage volume of 0.027 m^3 (0.95 ft^3) per passenger is provided. Underseat bags up to 23 x 41 x 51 cm (9 x 16 x 20 in) in size are accommodated. Aft preloaded baggage volume is 0.24 m^3 (8.3 ft^3) per passenger.

Passenger cabin comfort levels for the study interiors are compared with the Douglas DC-9-30 in Table 5. The DC-9 interior presented is the 110 passenger, all-coach interior used by USAir since 1979. The 3-abreast interior has a clear advantage over the 2-abreast configuration; and except for aisle height and pressurization level, the 3-abreast interiors compare favorably with the DC-9-30. The 42 KPa (6.0 psi) pressurization level for the study aircraft provides a sea level cabin to 4115 m (13,500 ft) altitude, and a 1219 m (4000 ft) cabin to 6096 m (20,000 ft) altitude.

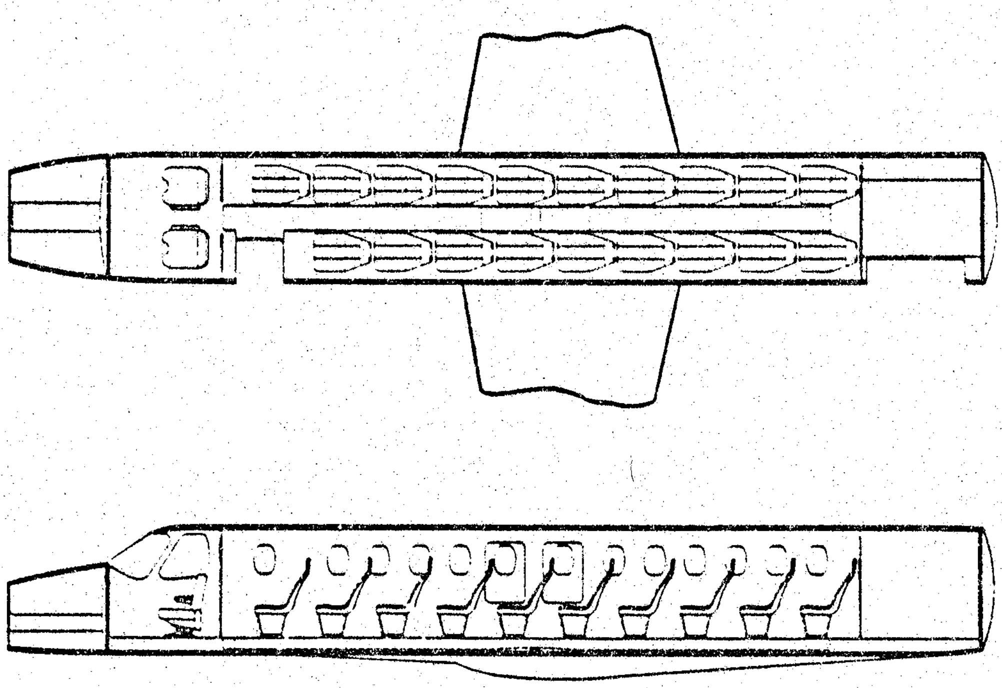

- 2-ABREAST SEATING
- 1.45 m (57 in) MINIMUM AISLE HEIGHT
- .36 m (14 in) MINIMUM AISLE WIDTH
- .76 m (30 in) SEAT PITCH
- UNDERSEAT BAGGAGE SIZE
  13 x 36 x 46 cm (5 x 14 x 18 in)
- AFT BAGGAGE HOLD VOLUME
  3.11 m^3 (110 ft^3)

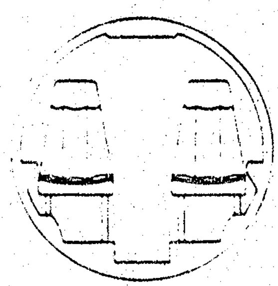

Figure 8. 2-Abreast Interior

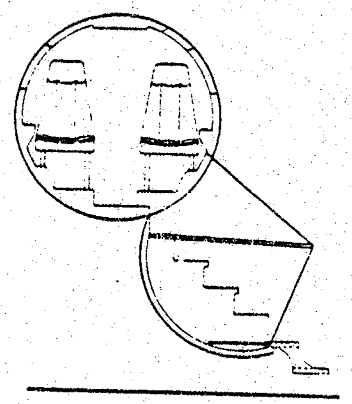

2-ABREAST SEATING

- 1.63 m (64 in) OUTSIDE FUSELAGE DIAMETER
- 1.45 m (57 in) MIN AISLE HEIGHT
- .36 m (14 in) MIN AISLE WIDTH
- .46 m (18 in) SEAT WIDTH

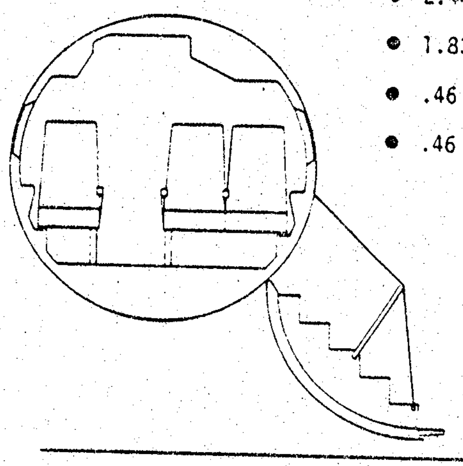

3-ABREAST SEATING

- 2.44 m (96 in) OUTSIDE FUSELAGE DIAMETER
- 1.83 m (72 in) MIN AISLE HEIGHT
- .46 m (18 in) MIN AISLE WIDTH
- .46 m (18 in) SEAT WIDTH

Figure 9. Cabin Cross Section Comparison

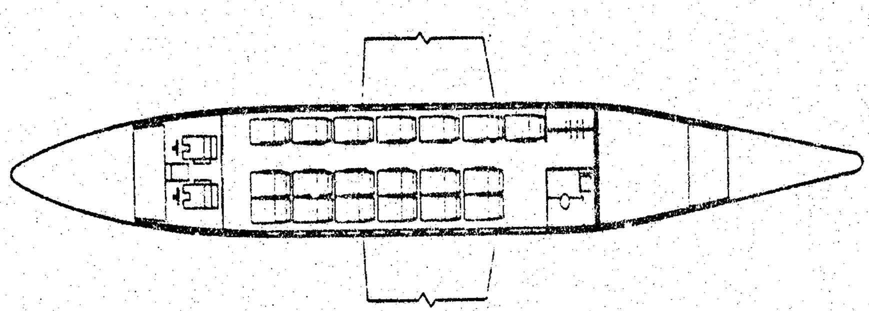

- 3-ABREAST SEATING
- 1.83 m (72 in) MIN AISLE HEIGHT
- .46 m (18 in) MIN AISLE WIDTH
- .81 m (32 in) SEAT PITCH
- UNDERSEAT BAGGAGE SIZE
  23 x 41 x 51 cm (9 x 16 x 20 in)
- .91 m (36 in) HANGING BAGGAGE LENGTH
- .49 m^3 (17.3 ft^3) OVERHEAD BAGGAGE VOLUME
- 7.1 m^3 (250 ft^3) AFT BAGGAGE HOLD VOLUME
- LAVATORY

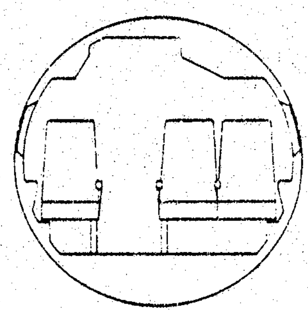

Figure 10. 3-Abreast 19 Passenger Interior

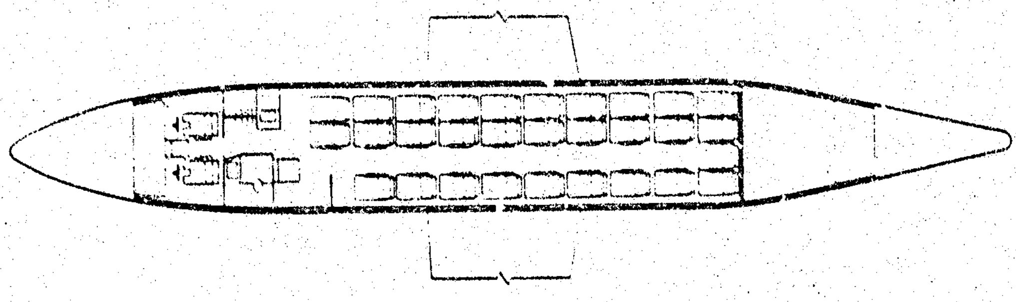

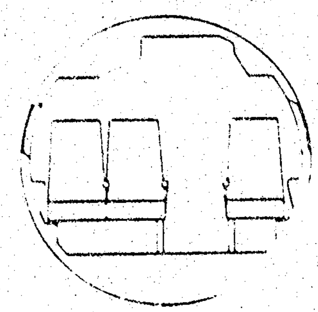

- 3-ABREAST SEATING
- 1.83 m (72 in) MIN AISLE HEIGHT
- .46 m (18 in) MIN AISLE WIDTH
- .81 m (32 in) SEAT PITCH
- UNDERSEAT BAGGAGE SIZE
  23 x 41 x 51 cm (9 x 16 x 20 in)
- .61 m (24 in) HANGING BAGGAGE LENGTH
- .81 m^3 (28.5 ft^3) OVERHEAD BAGGAGE VOLUME
- 7.1 m^3 (250 ft^3) AFT BAGGAGE HOLD VOLUME
- LAVATORY
- BEVERAGE SERVICE AREA

Figure 11. 30 Passenger Interior

ORIGINAL PAGE IS
OF POOR QUALITY

Table 5. Cabin Data Comparison

CABIN CONFIGURATION	CABIN DATA					LAVATORIES	
	SEAT WIDTH m (IN)	SEAT PITCH m (IN)	MINIMUM AISLE WIDTH m (IN)	AISLE HEIGHT m (IN)	CABIN PRESS kPa (PSI)	NUMBER	PAX/LAV
19 PASSENGER 2-ABREAST	.46 (18)	.76 (30)	.36 (14)	1.45 (57)	42 (6.0)	0	--
19 PASSENGER 3-ABREAST	.46 (18)	.81 (32)	.46 (18)	1.83 (72)	42 (6.0)	1	19
30 PASSENGER 3-ABREAST	.46 (18)	.81 (32)	.46 (18)	1.83 (72)	42 (6.0)	1	30
DOUGLAS DC-9-30	.44 (17.5)	.84 (33)	.50 (19.5)	2.03 (80)	51 (7.45)	3	31

CABIN CONFIGURATION	BAGGAGE ALLOWANCES PER PASSENGER				CLOSET SPACE	
	PRELOADED	UNDERSEAT		OVERHEAD		
	VOLUME m^3 (FT^3)	VOLUME m^3 (FT^3)	SIZE m (IN)	VOLUME m^3 (FT^3)	TOTAL LENGTH m (IN)	LENGTH PER PAX m (IN)
19 PASSENGER 2-ABREAST	.16 (5.8)	.02 (.8)	.13x.36x.46 (5x14x18)	--	--	--
19 PASSENGER 3-ABREAST	.37 (13.2)	.05 (1.7)	.23x.41x.51 (9x16x20)	.026 (.91)	.91 (36)	.048 (1.89)
30 PASSENGER 3-ABREAST	.24 (8.3)	.05 (1.7)	.23x.41x.51 (9x16x20)	.027 (.95)	.61 (24)	.020 (.80)
DOUGLAS DC-9-30	.23 (8.1)	.05 (1.8)	.23x.41x.53 (9x15x21)	.028 (.98)	2.03 (80)	.019 (.73)

NOTES: 1. COCKPIT CREW PROVISIONS INCLUDE A CHART HOLDER AND A TOTAL WEIGHT ALLOWANCE OF 28kg (60 lb)
2. DOUGLAS DC-9-30 DATA BASED ON 110 PASSENGERS.

5.4.1.3 Baseline 3-Views

The four baseline airplane 3-views are shown in Figure 12, 13, 14, and 15. These configurations were optimized for minimum DOC using the carpet plot technique described in Section 4.1. Figure 16 shows the final carpet plot for the optimized 19 passenger, 2-abreast baseline. Point A defines the aircraft that has the minimum direct operating cost and still satifies all the performance requirements. Lines of constant direct operating cost (DOC) are shown for reference. All of the baselines were constrained by the cruise speed and takeoff field length requirements. Neither approach speed nor climb gradient requirements constrained any of the designs. In fact, the 222 km/hr (120 KIAS) approach speed constraint line and the FAR Part 135 climb gradient constraint line lie off the sizing grid. The design data associated with point A is shown in the first column of Table 4.

The optimization trends for all of the baselines were very similar. Figure 17 shows the effect of aspect ratio on DOC for Baseline 1. The curve indicates a moderate variation in DOC through the range of aspect ratios analyzed. This flat variation is typical for very short range, low altitude missions. For these missions, the sizing relationship between wing area and engine size is of greater importance than the wing geometry.

The propeller optimization trend is shown in Figure 18 for Baseline 1. Note that DOC is very flat for propeller diameters from 3.05 m through 3.20 m (120-126 in), with the optimum occuring at 3.12 m (123 in).

A diameter of 3.05 m (120 in) was selected to provide the lowest tip speed consistent with the desire for minimum DOC. This diameter gives a maximum rotational tip speed of 271 mps (890 fps) at the selected maximum propeller speed of 1700 rpm.

Propellers smaller than 3.05 m (120 in) suffer a penalty due to high disc loading, while propellers larger than 3.20 m (126 in) encounter high tip Mach number losses. Also, the clearance between the propeller tips and the ground was held constant in this study; so larger propellers drove the size and weight of the airplane higher, due mostly to the higher propeller weight and the longer gear length required.

Baseline 2 differs from Baseline 1 in that it's design field length is 25% lower. Figure 13 shows that the short-field airplane has a lower aspect ratio than the longer-field airplane (Figure 12). The opposite trend may be expected. However, the sizing of these aircraft followed the pattern of Figure 2. The shorter field length requirement, along with the fixed cruise speed and range requirements, resulted in a heavier airplane with larger wing area and higher engine power. Since minimum DOC is closely tied to minimum weight, the optimization tended toward a lighter, lower aspect ratio wing. The heavier 3-abreast airplanes also optimized with lower aspect ratios than Baseline 1.

BASELINE 1

- 19 PASSENGERS
- 2-ABREAST SEATING
- CURRENT TECHNOLOGY
- 1219 m (4000 ft) TOFL

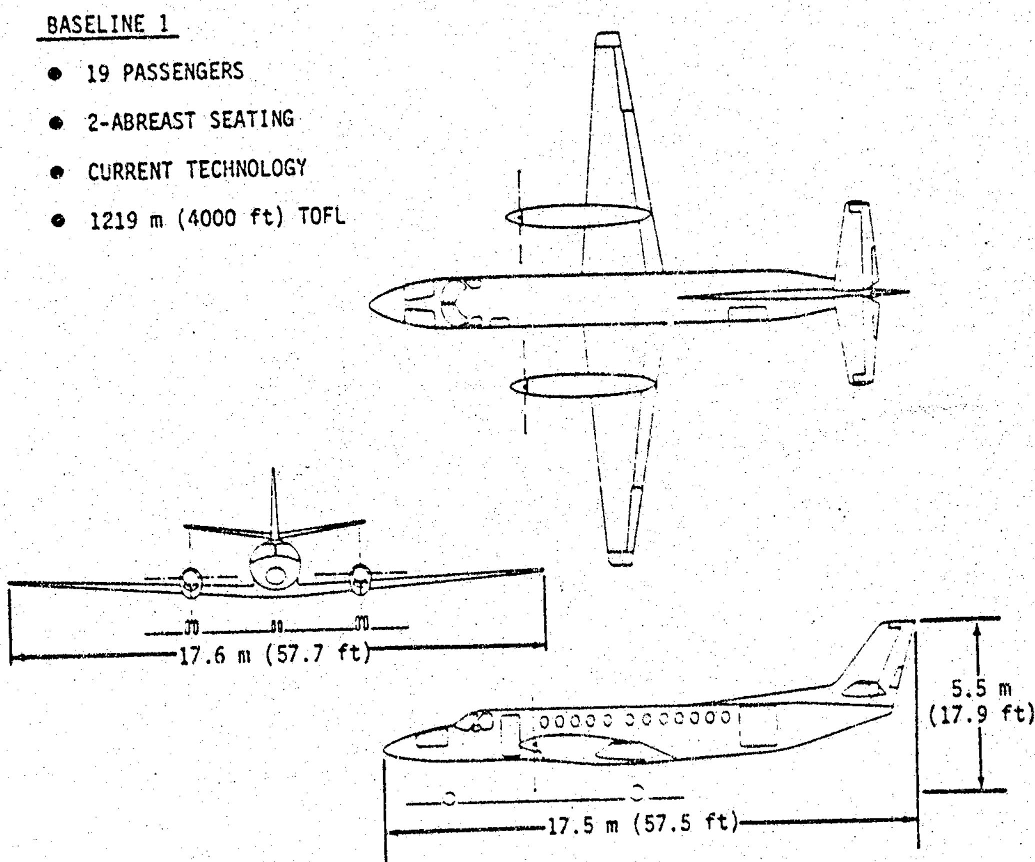

TOGW	7239 kg	(15,960 lb)
POWER/ENGINE	928 kW	(1245 shp)
PROPELLER DIAMETER	3.0 m	(10.0 ft)
WING AREA	30.2 m^2	(325 ft^2)
WING SPAN	17.6 m	(57.7 ft)
ASPECT RATIO	10.25	

Figure 12. Baseline 1 -- 19 Passenger, 2-Abreast, 4000 Ft Field Length

BASELINE 2

- 19 PASSENGERS
- 2-ABREAST SEATING
- CURRENT TECHNOLOGY
- 1219 m (4000 ft) TOFL

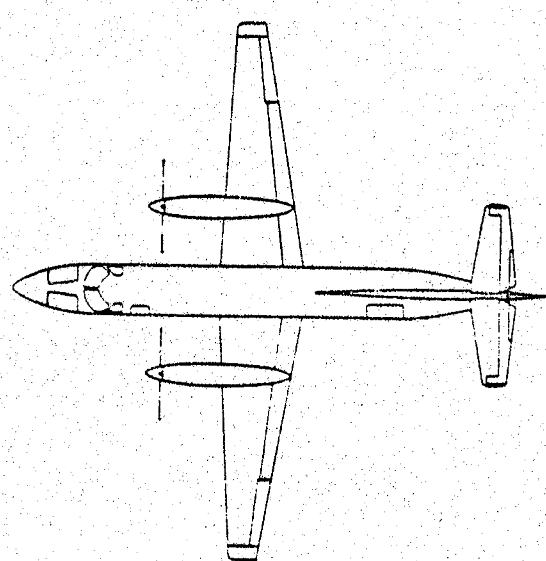

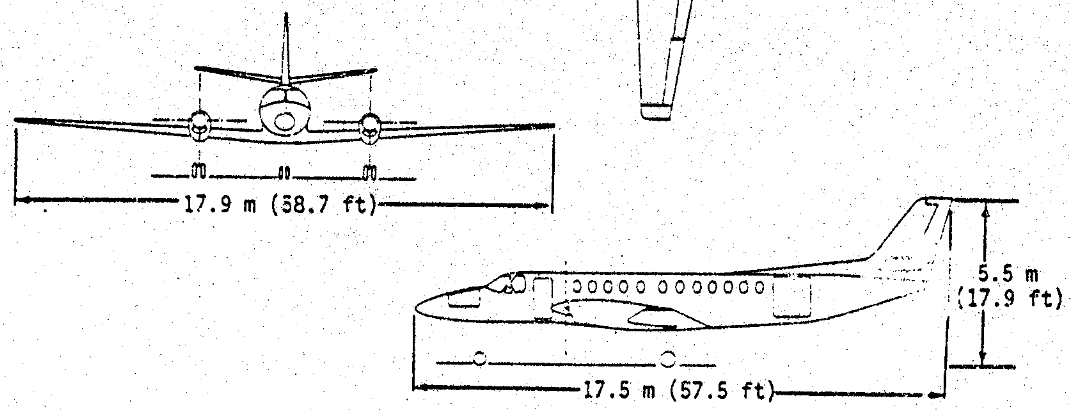

TOGW	7468 kg (16,465 lb)
POWER/ENGINE	1040 kW (1395 shp)
PROPELLER DIAMETER	3.0 m (10.0 ft)
WING AREA	34.7 m^2 (373 ft^2)
WING SPAN	17.9 m (58.7 ft)
ASPECT RATIO	9.25

Figure 13. Baseline 2 -- 19 Passenger, 2-Abreast, 3000 Ft Field Length

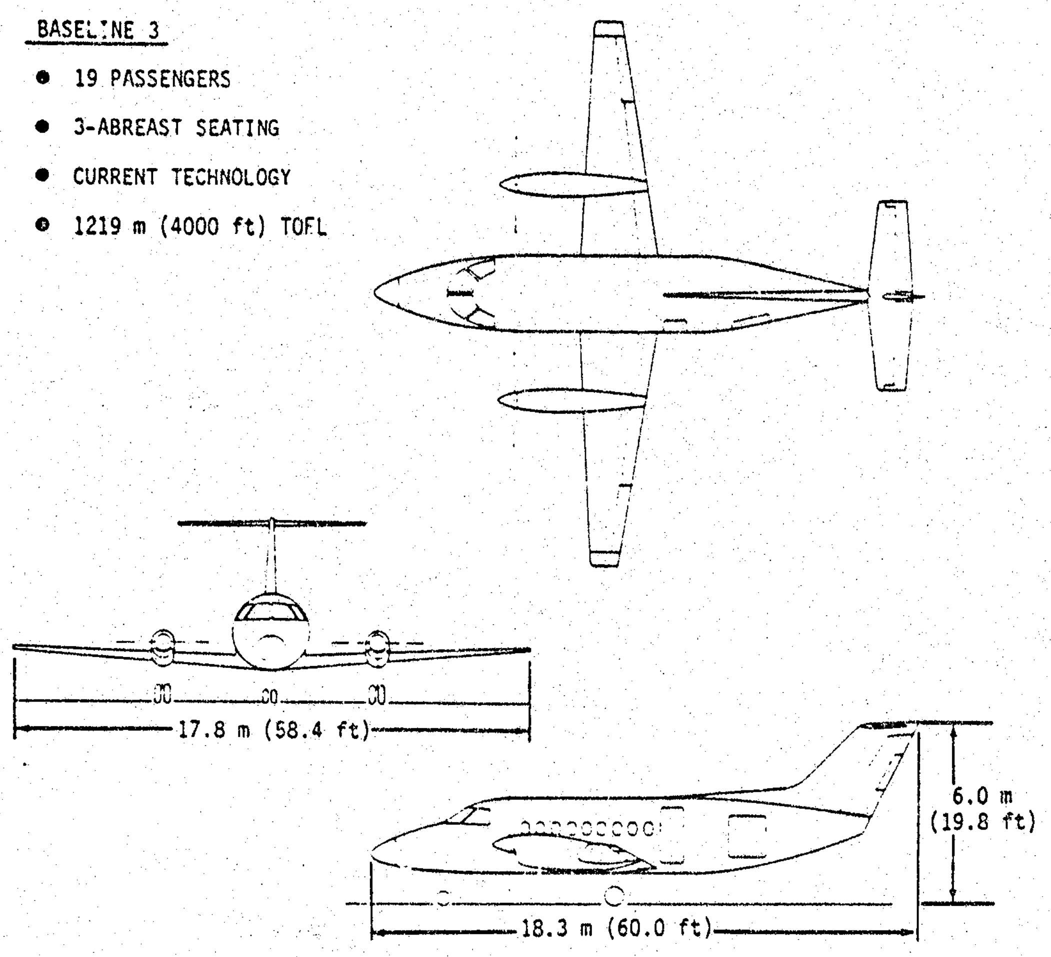

TOGW	8140 kg	(17,945 lb)
POWER/ENGINE	1070 kW	(1435 shp)
PROPELLER DIAMETER	3.0 m	(10.0 ft)
WING AREA	32.5 m^2	(350 ft^2)
WING SPAN	17.8 m	(58.4 ft)
ASPECT RATIO	9.75	

Figure 14. Baseline 3 -- 19 Passenger, 3-Abreast, 4000 Ft Field Length

BASELINE 4

- 30 PASSENGERS
- 3-ABREAST SEATING
- CURRENT TECHNOLOGY
- 1219 m (4000 ft) TOFL

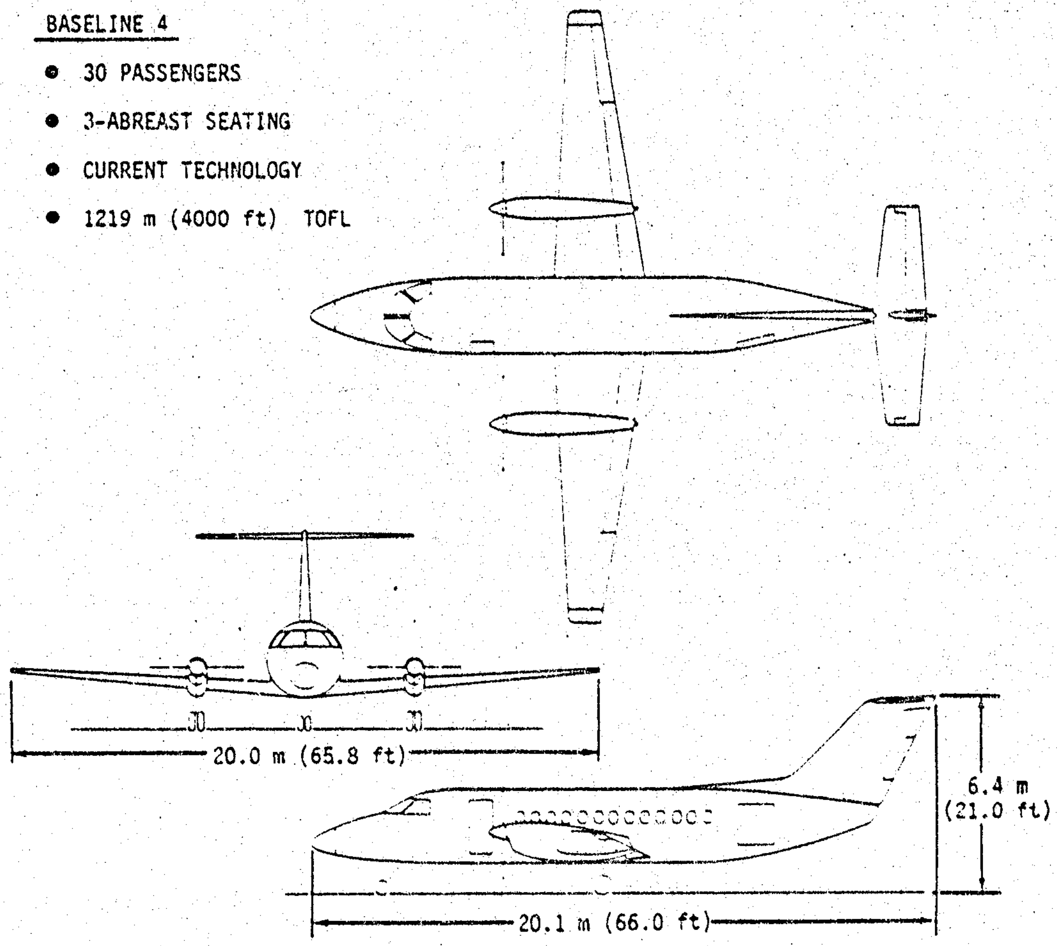

TOGW	10,981 kg	(24,210 lb)
POWER/ENGINE	1439 kW	(1930 shp)
PROPELLER DIAMETER	3.0 m	(10.0 ft)
WING AREA	42.4 m^2	(456 ft^2)
WING SPAN	20.0 m	(65.8 ft)
ASPECT RATIO	9.50	

Figure 15. Baseline 4 -- 30 Passenger, 3-Abreast, 4000 Ft Field Length

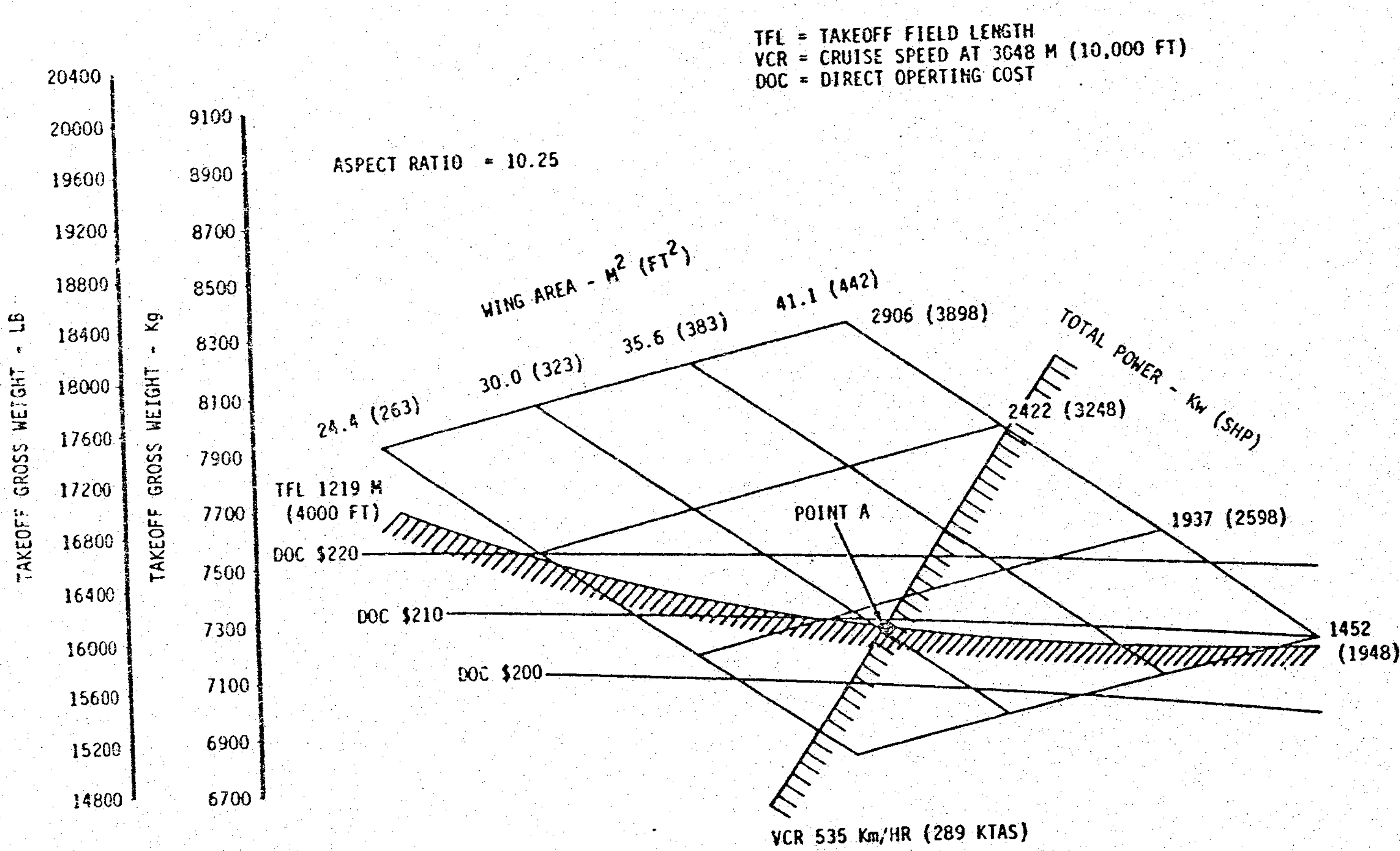

Figure 16. Baseline 1 Car: Plot

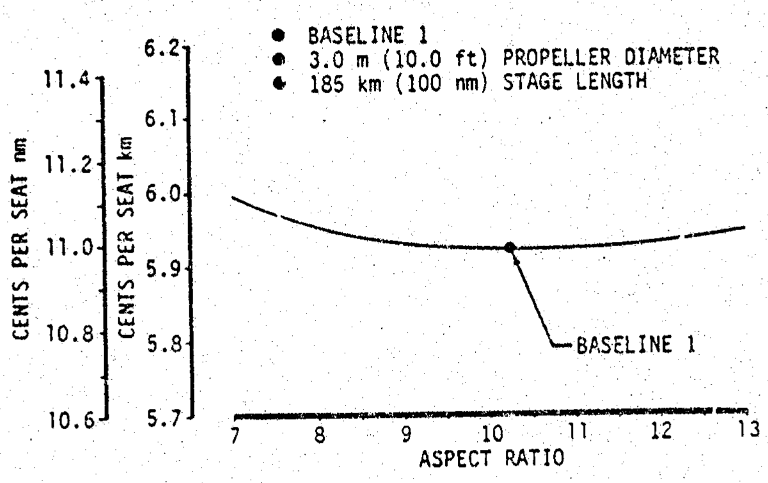

Figure 17. Effect of Aspect Ratio on DOC for Baseline 1

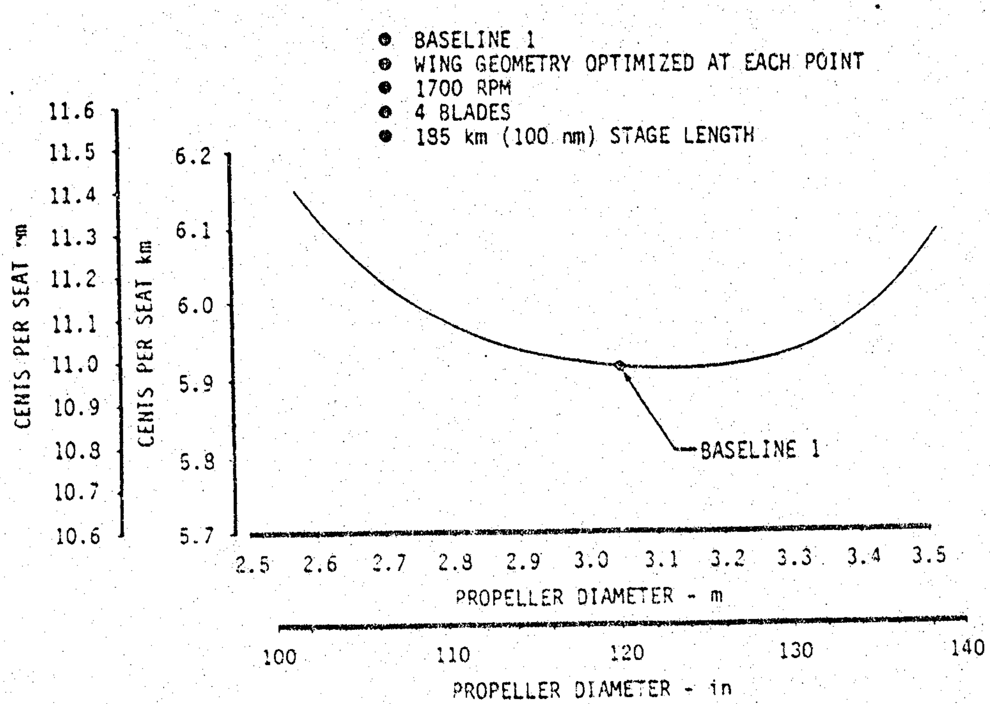

Figure 18. Effect of Propeller Diameter on DOC for Baseline 1

The empennage designs for the 3-abreast airplanes differ from those of the 2-abreast airplanes. The 2-abreast designs derive from existing Citation hardware that utilizes the cruciform tail. In these aircraft, maximum commonality dictates retaining the tail configuration. The 3-abreast aircraft are all new and are unconstrained by commonality goals. T-tails are used on the 3-abreast aircraft for three principal reasons: noise, aerodynamic efficiency, and ground vehicle clearance. The T-tail reduces cabin noise by raising the horizontal tail well above the propwash in all normal flight attitudes. Aerodynamic efficiency benefits include both lower drag and improved fin/rudder effectiveness, relative to a cruciform tail of the same size. Ground vehicle clearance for the T-tail is approximately 5.8 m (19 ft), almost 2.7 m (9 ft) higher than for the cruciform tail.

5.4.1.4 Baseline Propulsion Data and Scaling

The Pratt and Whitney PT6-series engines were used to develop baseline engine data and scaling factors. This engine series provides a good parametric data base because it includes 29 different engines, with output ranging from 354 kW (475 shp) to 969 kW (1299 shp). The performance of the PT6A-65 engine was scaled for the baseline airplane sizing studies. No flat rating or water injection was employed. Characteristics of the baseline engine are given in Table 6.

Figure 19 shows parametric PT6 dry engine weight as a function of power and propeller speed. The nominal dry weight shown represents a bare engine without additional equipment, options, or accessories. The 1700 rpm line was used for weight scaling. Considering that all PT6 engines have a nominal diameter of 0.48 m (19 in), the engine diameter was not scaled with power. A minimum length of 1.88 m (74 in) was used, which is the length of the PT6A-65. This was scaled upwards as power increased above the 969 kW (1299 shp) thermodynamic level.

A typical PT6 installation is shown in Figure 20. The gas path is reversed, with exhaust stacks forward and an inlet plenum aft. The installation losses were scheduled with power setting and flight condition and scaled to aircraft size. Maximum assumed installation losses for the baseline aircraft are given in Table 7.

Propeller performance and weight were based on data from the Hamilton Standard STAT propeller study (Reference 14). The weight relationship recommended by Hamilton Standard for a single acting, solid aluminum propeller is:

$$W_T = 220\left[\left(\frac{D}{10}\right)^2 \left(\frac{B \times AF}{400}\right)^{0.7} \left(\frac{N \times D}{20,000}\right)^{0.4} \left(\frac{SHP}{10D^2}\right)^{0.12} \left(1 + M\right)^{0.5}\right]$$

$$+5B\left(\frac{D \times AF}{1000}\right)^2 \left(\frac{20,000}{N \times D}\right)^{0.3}$$

where: W_T = Propeller weight, less spinner, deice, and governor (lb)

D = Propeller diameter (ft)

B = Number of blades

AF = Blade activity factor

N = Maximum propeller speed (rpm)

SHP = Takeoff shaft power (HP)

M = Maximum cruise Mach number

Table 6. PT6A-65 Engine Characteristics

TAKEOFF SHAFT POWER, SEA LEVEL, STD. DAY	969 kW (1299 shp)
SPECIFIC FUEL CONSUMPTION, MAX TAKEOFF POWER	.334 kg/kW/hr (0.549 lb/eshp/hr)
MASS FLOW, MAX TAKEOFF POWER	4.5 kg/sec (9.9 lbm/sec)
PRESSURE RATIO	10.35
MAXIMUM SHAFT SPEED	1700 rpm
DRY WEIGHT	210 kg (464 lb)
LENGTH	1.88 m (74 in)
NOMINAL DIAMETER	0.48 m (19 in)

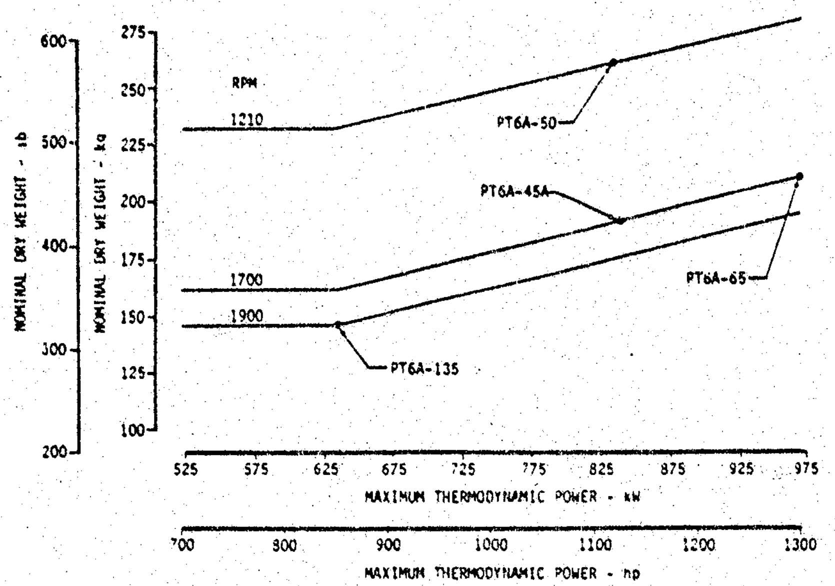

Figure 19. Engine Weight

Table 7. Peak Installation Losses

AIRCRAFT	BASELINE 1 19 PASSENGER 2-ABREAST	BASELINE 2 19 PASSENGER 2-ABREAST SHORT FIELD	BASELINE 3 19 PASSENGER 3-ABREAST	BASELINE 4 30 PASSENGER
INLET PRESSURE LOSS RATIO	.15	.15	.15	.15
POWER EXTRACTION/ENGINE	8.9 kW (12 hp)	8.9 kW (12 hp)	11.2 kW (15 hp)	14.9 kW (20 hp)
BLEED EXTRACTION/ENGINE	4.5 kg/min (10 lbm/min)	4.5 kg/min (10 lbm/min)	5.4 kg/min (12 lbm/min)	8.2 kg/min (18 lbm/min)

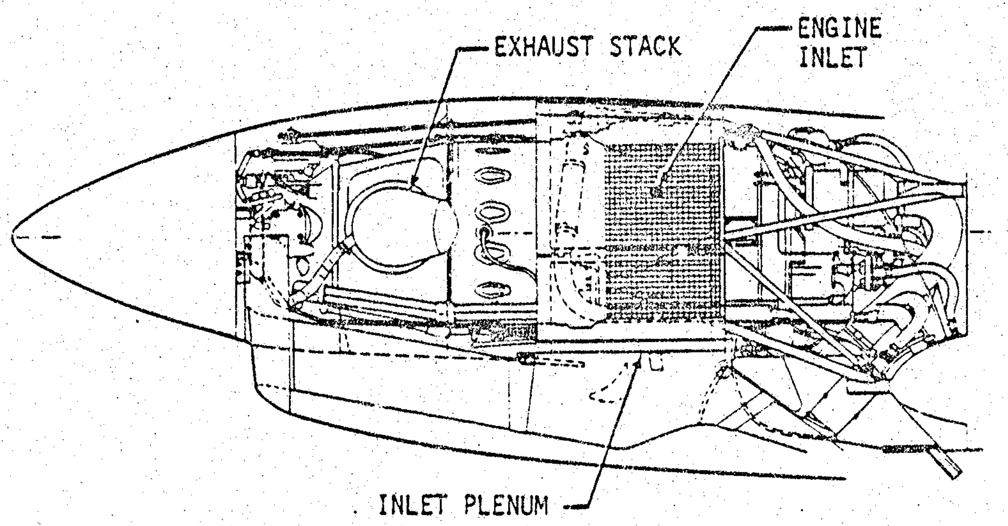

Figure 20. Baseline Engine Installation

5.4.1.5 Baseline Aircraft Systems

The baseline aircraft systems utilize current technology and meet FAR Part 25 requirements. In choosing the system concepts, special emphasis was placed on simplicity, maintainability and reliability. System weights were derived from those of the Citation I and II business jet aircraft.

The speed range of the aircraft permits the use of manual primary flight controls through a mechanical control system. Flight adjustable trim tabs are located on the primary control surfaces. Trim tabs are both electrically and manually operated.

The tricycle landing gear are hydraulically actuated and incorporate dual wheels on each strut. The nose gear retracts forward into the fuselage nose, and the main gear retract into the engine nacelles. A 10,300 kPa (1500 psi) hydraulic system was chosen to operate the landing gear as well as the wing flaps, power steering system and brakes.

Pneumatic boots were chosen for deicing the wing, horizontal stabilizer and vertical fin. Conventional electric anti-ice systems are used for the propellers and windshields. Bleed air was chosen as the means for anti-icing the engine air inlet. Electrically reheated cabin air is used to de-fog cockpit windows.

The baseline structure employs conventional riveted aluminum construction with spars, ribs, bulkheads, stringers and skins. Metal bonding and composites were considered only for the advanced technology aircraft. The structural weight reflects an airframe design life of 30,000 hours and 60,000 cycles.

The aircraft is pressurized to 42 kPa (6 psi), providing a sea level cabin at an aircraft altitude of 4115 m (13,500 ft). Engine bleed air is used for cockpit and cabin heating. An air-cycle machine is provided for cooling. An oxygen system is included that meets the requirements of FAR Part 135.

The 28 volt DC, dual bus electrical system is powered by engine mounted starter-generators and two NiCad-type aircraft batteries. An external power receptacle is provided. 115 volt AC current is provided by static inverters.

5.4.1.6 Weights

A summary of baseline aircraft component weights is presented in Table 8. Operating weights are shown in Table 9.

5.4.2 Aerodynamic Design

Conventional aerodynamic arrangements were used in the design of the baseline aircraft. The wing sections were developed from the NACA 23018 airfoil at the root and the NACA 23012 airfoil at the tip. The flapped portion of the wing runs from the fuselage side to 0.70 semi-span. The flap/wing chord ratio is 0.30. Hinged, single-slotted flaps were used. For the baseline airplanes, maximum takeoff lift coefficient is 1.69, and the maximum landing configuration lift coefficient is 2.0.

ORIGINAL PAGE IS
OF POOR QUALITY

Table 8. Baseline Aircraft Weight Summary
(lb)

AIRCRAFT	BASELINE 1 19 PASSENGER 2-ABREAST	BASELINE 2 19 PASSENGER 2-ABREAST SHORT FIELD	BASELINE 3 19 PASSENGER 3-ABREAST	BASELINE 4 30 PASSENGER
WING	1300	1340	1530	2230
TAIL	295	295	430	485
BODY	2150	2150	2240	2740
GEAR & ROLLING ASSY.	705	715	735	1005
CONTROLS	200	210	300	325
PROPULSION SYSTEM	1745	1830	2010	2360
NACELLES	320	335	385	400
HYDRAULIC SYSTEM	100	105	115	140
ELECTRIC SYSTEM	390	390	420	535
ELECTRONIC SYSTEM & INSTRUMENTATION	325	325	325	325
ENVIRONMENTAL SYSTEM	455	455	625	810
INTERIOR FURNISHINGS	615	615	1000	1400
AUXILIARY GEAR	10	10	10	15
EXTERIOR FINISH	60	60	80	110
TRAPPED AND UNUSABLE FLUIDS	110	110	110	120
STD. EMPTY WEIGHT	8780	8945	10,315	13,000

Table 9. Operating Weights
(lb)

AIRCRAFT	BASELINE 1 19 PASSENGER 2-ABREAST	BASELINE 2 19 PASSENGER 2-ABREAST SHORT FIELD	BASELINE 3 19 PASSENGER 3-ABREAST	BASELINE 4 30 PASSENGER
STD. EMPTY WEIGHT	8780	8945	10,315	13,000
ZERO FUEL WEIGHT	12,980	13,145	14,515	19,600
MAXIMUM FUEL CAPACITY	2980	3320	3430	4610
MAXIMUM PAYLOAD	4200	4200	4200	6600
MAXIMUM USEFUL LOAD	7180	7520	7630	11,210
MAXIMUM LANDING WEIGHT	15,960	16,465	17,945	24,210
MAXIMUM TAKEOFF WEIGHT	15,960	16,465	17,945	24,210

The baseline aircraft drag polars are given in Figures 21 through 24. The twin-engine cruise, takeoff, and landing configuration polars are shown. For single-engine conditions, drag adjustments were made for the effects of yaw, trim, propeller slipstream, the feathered propeller, and a windmilling turbine. These adjustments resulted in single-engine C_D levels 10% to 15% higher than the twin-engine C_D levels for the aircraft in this study.

5.4.3 Operating Costs

The baseline aircraft direct operating costs are detailed in Table 10. The individual DOC elements are shown for 50, 100, 150, 200, 400, and 600 nm stage length.

The baseline DOC's are compared in Figure 25. The high costs associated with short stage lengths below 280 km (150 nm) are immediately evident. The DOC's at 93 km (50 nm) are approximately 50% higher than for 185 km (100 nm). This illustrates some of the cost pressure that has historically driven short-haul airlines to longer and longer routes.

5.5 Design Sensitivities

Both configuration and technology sensitivities were analyzed. The configuration sensitivities were conducted on the four baseline airplanes, because they have the same level of technology. The technology sensitivities were conducted on Baseline 1 by making systematic changes in several technical parameters. The primary sensitivity measures were DOC and fuel efficiency for a 185 km (100 nm) stage length.

5.5.1 Configuration Sensitivities

The configuration sensitivity analyses show the effects of the takeoff field length requirement, cabin comfort level, and the number of passenger seats on DOC and fuel use.

5.5.1.1 Takeoff Field Length

Figure 26 shows the hot day field performance for Baseline 1 at sea level and at 1830 m (6000 ft) altitude. The takeoff field length is shown to be 1220 m (4000 ft) at sea level with a full 19 passenger payload. In order to operate from a 915 m (3000 ft) field at sea level, this airplane must offload 8 passengers, increasing it's available seat-mile operating costs from 10.993¢/available seat-nm to 18.988¢/available seat-nm, a 73% increase.

For airlines operating regularly from shorter fields, Baseline 2 offers a significant economic advantage because it is designed specifically for a 915 m (3000 ft) runway. The 100 nm DOC for Baseline 2 is 11.627¢/available seat-nm, which is 5.8% higher than Baseline 1 at it's full capacity, but 39% lower than Baseline 1 offloaded to 11 passengers. The tradeoff between field length and DOC is presented in Figure 27, which shows Baseline 2 to be more economical up to a runway length of 1196 m (3920 ft).

ORIGINAL PAGE IS
OF POOR QUALITY

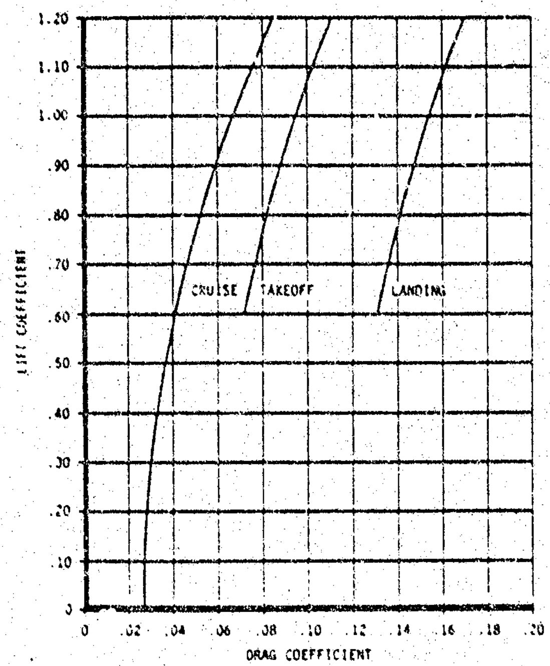

Figure 21. Drag Polars - Baseline 1

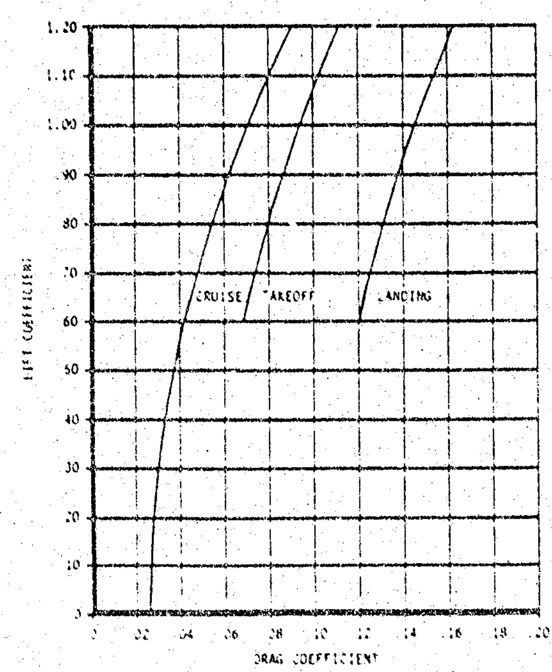

Figure 22. Drag Polars - Baseline 2

ORIGINAL PAGE IS
OF POOR QUALITY

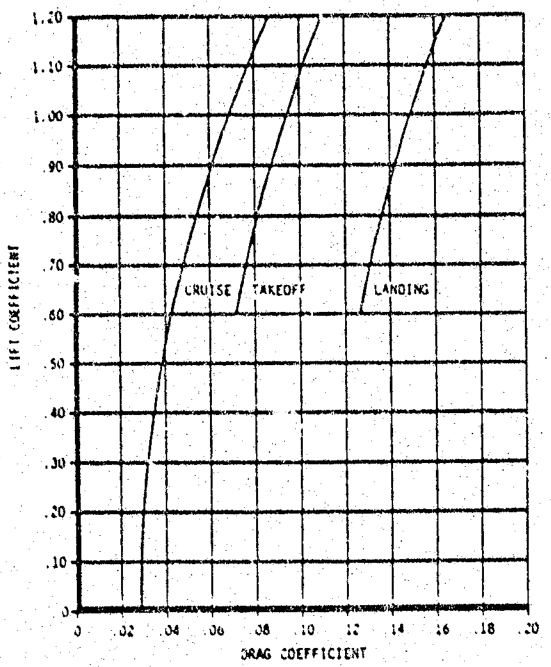

Figure 23. Drag Polars - Baseline 3

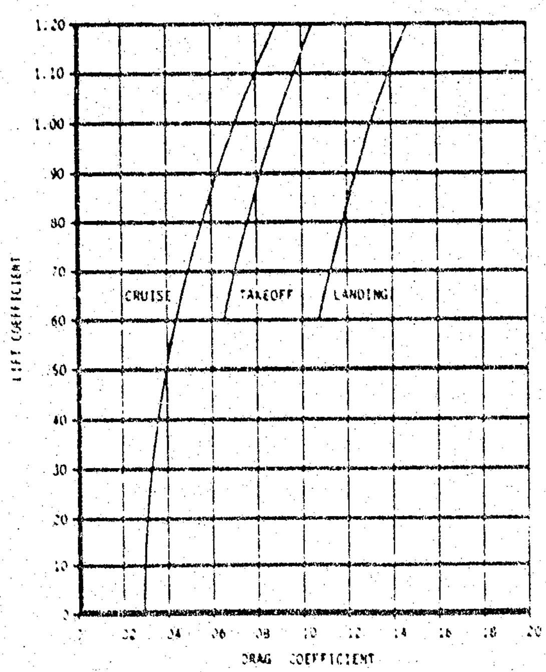

Figure 24. Drag Polars - Baseline 4

Table 10. Baseline Aircraft DOC Summary

STAGE LENGTH		BASELINE 1 19 PASSENGER 2-ABREAST	BASELINE 2 19 PASSENGER 2-ABREAST SHORT FIELD	BASELINE 3 19 PASSENGER 3-ABREAST	BASELINE 4 30 PASSENGER
		¢/skm(¢/snm)	¢/skm(¢/snm)	¢/skm(¢/snm)	¢/skm(¢/snm)
93 km (50 nm)	Crew	1.10 (2.04)	1.10 (2.04)	1.10 (2.04)	1.10 (2.04)
	Insurance	.17 (.32)	.18 (.33)	.20 (.37)	.16 (.30)
	Depreciation	.87 (1.60)	.90 (1.67)	1.00 (1.87)	.82 (1.52)
	Maintenance	3.50 (6.48)	3.67 (6.80)	4.14 (7.66)	3.42 (6.33)
	Fuel	3.40 (6.30)	3.65 (6.77)	3.78 (6.99)	3.04 (5.62)
	TOTAL	9.04 (16.74)	9.50 (17.59)	10.22 (18.93)	8.54 (15.81)
185 km (100 nm)	Crew	.80 (1.48)	.80 (1.48)	.80 (1.48)	.80 (1.48)
	Insurance	.12 (.23)	.13 (.24)	.15 (.27)	.12 (.22)
	Depreciation	.63 (1.17)	.66 (1.22)	.74 (1.36)	.60 (1.11)
	Maintenance	2.03 (3.76)	2.15 (3.97)	2.40 (4.44)	1.99 (3.68)
	Fuel	2.35 (4.34)	2.55 (4.72)	2.63 (4.87)	2.15 (3.98)
	TOTAL	5.94 (10.99)	6.29 (11.63)	6.72 (12.43)	5.66 (10.47)
278 km (150 nm)	Crew	.70 (1.30)	.70 (1.30)	.70 (1.30)	.70 (1.30)
	Insurance	.11 (.20)	.11 (.21)	.13 (.24)	.10 (.19)
	Depreciation	.55 (1.02)	.58 (1.07)	.64 (1.19)	.52 (.97)
	Maintenance	1.54 (2.86)	1.63 (3.02)	1.82 (3.36)	1.51 (2.79)
	Fuel	1.99 (3.69)	2.18 (4.03)	2.25 (4.18)	1.86 (3.44)
	TOTAL	4.90 (9.07)	5.20 (9.64)	5.54 (10.26)	4.69 (8.69)
370 km (200 nm)	Crew	.65 (1.21)	.65 (1.21)	.65 (1.21)	.65 (1.21)
	Insurance	.11 (.19)	.11 (.20)	.12 (.20)	.10 (.18)
	Depreciation	.51 (.95)	.54 (1.00)	.60 (1.11)	.49 (.90)
	Maintenance	1.30 (2.40)	1.38 (2.55)	1.53 (2.83)	1.27 (2.35)
	Fuel	1.82 (3.36)	1.99 (3.69)	2.06 (3.81)	1.71 (3.16)
	TOTAL	4.39 (8.12)	4.67 (8.64)	4.96 (9.18)	4.22 (7.80)
741 km (400 nm)	Crew	.58 (1.07)	.58 (1.07)	.58 (1.07)	.58 (1.07)
	Insurance	.09 (.17)	.09 (.17)	.10 (.19)	.09 (.16)
	Depreciation	.45 (.84)	.48 (.88)	.53 (.98)	.43 (.80)
	Maintenance	.93 (1.72)	.99 (1.84)	1.09 (2.02)	.91 (1.68)
	Fuel	1.55 (2.87)	1.72 (3.18)	1.77 (3.28)	1.48 (2.75)
	TOTAL	3.60 (6.67)	3.86 (7.14)	4.07 (7.54)	3.49 (6.46)
1111 km (600 nm)	Crew	.55 (1.02)	.55 (1.02)	.55 (1.02)	.55 (1.02)
	Insurance	.09 (.16)	.09 (.17)	.10 (.19)	.08 (.15)
	Depreciation	.43 (.80)	.46 (.84)	.51 (.94)	.41 (.76)
	Maintenance	.80 (1.49)	.87 (1.60)	.94 (1.75)	.79 (1.46)
	Fuel	1.46 (2.70)	1.62 (3.00)	1.67 (3.10)	1.41 (2.61)
	TOTAL	3.34 (6.18)	3.58 (6.64)	3.78 (6.99)	3.24 (6.01)

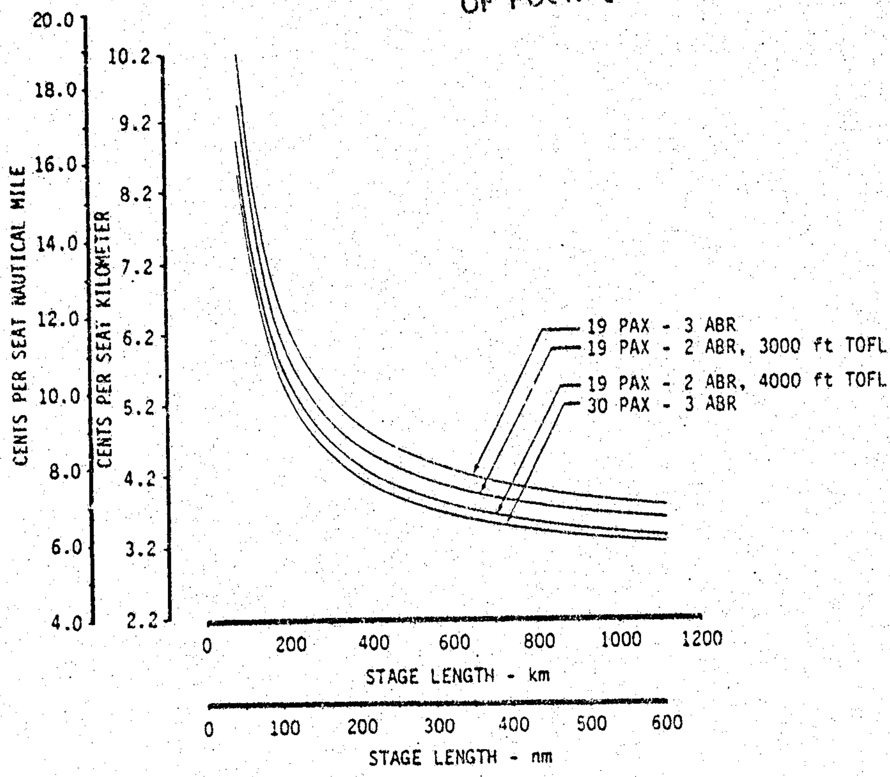

Figure 25. DOC Comparison

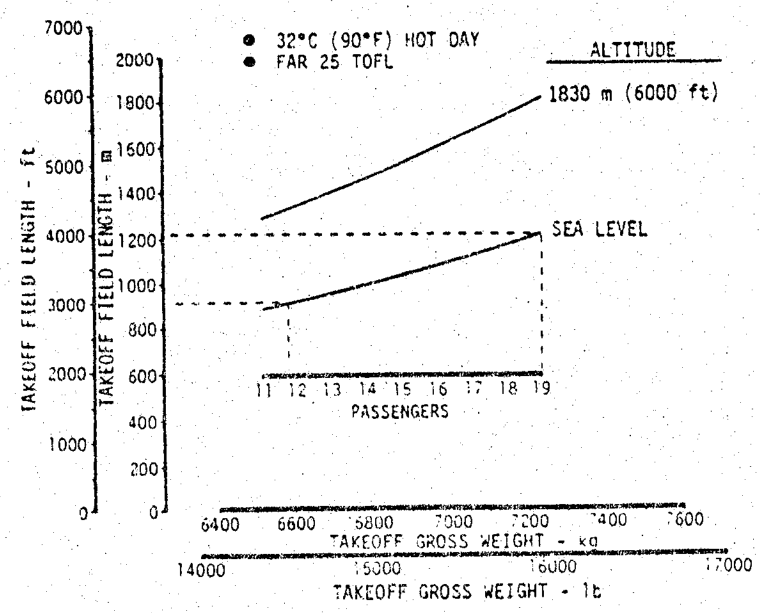

Figure 26. Offloaded Takeoff Performance of Baseline 1

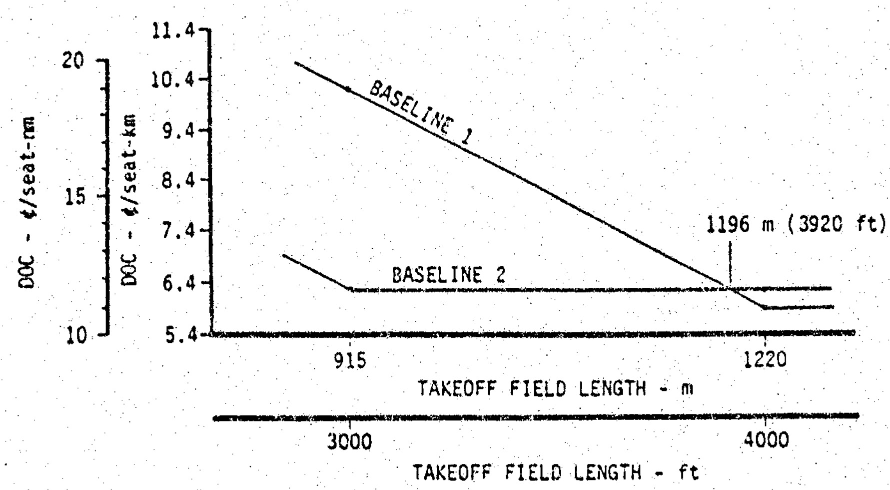

Figure 27. Tradeoff Between Design Field Length and DOC

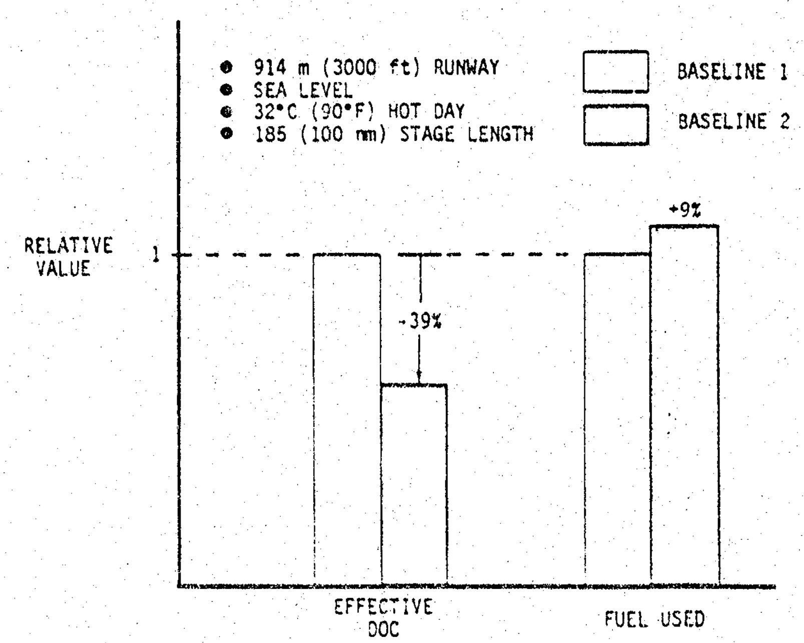

Figure 28. Hot Day, Short-Field Tradeoff for Baseline 2

Baseline 2 has a short-field DOC advantage, but pays a 9% penalty in fuel economy, due to its larger size. Figure 28 summarizes the relative DOC and fuel tradeoffs for short runway, hot day operations.

5.5.1.2 Cabin Comfort Level

The costs associated with providing a high level of cabin comfort can be determined by comparing Baselines 1 and 3. Table 11 summarizes the DOC and fuel penalties associated with the wide body design. These penalties are smaller than expected.

Assuming a fare yield of 27¢ per seat-nm, the breakeven load factor is 41% for the 2-abreast airplane on a 100 nm stage length, and 46% for the 3-abreast airplane. The additional 5% load factor requirement for the 3-abreast aircraft represents an average of 1 additional person per flight.

Consequently, the larger, more appealing airplane would have to attract an average of 1 more passenger per flight or fares would have to increase about 8% in order to maintain the same net margin of total trip yield over costs. For example, the 2-abreast airplane at 63% load factor (12 passengers) yields $324 per 100 nm flight at 27¢ per seat-nm fare. The margin over cost is $324-$208.87 = $115.13. The 3-abreast airplane at 68.4% load factor (13 passengers) yields $351 on the same flight. The margin is $114.83, which is very close to the 2-breast airplane margin. Alternatively, the 3-abreast airplane with 12 passengers and an 8.43% higher fare provides a margin of $351.30-$236.17 = $115.13.

5.5.1.3 Passenger Seating Capacity

Figure 25 and Table 10 show the large improvement in seat-mile DOC's that result from an increase in design seating capacity. Table 12 summarizes these results for Baselines 3 and 4 on the average 185 km (100 nm) stage length. These baselines were chosen for the comparison because they share the 3-abreast cabin design.

The larger airplane costs 33% more to operate on the 185 km (100 nm) stage, but because of its higher seating capacity its seat-mile DOC's are 16% lower. Similarly, mission fuel is 29% higher, but seat-mile fuel efficiency is 18% better.

5.5.2 Technology Sensitivities

Technology sensitivity studies were conducted in order to indicate the appropriate emphasis to give to each of the candidate advanced technologies. Figures 29 through 32 show the sensitivities of DOC and fuel consumption to four basic design parameters (drag, takeoff $C_{L\,MAX}$, weight, and SFC) that relate to the candidate technologies. The resizing effects on takeoff weight, engine power, and wing area are also presented in these Figures for added trend information. Each trend line is based on four points, and each point represents a resized and reoptimized airplane using factored technology levels in the sizing/optimization process. The sensitivities presented were generated for Baseline 1 on a 185 km (100 nm) stage length. A cross-check of several sensitivities using the other baselines showed very similar results.

Table 11. DOC and Fuel Effect of a More Comfortable Cabin

185 km (100 nm) STAGE LENGTH

CONFIGURATION	DOC				BLOCK FUEL			
	$/km	($/nm)	¢/skm	(¢/snm)	kg	(lb)	kg/skm	(lb/snm)
BASELINE 1 19 PASSENGER 2-ABREAST	1.13	(2.09)	5.94	(10.993)	249	(550)	.071	(.291)
BASELINE 3 19 PASSENGER 3-ABREAST	1.28	(2.36)	6.72	(12.430)	281	(620)	.080	(.327)
Δ	+13%	+13%	+13%	+13%	+12%	+12%	+12%	+12%

Table 12. DOC and Fuel Effect of Increased Seating Capacity

185 km (100 nm) STAGE LENGTH

CONFIGURATION	DOC				BLOCK FUEL			
	$/km	($/nm)	¢/skm	(¢/snm)	kg	(lb)	kg/skm	(lb/snm)
BASELINE 3 19 PASSENGER 3-ABREAST	1.28	(2.36)	6.72	(12.430)	281	(620)	.080	(.327)
BASELINE 4 30 PASSENGER 3-ABREAST	1.70	(3.14)	5.66	(10.476)	363	(800)	.065	(.267)
Δ	+33%	+33%	-16%	-16%	+29%	+29%	-18%	-18%

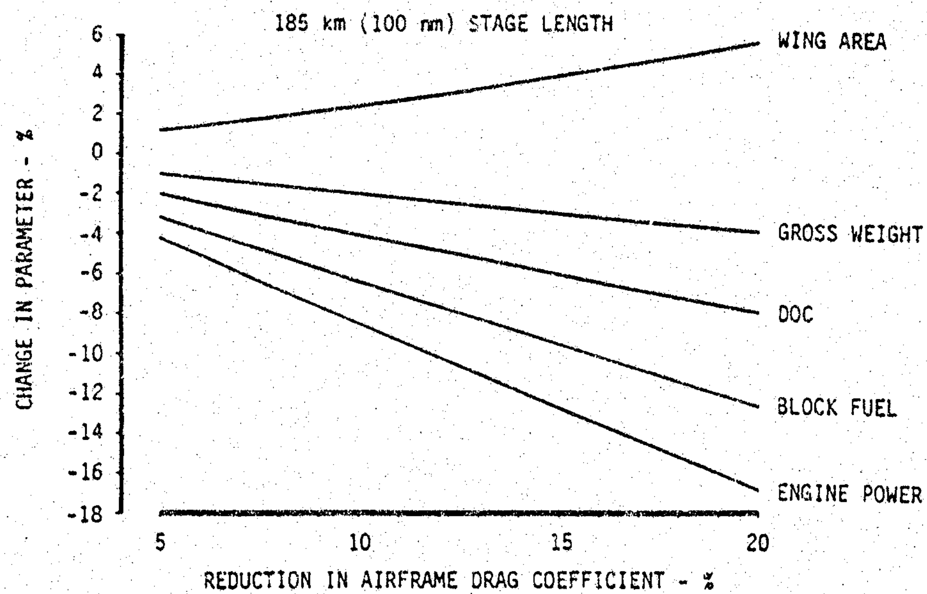

Figure 29. Design Sensitivities to Reductions in Cruise Drag

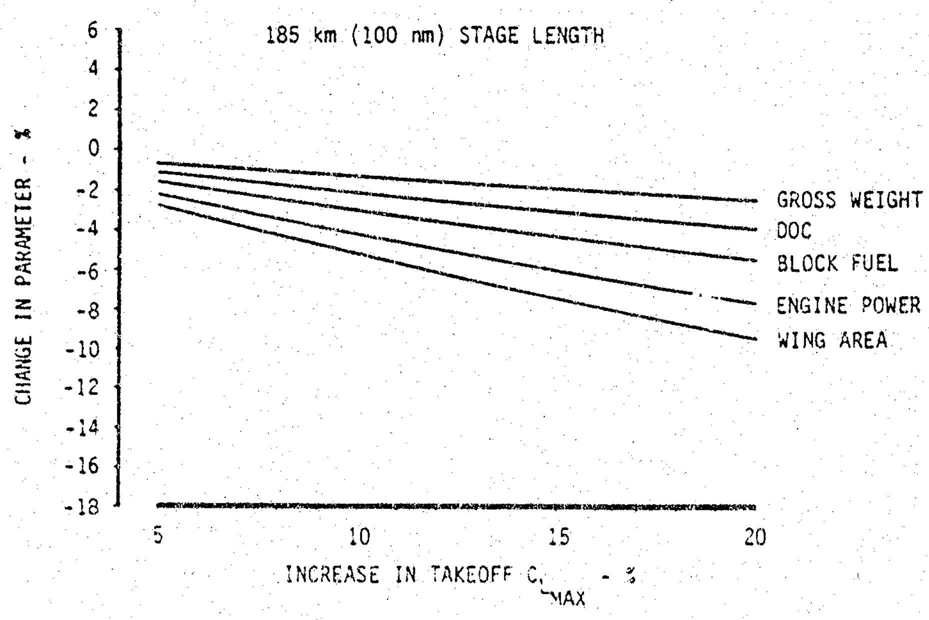

Figure 30. Design Sensitivities to Increase in Takeoff L/D

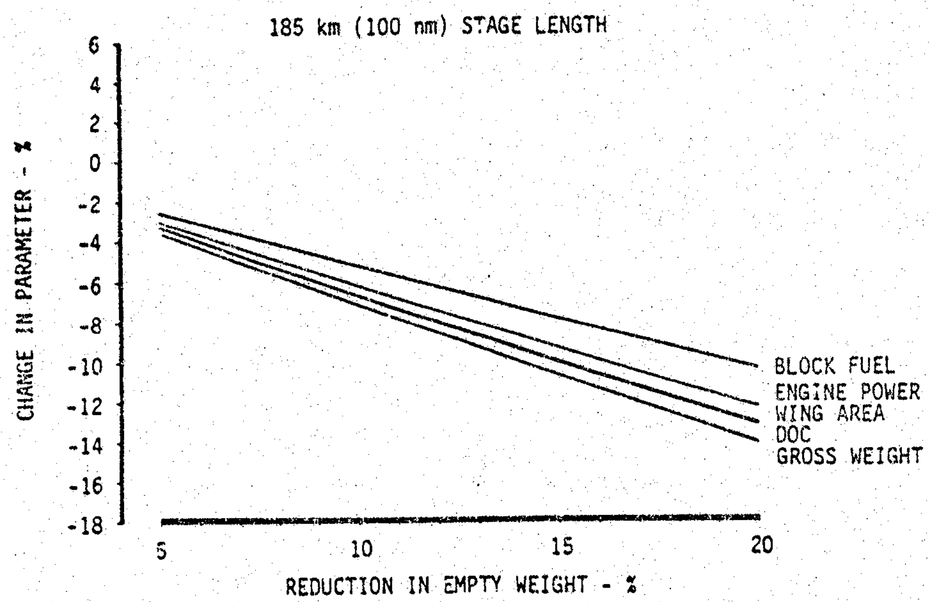

Figure 31. Design Sensitivities to Reductions in Empty Weight

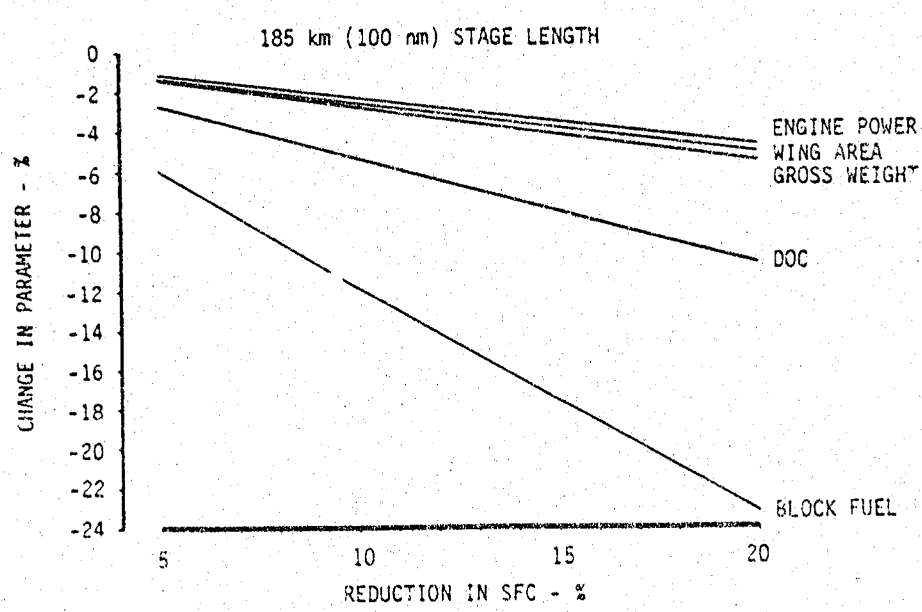

Figure 32. Design Sensitivities to Reductions in Engine SFC

ORIGINAL PAGE IS
OF POOR QUALITY

Figure 29 shows an interesting sizing effect. As the airframe drag coefficient is reduced, the airplane re-optimizes with relatively more wing and less engine. This result would be expected, because with a lower drag coefficient the drag penalty of additional wetted area is lower, and the optimum shifts toward more wing and less engine.

Figure 33 provides the sensitivity of DOC to aircraft price. The effect is quite small, with a 10% increase in airplane price causing a DOC increase of less than 2%. This result encourages the pursuit of seemingly expensive technologies in Section 6.0.

Given equal improvements in all parameters, DOC is shown in Figure 34 to be most sensitive to empty weight, followed in order by SFC, airframe drag, takeoff $C_{L\ MAX}$, and aircraft price. Figure 35 shows fuel consumption to be most sensitive to engine SFC, followed by airframe drag, empty weight, and takeoff $C_{L\ MAX}$.

The overall design emphasis in this study is on minimum DOC. Therefore, as a result of these sensitivity studies, the advanced structural and propulsion technology applications chosen in Section 6.0 are more aggressive than the selected aerodynamic technologies.

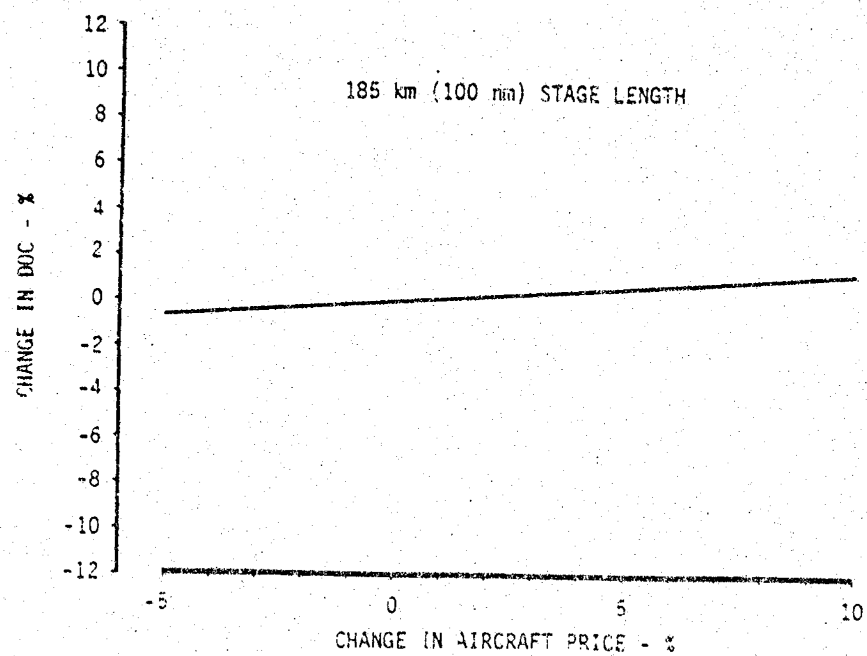

Figure 33. Design Sensitivity to Changes in Aircraft Price

ORIGINAL PAGE IS
OF POOR QUALITY

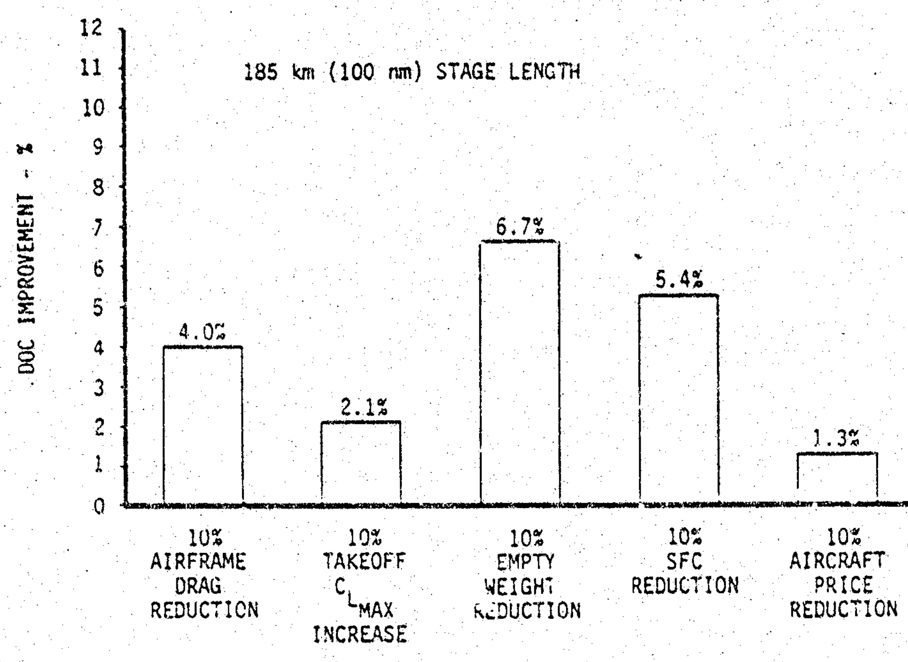

Figure 34. Summary of DOC Sensitivities

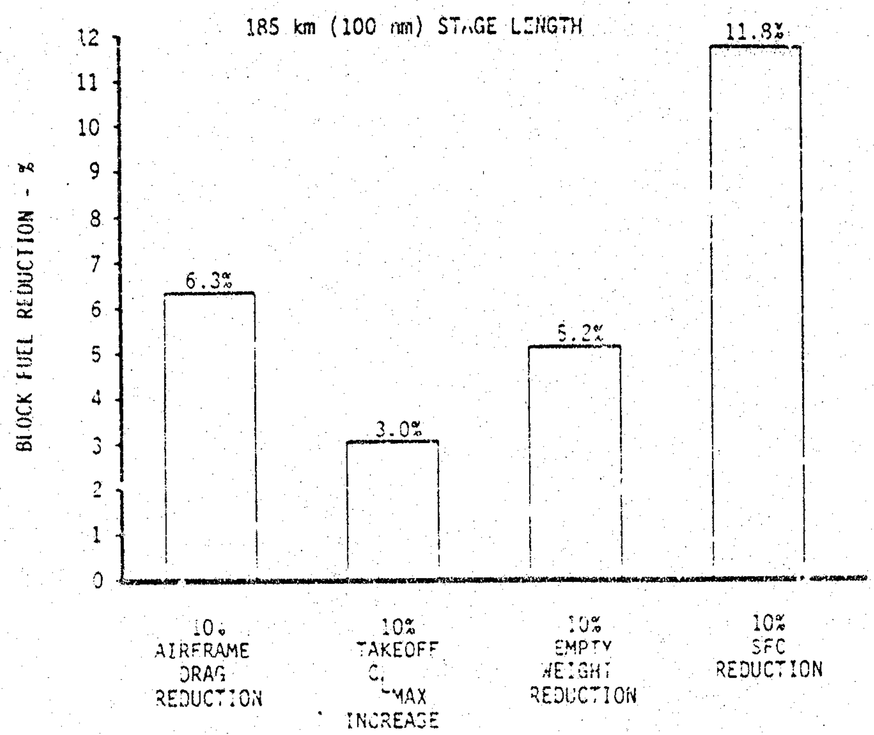

Figure 35. Summary of Block Fuel Sensitivities

6.0 ADVANCED TECHNOLOGY ASSESSMENT

Beginning as early as 1969, the CAB, DOT and FAA recognized that the commuter airline industry would require specific technology improvements directed towards improving commuter aircraft (Reference 15). With this goal in mind various investigations by NASA and industry were initiated to improve the technology base available to the commuter industry. In this section, promising advanced technologies for turboprop commuter aircraft are examined, and an assessment is made of their potential for improving the efficiencies and operating costs of the baseline aircraft. The selected technologies fall into four groups:

- Advanced Airfoils and High Lift Systems
- Advanced Propulsion Systems
- Advanced Materials and Structures
- Ride Quality Improvements

Technology improvements are often introduced in gradual stages. Recognizing this, two levels of advanced technology are examined in each of the four technology groups. Selected technologies which are sufficiently developed and proven to allow immediate incorporation on turboprop commuter aircraft are identified as Level 1 technologies. Level 2 technologies are those which require additional development effort before successful application in production is feasible. In this study, Level 1 is relatively low-risk technology appropriate for the pre-1990 time period, whereas the moderate-to-high-risk Level 2 technology is identified for the post-1990 time period.

6.1 Advanced Airfoils and High Lift Systems

Improved airfoils and high lift systems provide the potential for increased aircraft efficiency and performance. Currently a wide range of airfoil data and design techniques are available for two-dimensional applications. Recent advances in aerodynamic computational methods have allowed designers to produce two-dimensional single and multi-element airfoil sections which satisfy specific design requirements. For three dimensional high C_L conditions, however, computational design methods and test data are scarce. Typically, empirical techniques must be employed to complete the design. In this study, the baseline aircraft lift system consists of NACA airfoil sections (230XX series) and a partial span, single-slotted flap system. Advanced technology airfoils and trailing edge flap systems are examined for their potential benefit to the baseline aircraft.

6.1.1 Airfoils

Airfoil design techniques are available which allow specific tailoring of airfoils to a given set of design requirements. These may include aerodynamic specifications such as drag, pitching moment, and lift, as well as geometric requirements like maximum thickness and thickness distribution required for structural and fuel volume considerations. The techniques can allow either partial contour modification (Reference 16) or complete section design (Reference 17). Figure 36 shows the contour and pressure distribution for the JCN-15 tailored airfoil. This section was designed to obtain the NASA LS series level of drag with the NACA 4-digit series level of pitching moment as shown in Figure 37. Work at Cessna has shown that tailored airfoils can provide improvements of 6 to 9% in two-dimensional drag levels and 10 to 15% in takeoff and climb L/D's, while still satisfying other design constraints such as fuel volume and handling qualities requirements. For normal twin-engine aircraft configurations, the adverse effects of propwash, and wing-body and wing-nacelle interference reduce these two-dimensional improvements to approximately 3% in drag and L/D.

Further improvement in airfoil drag is possible by designing for natural laminar flow (NLF). A reduction of up to 50% in section drag coefficient could be achieved (Reference 18), provided the practical problems of leading edge contamination and interference flow-tripping can be overcome. Again for normal aircraft configurations, propwash and interference effects may limit the portion of the wing that can actually achieve the full benefits of significant laminar flow, so that a 5% improvement in overall airplane drag and L/D was estimated for NLF. However, since commuter aircraft operate predominantly at low altitudes, where leading edge contamination due to insects is likely, improvements due to natural laminar flow were not included in this study. It should be noted, however, that by using properly faired, liquid wing de-icing systems, and by cleaning the wing leading edge between flights, extensive laminar flow could be achieved in commuter operations.

6.1.2 High Lift Systems

For a given takeoff and landing field requirement, high lift devices offer the potential of reducing wing area, thus improving aircraft weight and fuel efficiency. On the other hand, increasing takeoff $C_{L\,MAX}$ by using high lift systems results in reduced takeoff speeds and distances. Equally important, high lift systems can improve takeoff climb L/D, which increases takeoff climb gradient. For landing, an increased $C_{L\,MAX}$ results in lower approach speeds and shorter landing distances. In practice, the design values of $C_{L\,MAX}$ and climb L/D, for both takeoff and landing, must be balanced to satisfy both field length and climb (second segment or balked landing) requirements before the design can be resized to take full advantage of the benefits of advanced high lift systems. As noted in Section 5.4.1.3, these designs were constrained by takeoff field length, but not approach speed. Therefore, the advanced flap analyses concentrated on improving maximum takeoff lift coefficient, rather than the landing lift coefficient.

Computational methods similar to those described in Section 6.1.1 are available for high lift systems. These techniques allow the designer to tailor the high lift system for specific design requirements up to a point. To complete the design of an improved lift system, especially in the area of $C_{L\,MAX}$, these computational methods must then be combined with empirical techniques and wind tunnel test methods. Some of these methods can be found in References 19, 20, 21 and 22. Starting with the baseline trailing edge flap system, techniques such as these methods, combined with careful design

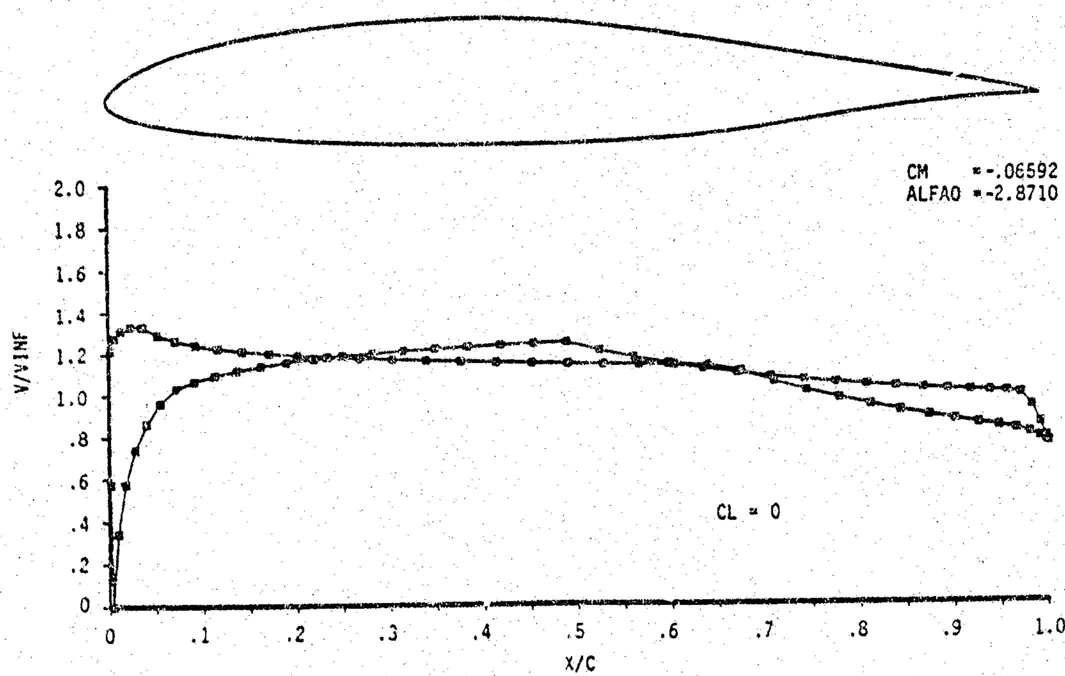

Figure 36. Theoretical Shape and Pressure Distribution for the JCN-15 Airfoil

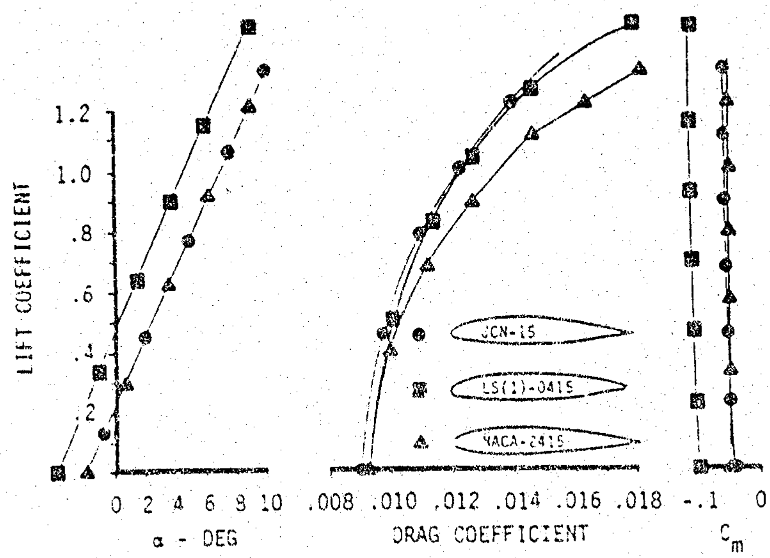

Figure 37. Performance Comparison of Three 15% Thick Airfoils

of gaps and overhang schedules, can provide up to 15% higher $C_{L\ MAX}$ and 3 to 4% higher L/D's. Further, $C_{L\ MAX}$ can be improved another 15 to 20% by using nearly full span flaps. This increase in flap span adds the extra requirement of an alternative roll control system such as drooped ailerons, spoilers, or flaperons. These devices can provide some additional benefit, since a combination of spoiler roll control and drooped ailerons can increase takeoff and climb L/D another 1% due to improved span loading.

6.1.3 Advanced Aerodynamics Applications

The baseline lift system is the NACA 230XX series airfoil with a partial span, single-slotted flap system. The pre-1990 Level 1 technology combines an advanced airfoil section with an improved partial span, double-slotted Fowler-type flap. The Level 1 technology characteristics are shown in Figure 38. The baseline flap $C_{L\ MAX}$ is shown for reference. The overall effects of this improved lift system for Level 1 are:

- 3% Lower Cruise Drag
- 3% Higher Takeoff and Climb L/D
- 15% Higher $C_{L\ MAX}$ at Takeoff
- 50% Higher Flap System Cost/lb
- 60% Higher Flap System Weight/ft^2

The higher flap system weight and cost factors are due to an increase in complexity for the advanced flap.

Level 2 represents an extension of the two-dimensional improvements of Level 1 to three dimensions. The selected Level 2 technology uses the Level 1 advanced airfoil/flap cross section on a nearly full span flap system with drooped ailerons and spoiler roll control augmentation. The Level 2 technology characteristics are given in Figure 39. Relative to the baseline, the overall effects for Level 2 are:

- 3% Lower Cruise Drag
- 4% Higher Takeoff and Climb L/D
- 35% Higher $C_{L\ MAX}$ at Takeoff
- 50% Higher Flap System Cost/lb
- 60% Higher Flap System Weight/ft^2

In Level 2 the flap system design remains the same as in Level 1, except the span is increased. Therefore, there are no changes in the weight & cost complexity factors. Figure 40 shows Baseline 3 configured with the Level 2 high lift system. A low speed drag comparison is shown in Figure 41. Note that the improvements shown in L/D due to Level 1 and Level 2 technologies are amplified by allowing the advanced aircraft to reoptimize weight, wing area, and aspect ratio. Figure 42 shows a comparison of the STAT flap technology levels to other commuter type aircraft.

ORIGINAL PAGE IS
OF POOR QUALITY

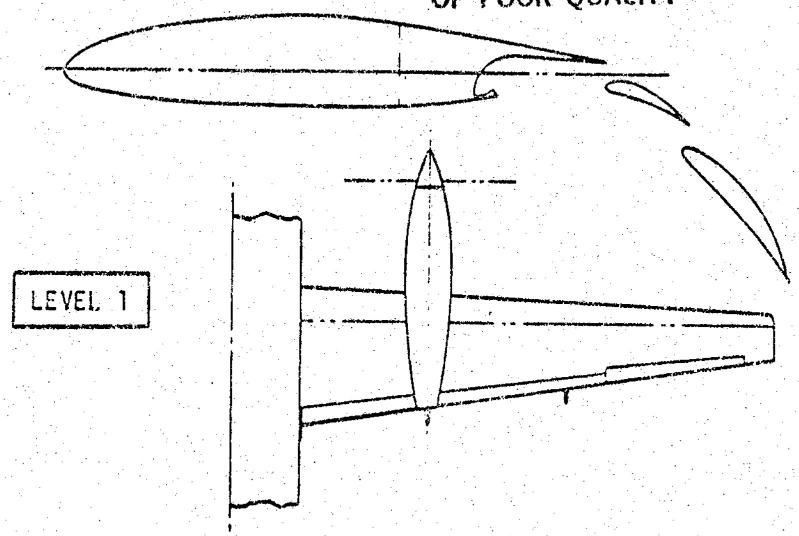

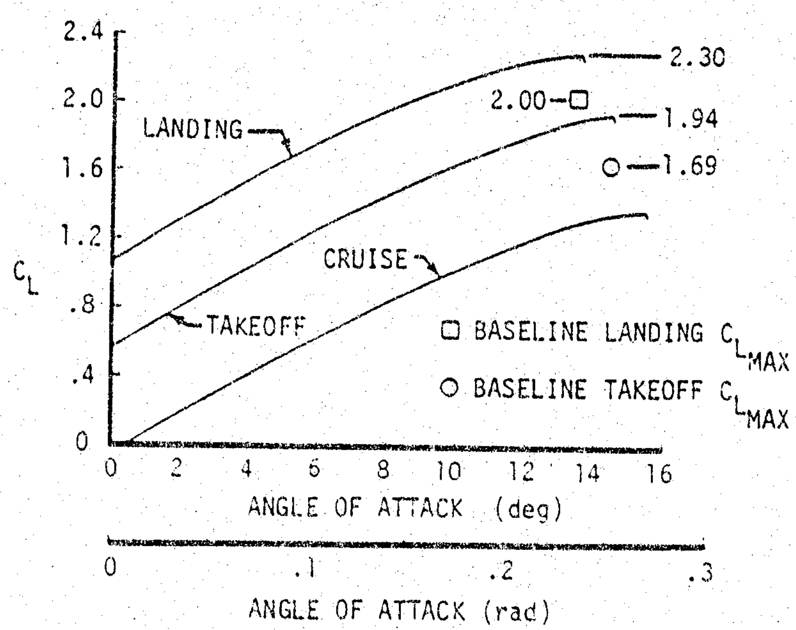

Figure 38. Geometry and 3-D Lift Characteristics for Level 1 Advanced Flaps

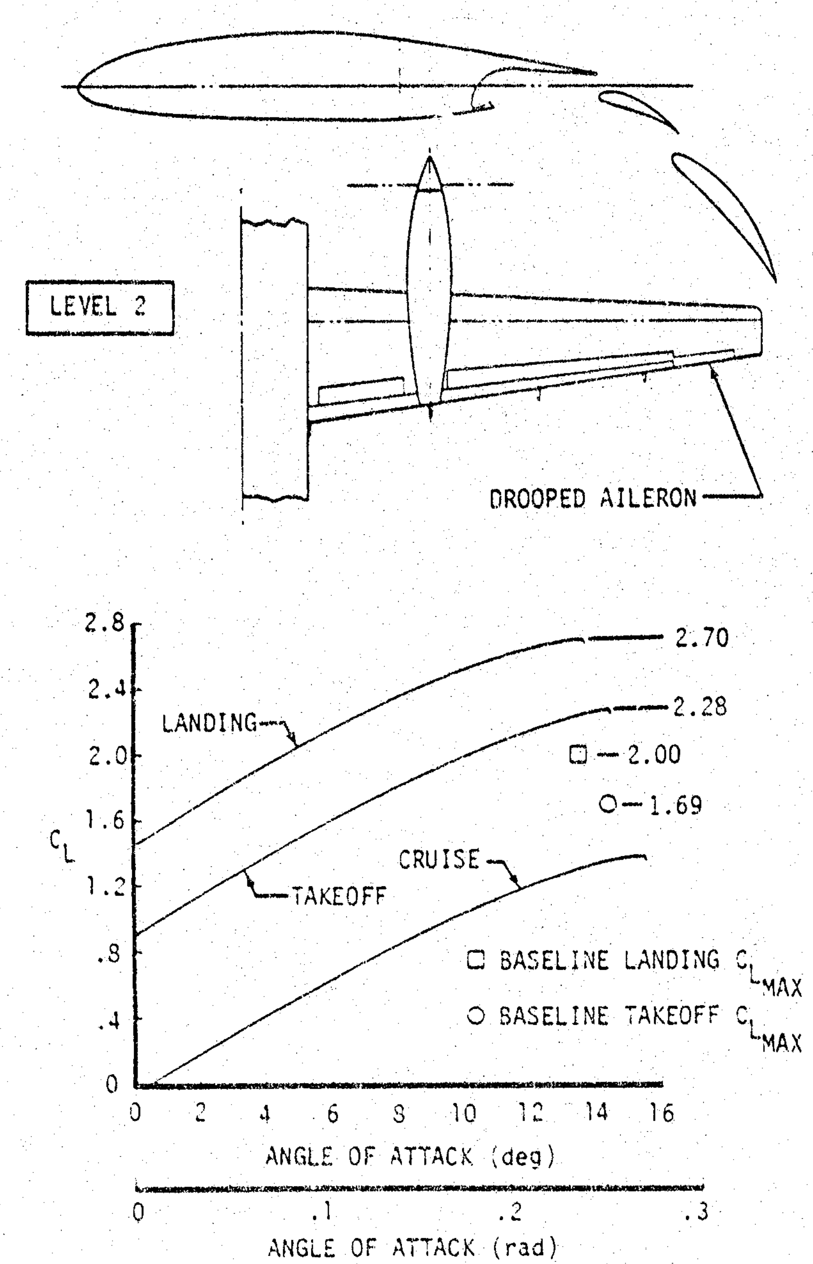

Figure 39. Geometry and 3-D Lift Characteristics for Level 2 Advanced Flap

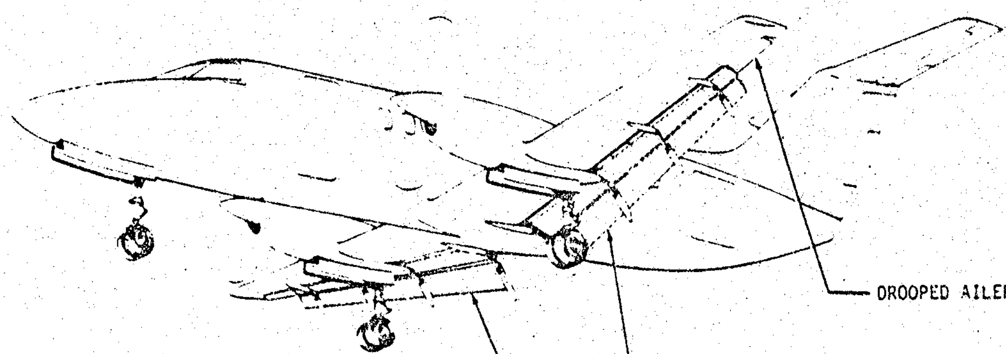

Figure 40. Advanced Flaps Deployed for Landing

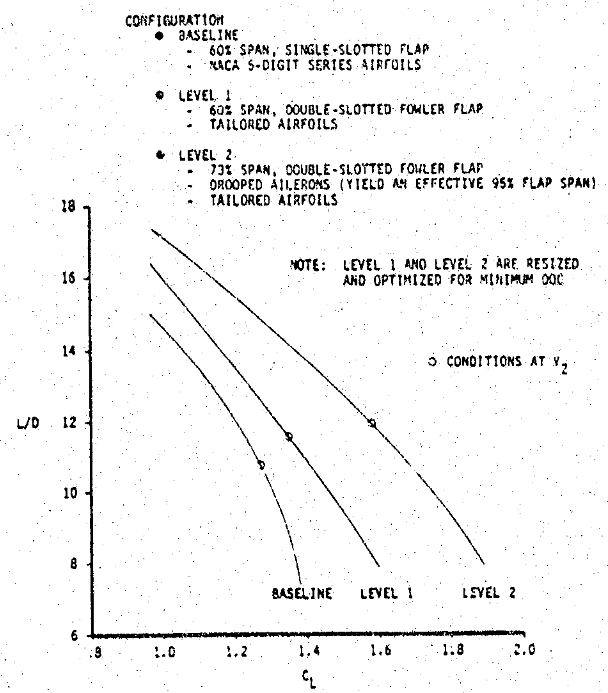

Figure 41. Second-Segment Climb L/D Comparison

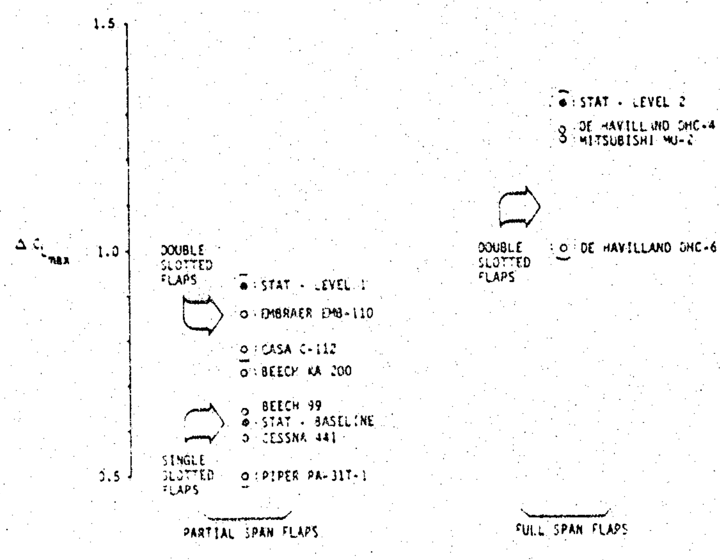

Figure 42. Landing Flap $\Delta C_{L\ Max}$ for Typical High Lift Systems

6.2 Advanced Propulsion

Improvements in engine and propeller efficiency directly affect aircraft fuel efficiency. In this study the effect of technology improvements on powerplants and propellers were examined separately. These effects were then combined and applied as Level 1 and Level 2 propulsion system improvements.

6.2.1 Turboprop Engines

The engine cycles for the baseline aircraft were based on the Pratt & Whitney PT6A-65 engine. This cycle was scaled to meet the power requirements of each baseline airplane. The top region of Figure 43 shows the variation of SFC with engine size for current technology turboprop engines, including the PT6A-65. This SFC scale effect was included in sizing the baseline aircraft. The significant benefit of scale results from better internal efficiencies, higher pressure ratios, and higher turbine inlet temperatures as engine size increases. Current technology commuter turboprop engines are characterized by overall pressure ratios of 8-10 and turbine inlet temperatures of 1700-1800°F. Significant SFC improvements can result from increases in pressure ratio and turbine inlet temperature. Additional gains can be made by means of more efficient cooling, higher work stages, closer clearances, variable geometry, and higher strength/lighter weight materials.

6.2.2 Advanced Engine Applications

Two advanced levels of engine technology are also indicated in Figure 43. Level 1 is appropriate for pre-1990 technology and represents a 12% overall SFC improvement. For engines now in development, this is achieved by increasing the overall pressure ratio to 14-17 and the maximum turbine inlet temperature to approximately 2200°F. To permit the higher turbine inlet temperatures, cooled inlet vanes and cooled turbine blades are used. Even though there are already two engines in the Level 1 band of Figure 43, neither currently match the 1000 shp or 1900 shp levels required by the 19 and 30 passenger baselines in this study. However, engines in the required sizes are attainable for production prior to 1990. The cost of Level 1 engines, based on $/hp for the two engines already in the Level 1 band, is assumed to be 7% higher than baseline engine cost.

Studies for the application of advanced technology to current turboprop propulsion systems were conducted under NASA-Lewis sponsership by Detroit Diesel Allison, Garrett AiResearch, and General Electric (Reference 23, 24, and 25). Their predicted levels of SFC using post-1990 technology are shown as Level 2 in Figure 43. Level 2 represents a 20% improvement in overall SFC, relative to current technology engines. For Level 2, overall pressure ratios increase to 17-20 by using higher work stages with high stage efficiencies. Monocrystal turbine blades with impingement or film cooling allow turbine inlet temperaures as high as 2400°F. Variable geometry guide vanes and reduced gas leakage are also a part of Level 2 engine technology. The cost of Level 2 technology engines, in terms of $/hp, is assumed to be 13% higher than for the baseline engines.

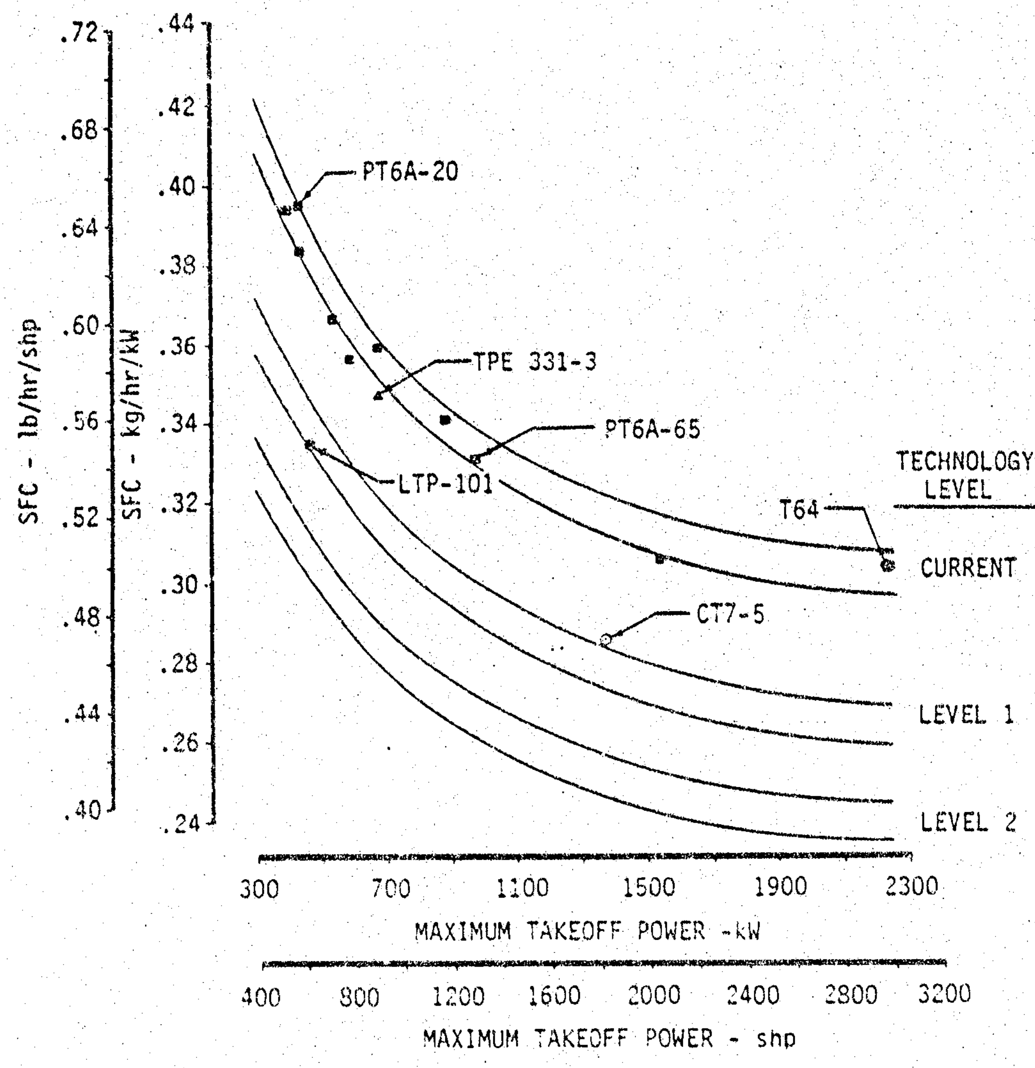

Figure 43. Effect of Engine Size on SFC

An advanced engine installation is shown in Figure 44. This installation provides for straight-through airflow with the exhaust exiting over the wing. The engine drives the forward-mounted gearbox through a long shaft, which permits a long inlet duct for good inlet pressure recovery. The high engine and gearbox location provides the ground clearance required for large, slow turning propellers. The nacelle lower contours were faired to include space for the dual-wheel main gear. This engine/nacelle/gear arrangement was used for all advanced technology aircraft in this study.

6.2.3 Propeller Technology

The baseline propellers are conventional-section, all-aluminum blade designs similar to those used on current Cessna turboprops. Propeller technology studies, such as Reference 26, have identified several approaches for improving efficiency and weight. These include advanced technology airfoils, optimized three-dimensional design, and composite blade construction.

Advanced airfoil sections can be specifically tailored for the flow conditions along the blade. Higher section L/D values can be achieved with these tailored airfoils especially at the shank, allowing a $\frac{1}{2}$ - $1\frac{1}{2}$% improvement in overall efficiency.

Three-dimensional optimization of propeller design includes both improved hub-blade intersection design and the use of more blades with lower blade activity factors. Current propeller blades have round shanks that pass through holes in the hub spinner. A loss of 5% in propeller efficiency is attributed to the round shank shape and shank-spinner interference. Fairing the blade airfoil shape into the hub requires some compromise in order to permit blade rotation, but efficiency could be improved up to 3% by careful design.

Figure 45 shows that peak ideal efficiency increases as the number of blades increases. The three curves represent three values of disk loading and the upper limit of each curve is indicated. Ideal efficiency includes vortex losses, but does not include hub or blade profile drag losses. Any propeller has a peak efficiency point, depending on speed-power coefficient and blade angle. The peak ideal efficiency for a group of propellers with different numbers of blades can then be plotted and lines drawn as in Figure 45. Note that the greatest efficiency improvement occurs as blade count increases from 2 to 7. To obtain the efficiency improvement indicated in Figure 45, it is necessary to optimize the blade design every time a blade is added, using tailored airfoil sections and shorter chord blades to maintain a constant disk activity factor.

The thinner blades required for higher efficiencies present a structural problem with standard aluminum construction. This can be solved using composite materials. Composites allow the construction of blades with activity factors as low as 60, and permit the use of advanced airfoils and optimized blade shapes. Damage tolerance is improved with composites and repairs are straightforward. The agressive use of composites can also reduce propeller weight up to 30% for standard blade shapes (Reference 26).

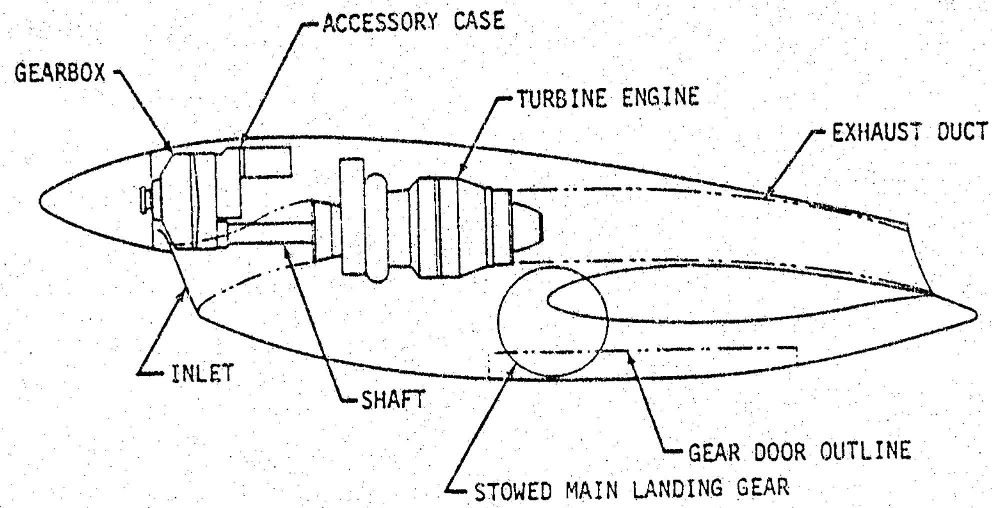

Figure 44. Advanced Technology Engine Installation

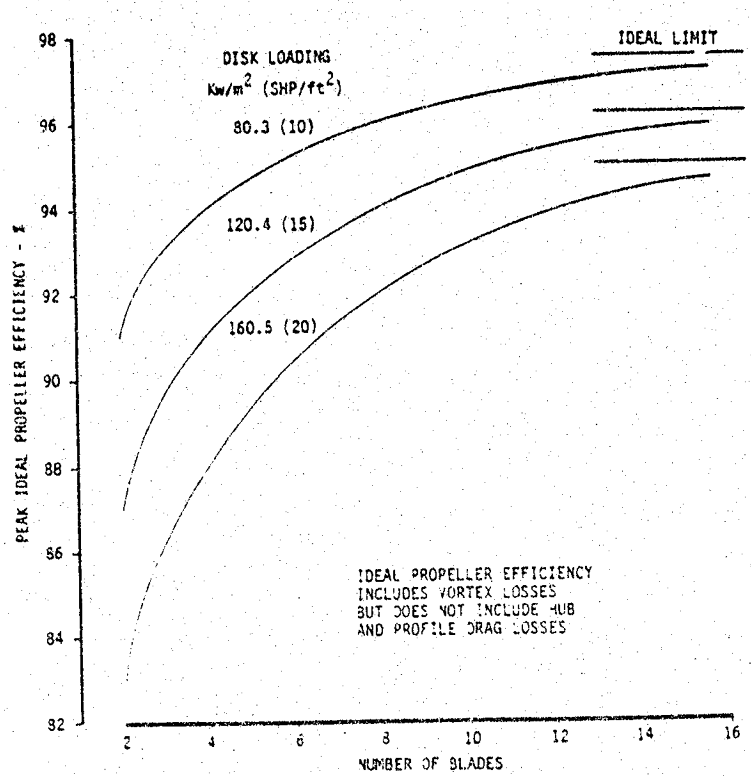

Figure 45. Effect of Number of Blades on Ideal Propeller Efficiency

The maximum improvement in blade weight is reduced as advanced airfoils and three-dimensional design optimization techniques are applied. The assumed tradeoff of maximum weight improvement vs. level of aerodynamic efficiency improvement is shown in Figure 46.

6.2.4 Advanced Propeller Applications

The two advanced levels of propeller technology are presented in Figure 47. Level 1 represents a 2½% propeller efficiency improvement. This is achieved by means of advanced airfoils and faired shanks. Conservative use of composite materials provides a 10% weight reduction which is less than the maximum weight reduction potential indicated in Figure 46.

Level 2 propeller technology provides a 5% efficiency improvement, relative to the baseline. In addition to advanced airfoils and faired shanks, Level 2 propellers include an increased number of blades, optimized shank-spinner intersections, and advanced composite construction.

The propeller blade structural arrangement for Level 2 incorporates an aluminum alloy shank which attaches to the hub in a conventional manner and extends outward almost to the tip. The skin is a fiberglas and Kevlar/epoxy shell, covered with a restorable plastic erosion coating, and supported by a low density core. The leading edge is protected by a deice boot near the hub and by a metal sheath near the tip. This structural approach, in combination with the design for a 5% aerodynamic efficiency improvement, provides a 15% propeller weight reduction (see Figure 46).

For round shank propellers, the maximum number of blades that can be mechanically accommodated at the hub is eight. With faired shanks, a practical compromise of seven blades was chosen for Level 2. Figure 48 shows the advanced seven blade propeller configuration.

6.2.5 Summary Of Advanced Propulsion Applications

The characteristics of the selected propulsion system technologies, relative to the baseline, are summarized as follows:

<u>Level 1</u>

- Powerplant
  - 12% Lower Engine SFC
  - 8% Lower Engine Weight/hp
  - 7% Higher Engine Cost/hp
- Propeller
  - 2.5% Higher Propeller Efficiency
  - 10% Lower Propeller Weight/hp
  - Same Propeller Cost/hp

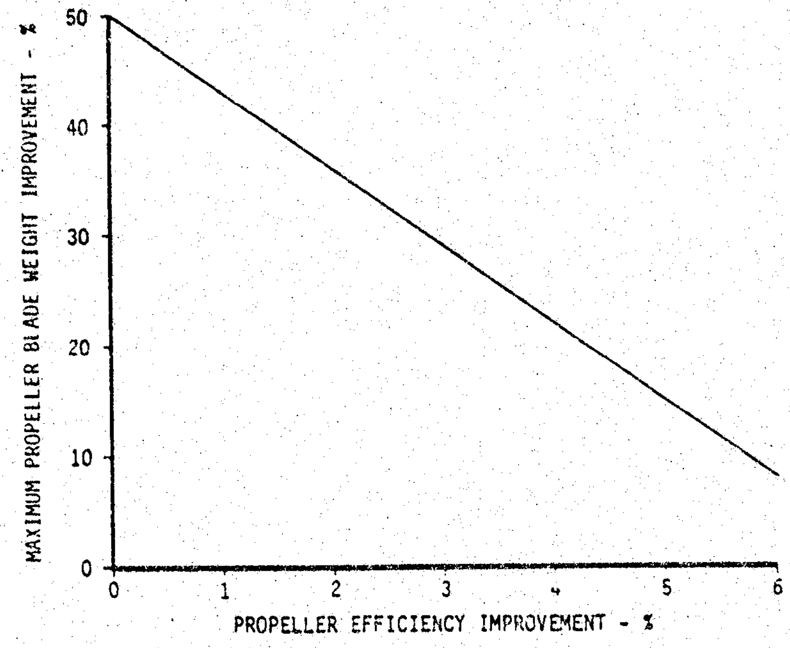

Figure 46. Tradeoff Between Aerodynamic Efficiency Improvement and Maximum Propeller Weight Reduction

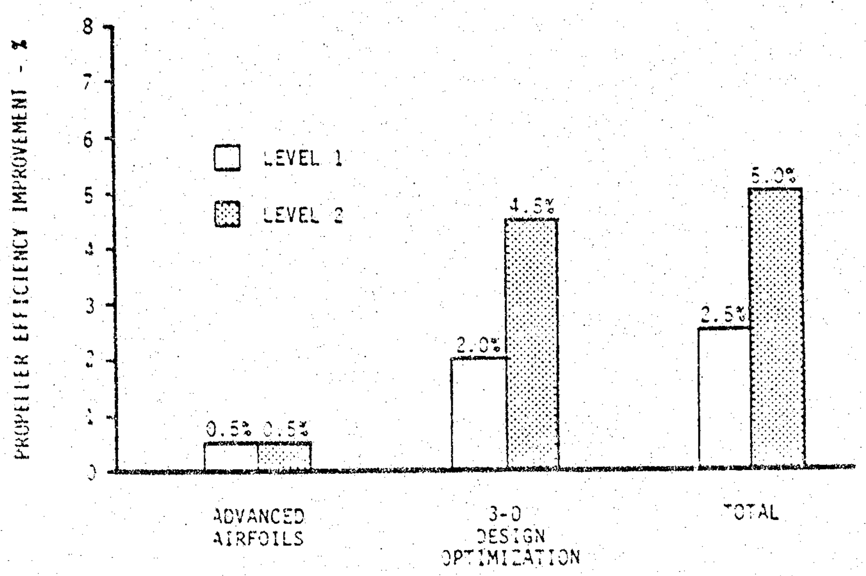

Figure 47. Effect of Advanced Propeller Technologies on Efficiency

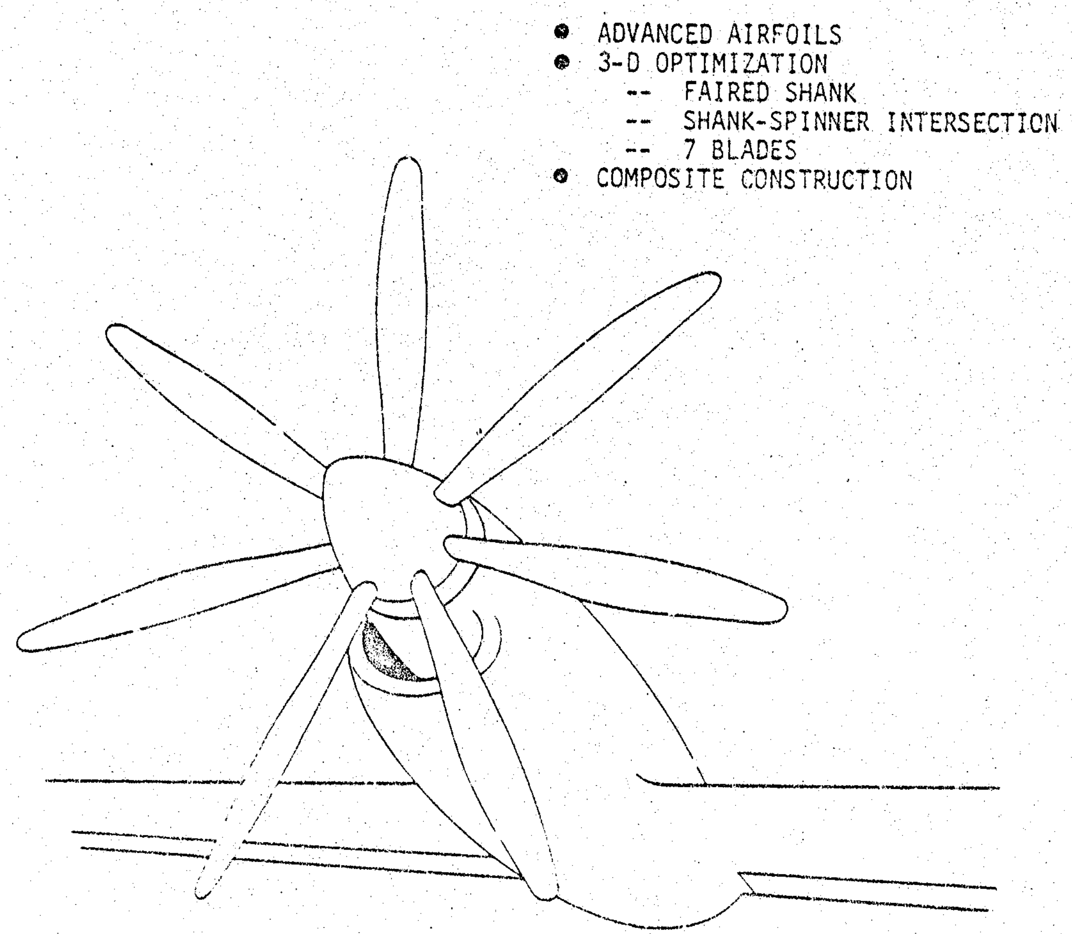

Figure 48. Advanced Seven Blade Propeller Configuration

Level 2

- Powerplant
  - 20% Lower Engine SFC
  - 10% Lower Engine Weight/hp
  - 13% Higher Engine Cost/hp

- Propeller
  - 5% Higher Propeller Efficiency
  - 15% Lower Propeller Weight/hp
  - Same Propeller Cost/hp

6.3 Advanced Materials and Structures

Both bonded metal and composite structural concepts are examined in this study. None of the 19 or 30 passenger commuter airplane in current service makes significant use of either of these structural approaches.

The use of metal-bonded assemblies normally requires fewer parts and results in more stiffness and fatigue resistance without added weight. Bonded construction also provides a smooth surface which can be held closely to desired contours for improved appearance and aerodynamic performance. Operational requirements for turboprop commuter aircraft dictate numerous short stage lengths, resulting in many more takeoffs and landing per year than the typical airplane. The application of bonded construction, with its reduced susceptibility to fatigue, is a logical method for achieving long service life under these rigorous operating conditions.

Applications of advanced composite structure in large commercial transports have been studied extensively. This structural concept has potential for significant weight savings, although predicted cost is usually higher than for conventional aluminum structure. The size and performance of the study aircraft are such that material gauges are thin, and the weight saving percentage will be somewhat less than for large jet transports. The items examined in this study include composite materials for primary and secondary structure, including the wing, nacelles, wing flaps, and empennage assemblies.

6.3.1 Bonded Metal

Cessna has accumulated extensive experience with bonded metal structure and has developed a large bonding production facility, including cleaning tanks, layup rooms, autoclaves, and nondestructive test equipment. Over 10,000 bonded assemblies have been produced each month in this facility. Strong and reliable bonded joints are consistently achieved. Cessna first used bonded metal on primary structure in the early 1970's with the production of bonded Citation wing spars. Extensive bonding was introduced in the wing panels of the Cessna 400-series twin-engine airplanes in 1975.

The parts in a typical bonded assembly are shown in Figure 49. These parts are bonded in a single autoclave cycle. When the parts are assembled, the skin panel has a "waffle" appearance due to the doubler cutouts. The waffle doubler provides a transition in stiffness from skin to stringer or frame. This aids in preventing stress concentration areas when fatigue cracks might start. Since load transfer from one structural member to the next takes place over a wider area than for conventional riveted construction, the working stresses are lower, resulting in fewer fatigue related problems. This structural design results in a weight and cost-effective method for achieving long service life.

Figure 50 shows the bonded waffle doubler concept as applied to a short-haul aircraft fuselage barrel. This advanced technology structure is currently used on the Citation III business jet. On a pressurized fuselage this metal-bonded structure has the additional benefit of minimizing the sealant required to prevent air leakage.

Another metal-bonding concept, useful for control surfaces, combines full depth aluminum honeycomb and minimum gage aluminum skins. As shown in Figure 51, this structure requires only two closure ribs, compared to fourteen trailing edge ribs and rib segments on a production aileron and tab using riveted construction. Another application of honeycomb is for stiffening of selected wing, fuselage, and empennage skin panels.

6.3.2 Composite Materials

As part of its composites R&D work, Cessna is conducting an ongoing design allowables test program on a variety of composite materials and configurations (Reference 27). The design allowables are calculated by subtracting three standard deviations from the mean of test results obtained from unaged specimens at room temperature. These numbers are then further reduced for the effects of heat and humidity (material water soaked at 160°F) and fatigue damage (10^5 cycles at 50 percent of static strength). Typical dry material test results are shown in Figure 52. Even with conservative design allowables, composite structure provides significantly greater weight savings than bonded metal. Its cost, however, is higher than for conventional aluminum structure. Weight and cost characteristics are discussed further in Sections 6.3.3 and 6.3.4.

Four examples of composite assemblies considered for the study aircraft are the wings, wing flaps, engine nacelles, and seats. The composite wing concept includes a combination of graphite-epoxy, Kevlar-epoxy and honeycomb core construction. This concept is shown in Figure 53. Large subassemblies and the use of bonding to join these subassemblies minimizes the need for joints and fasteners. This concept helps to reduce the number of parts, an aid in minimizing cost, and allows skin panels to be worked to higher stress levels and still meet the required fatigue life.

The leading edge and interspar skin panels have an inner and outer skin bonded to a honeycomb core. The outer skins are Kevlar-epoxy which exhibits high impact and abrasion resistance. Kevlar is not as good as graphite in compression, but when stabilized by the core and used in conjunction with a

ORIGINAL PAGE IS OF POOR QUALITY

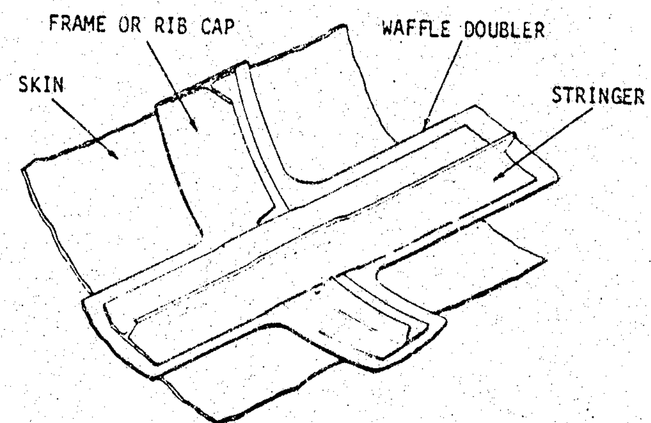

Figure 49. Typical Bonded Waffle Doubler Assembly

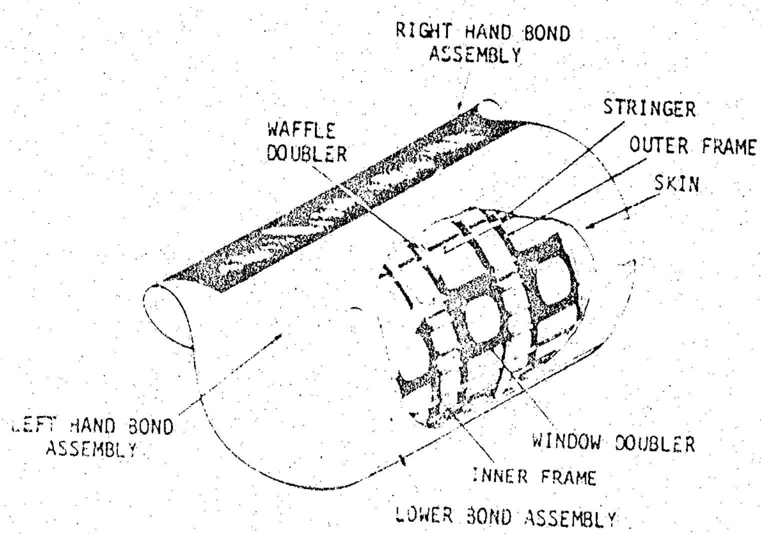

Figure 50. Bonded Fuselage Assembly

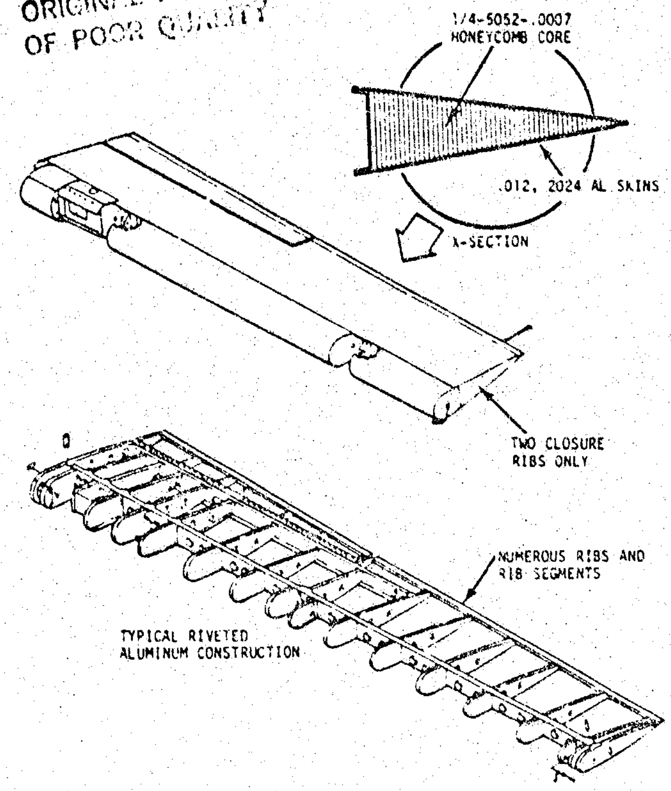

Figure 51. Metal-Bonded Aileron Compared with Riveted Structure

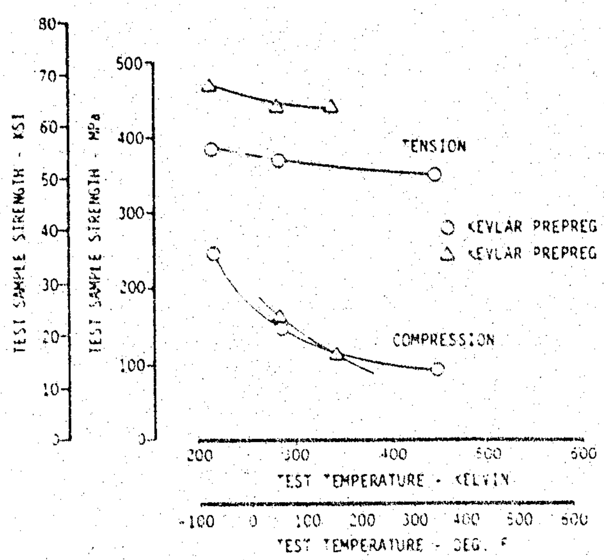

Figure 52. Effect of Temperature on Typical Kevlar-Epoxy Composite Materials

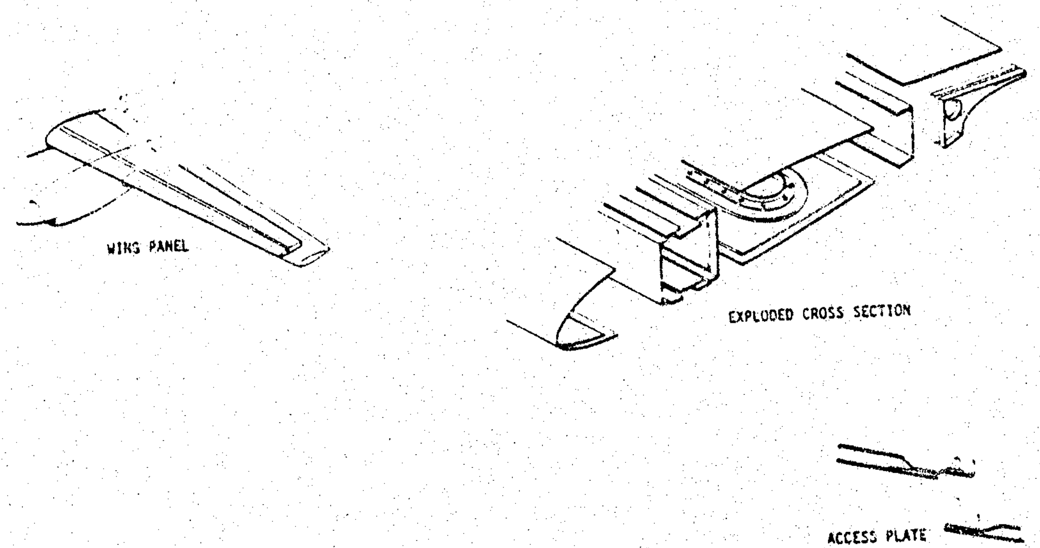

Figure 53. Composite Wing Structure

graphite inner skin an efficient structure results. An outside layer of aluminized E-glass, such as Thorstrand, provides lightning strike protection and good paint adhesion. The core material is aluminum or Nomex, as appropriate. The lower skin incorporates access openings for inspection of structure and fuel tanks. The external contour on the leading edge is indented to permit flush installation of deice boots.

The wing spars are graphite-epoxy. The required cap material strength is achieved through layers of unidirectional graphite. The spars taper spanwise to match the airfoil contours and load requirements.

The number of ribs is significantly reduced from the quantity normally required for conventional riveted metal structure. Ribs are located at the inboard and outboard ends and at spanwise locations experiencing high local loads, such as at engine mount attachments, gear attachments and flap track locations.

The wing incorporates an integral fuel tankage system. The bonded wing box structure provides the basic sealed tank. Additional sealing and protection could be achieved by using a controlled sloshing procedure to deposit a uniform layer of fuel resistant material on the inside surface.

Metal main fittings attach the wing outer panels to the carry-through structure. These metal fittings are bonded and mechanically fastened to the graphite outer wings.

ORIGINAL PAGE IS
OF POOR QUALITY

Figure 54 shows a Cessna composite wing flap. The upper and lower skin panels are of sandwich construction, with Kevlar outer skins for good resistance to foreign object damage. A Nomex core and a graphite inner skin provide desired panel stiffness. The two spars are made of unidirectional and woven graphite and transfer the flap shear loads to the flap tracks.

Extensive tests have shown this flap design to be very durable. After a high temperature water soak, 60,000 limit load cycles were applied with no failures. The front spar was then cut at the centerline, the flap was cycled to represent 15,000 flights, and a test load of 130 percent of limit load was applied with no failure. The same test was successful after cutting the rear spar at the centerline. Yet this flap is 23% lighter than a less durable riveted aluminum flap.

A third example of composite structure is shown in Figure 55. This is a jet engine nacelle designed, fabricated, tested, and flown by Cessna. Similar construction would be applicable on turboprop engine nacelles. A fiberglass and Kevlar layup is used for the aft cowl assembly, lower cowl door, upper cowl panel, and all of the inlet cowl assembly except for the heated inlet lip.

Composite materials are also used for cabin furnishings and trim on the advanced technology study aircraft. One example of composite interior design is the Cessna Enviroform Seat, shown in Figure 56. The seat assembly shown uses a molded fiberglass pedestal, and a fiberglass/aluminum honeycomb sandwich forms the seat pan and back, which are then upholstered. The contoured shape is functional and the slim seat lines give the interior a more spacious look. The thin, curved back gives plenty of knee room in high density seating arrangements and footrests are molded into the base. For this study, the pedestal and base are replaced with a composite framework that allows space for underseat storage.

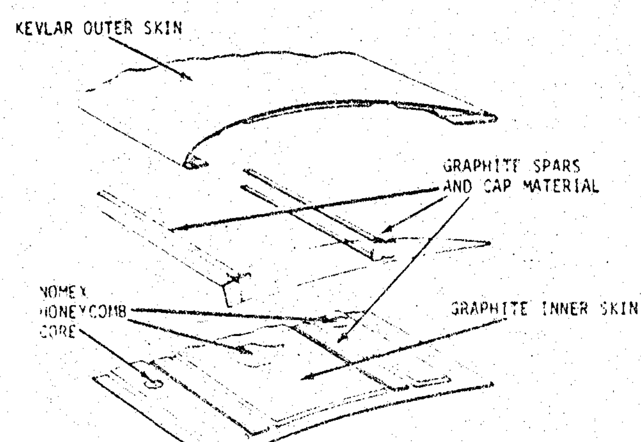

Figure 54. Cessna Composite Wing Flap Construction

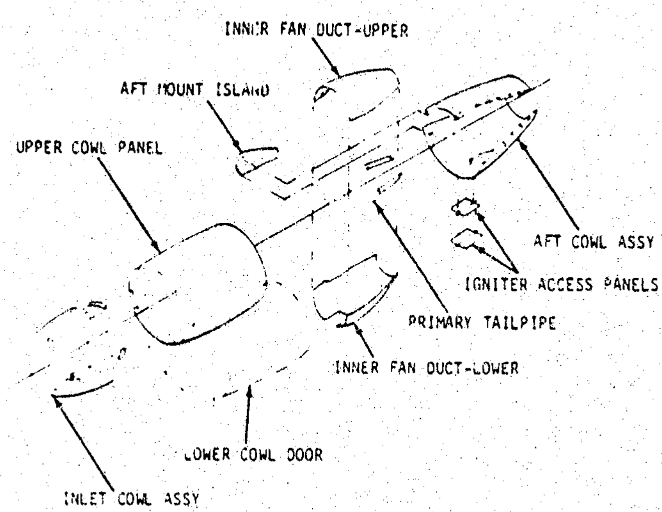

Figure 55. Cessna Composite Nacelle Configuration

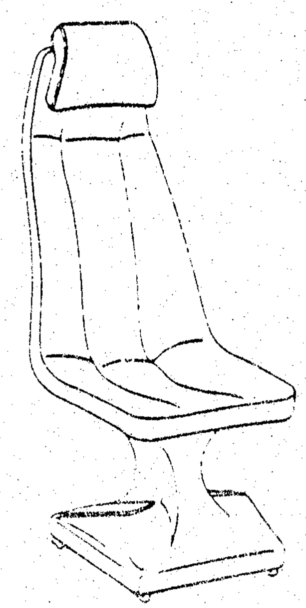

Figure 56. Enviroform Seat

6.3.3 Comparative Weight Savings

Experience with current bonded metal structure indicates a modest 0 to 10% weight savings relative to riveted aluminum construction, depending on the application. One reason for the small weight saving is that some parts are enlarged to facilitate the bond layup process. Another reason is that designers have used bonding primarily to increase fatigue life and damage tolerance rather than to reduce weight. However, with further development and test verification, more weight reductions could be achieved. It is anticipated that metal bonding could provide weight savings up to 20% with more advanced methods in design and construction.

Most applications of composite structure result in a 15 to 30% weight saving relative to riveted metal structure (Reference 2, 28 & 29). Weight savings for composite assemblies from various manufacturers are shown in Figure 57. This data indicates that component weight savings currently average 25% through use of advanced composites. Based on continuing research, it is anticipated that future composite component weight savings could average 35% relative to riveted metal structure.

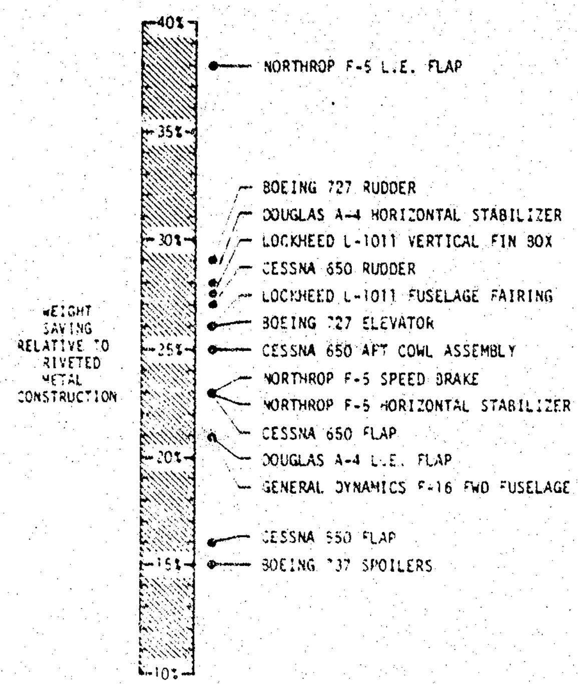

Figure 57. Composite Weight Savings in Aircraft Structural Applications

6.3.4 Advanced Structural Applications

The application of bonded and composite structure to the baseline airplane is shown in Figure 58. The individual structural breakdown is given in Table 13. Two levels of technology applications are shown. In Level 1, 50% of the baseline airframe weight is replaced with bonded metal structure and 10% is redesigned with advanced composites. Level 2 expands the use of advanced composites to replace 43.8% of the baseline airframe weight, and metal bonding is reduced to 20.8%. The largest item in Level 2 is the composite outer wing, which includes virtually all of the wing except for the fuselage carry-through structure.

The component weight savings selected for Level 1 are 10% for metal bonding and 25% for composites. For post-1990 Level 2, these savings increase to 20% for metal bonding and 35% for composites. Table 14 shows the unresized weight benefits of these advanced structural applications. The unresized weight benefits are the weight reductions that would result from substituting the advanced structural components identified in Table 13 for riveted aluminum components in an existing airframe. For example, Level 1 uses 50% metal bonding with a 10% average component weight saving, resulting in an airframe weight reduction of 5%. Since the airframe weight for Baseline 1 is 38% of the total empty weight, the 5% airframe number reduces to a 1.9% empty weight saving for the entire airplane. Level 1 composites add another 1.0% improvement, for a total empty weight reduction of 2.9%. Since the empty weight for Baseline 1 is 8780 lb, this amounts to a 255 lb weight saving. The 7.5% value for Level 2 provides a significant 659 lb weight reduction. The resized weight effects are discussed in Section 7.0.

The structural cost complexity factors presented in Table 14 were used as described in Section 4.3. Extensive experience with metal bonding shows that its cost per pound installed is equivalent to riveted structure. Material, tooling, & energy costs are higher with bonding, but final assembly and finishing costs are lower because the bonded subassemblies are larger and require less fitting and sealing. Where weight savings are experienced with bonding a cost benefit also results; so that Level 1 bonded components weigh and cost 10% less than their riveted counterparts, and Level 2 bonded components cost 20% less than riveted parts.

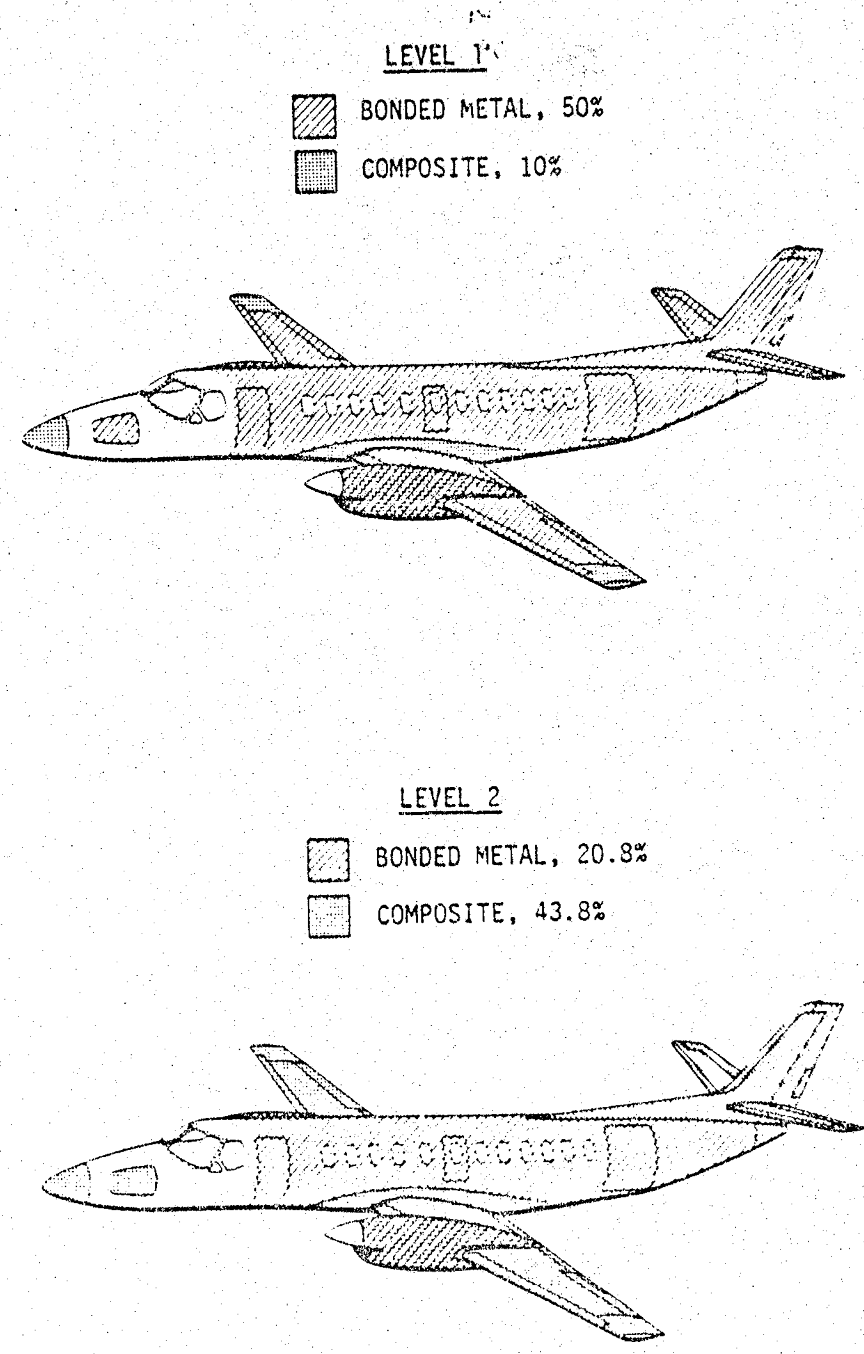

Figure 58. Areas of Advanced Structures Applications

Table 13. Breakdown of Advanced Structures Applications

ITEM	% OF TOTAL BASELINE AIRFRAME STRUCTURAL WEIGHTS			
	LEVEL 1		LEVEL 2	
	BONDED METAL	COMPOSITE	BONDED METAL	COMPOSITE
OUTER WING PANEL				
UPPER & LOWER PANELS	11.5%	--	--	11.5%
SPARS & RIBS	--	--	--	4.6%
FLAPS	--	3.4%	--	3.4%
AILERONS	3.2%	--	--	3.2%
ACCESS DOORS	1.8%	--	--	1.8%
TIPS	--	1.2%	--	1.2%
WING CARRY-THROUGH	5.3%	--	5.3%	--
FUSELAGE BARRELS	6.7%	--	6.7%	--
HORIZONTAL STABILIZER	4.2%	--	--	4.2%
VERTICAL FIN	2.8%	--	--	2.8%
ELEVATORS	2.3%	--	--	2.3%
RUDDER	1.8%	--	--	1.8%
TAILCONE SKIN & STIFFENERS	2.7%	--	2.7%	--
NACELLE COWLING	2.6%	2.2%	2.6%	2.2%
CABIN FLOOR AND SUPPORTS	2.3%	--	2.3%	--
WING/FUSELAGE FAIRINGS	--	1.5%	--	1.5%
MAIN AND NOSE GEAR DOORS	0.8%	--	--	0.8%
WINDSHIELD FRAME	--	0.8%	--	0.8%
CABIN ENTRANCE DOOR	0.7%	--	0.7%	--
FUSELAGE NOSE CAP	--	0.7%	--	0.7%
CABIN ESCAPE HATCH	0.5%	--	0.5%	--
NOSE BAGGAGE DOORS	0.4%	--	--	0.4%
TAILCONE ACCESS DOOR	0.4%	--	--	0.4%
TAILCONE STINGER	--	0.2%	--	0.2%
TOTAL	50.0%	10.0%	20.8%	43.8%

ORIGINAL PAGE IS
OF POOR QUALITY

Table 14. Unresized Effects of Advanced Materials Substitution on Baseline 1

	LEVEL 1	LEVEL 2
BONDED METAL		
% OF AIRFRAME STRUCTURAL WEIGHT	50%	20.8%
AVERAGE COMPONENT WEIGHT REDUCTION	10%	20.0%
UNRESIZED AIRFRAME STRUCTURAL WEIGHT SAVING	5%	4.2%
UNRESIZED AIRCRAFT EMPTY WEIGHT SAVING	1.9%	1.6%
COMPOSITE		
% OF AIRFRAME STRUCTURAL WEIGHT	10%	43.8%
AVERAGE COMPONENT WEIGHT REDUCTION	25%	35%
UNRESIZED AIRFRAME STRUCTURAL WEIGHT SAVING	2.5%	15.[illegible]%
UNRESIZED AIRCRAFT EMPTY WEIGHT SAVING	1.0%	5.[illegible]%
TOTAL BONDED METAL AND COMPOSITE		
% OF AIRFRAME STRUCTURAL WEIGHT	60%	[illegible]4.6%
UNRESIZED AIRFRAME STRUCTURAL WEIGHT SAVING	[illegible]	19.5%
UNRESIZED AIRCRAFT EMPTY WEIGHT SAVING	[illegible]	7.5%
COST COMPLEXITY FACTORS		
BONDED METAL - AVERAGE	1.0	1.0
COMPOSITE - AVERAGE	1.5	1.5

Composite construction averages 50% higher cost per finished pound than finished metal components. While composites eliminate many machined and forged parts, the material, energy, labor, and inspection costs are higher. The 1.5 complexity factor for composites is lower than current experience, but is based on rapidly decreasing materials costs along with maximum use of prepreg materials and new automated layup techniques. The reduced weight of composite structure largely offsets or even eliminates the cost penalty, even without resizing. For example, the Level 1 composite parts weigh (1 - 0.25) = 0.75 times as much as riveted metal parts, so the net cost factor is 0.75 x 1.5 = 1.13. For Level 2 composites, the 35% weight saving results in a net cost factor of 0.65 x 1.5 = 0.98. Thus, unresized Level 1 composite components cost 13% more than the metal parts they replace, and the Level 2 composite component costs are equivalent to those for metal construction.

The structural cost complexity factors are the same for Level 1 and Level 2, which implies that manufacturing process efficiencies improve over time at the same rate as structural efficiencies. This assumption is appropriate, since advanced structural R&D is concerned with improving manufacturing processes as well as with increasing structural efficiency.

6.4 Ride Quality Improvements

The analysis of aircraft response to turbulence begins with the development of a turbulence model. The model used for these analyses was derived from non-storm turbulence data collected by the NACA from 1952 through 1959 for transport aircraft. The turbulence model format shown in Figure 59 is that of Notess and Gregory (Reference 30). The second important element in ride quality analysis is a passenger discomfort model. Figure 60 shows the model generated by Holloway and Brumaghim (Reference 31) in a simulator test program. This model shows the threshold levels of acceleration at which a given percentage of passengers would object to the ride. The frequency-acceleration range of motion sickness is also indicated.

By applying the atmospheric power spectral density derived from the turbulence model to the aircraft gust load transfer function, the probability distribution of aircraft acceleration response may be determined. Results of these analyses for current large and small transport aircraft from References 32 and 33 have been overlayed on the passenger discomfort model for an RMS vertical gust of 6 ft/sec. Small transport aircraft are shown to have both a higher predominant frequency as well as higher acceleration response to turbulence. Reference 33 indicates that a goal of .03 RMS vertical g's at a predominant frequency of 1.5 Hz is a reasonable goal for a small short-haul transport. This point is indicated on the passenger discomfort model in Figure 60 as the STAT goal. For the 6 ft/sec gust the predominant frequencies of small transport aircraft tend to fall in the range of 1.3 to 1.7 Hz. The threshold lines of passengers objecting tend to be fairly horizontal in this range. This allows the data to be cross plotted as shown in Figure 61. The DeHavilland Twin Otter (DHC-6), the STAT Baseline 1, and the Level 1 and Level 2 results are superimposed on this Figure.

Level 1 employs higher wing loadings but no active ride control system. The high wing loadings were achieved by using the Level 2 flap system and advanced airfoils described in Section 6.1.3. The effectiveness of the Level 1 approach is shown in Figure 62, which shows the parametric response of Baseline 1 in terms of cruise wing loading and aspect ratio. Higher wing loadings and lower aspect ratios can improve the vertical g response of any of the baselines; however, the aspect ratio effect is relatively small and the wing loading effect is limited by either fuel volume or approach speed requirements. For example, Table 15 shows the limiting values of wing loading and the limiting parameter for three of the baseline technology airplanes. Because of these limits, the maximum reduction in vertical acceleration which can be expected from the Level 1 approach is approximately 10 percent.

The Level 2 approach combines an active ride control system (RCS) with higher wing loadings. The active ride control system includes separate aileron, spoiler, and elevator surface controls and a self-adaptive feedback system for vertical acceleration and pitch. One approach for implementing this type of system would include the use of spoilers, split ailerons, and a split elevator.

Reference 33 studied the effectiveness of this type of system on a DHC-6 Twin Otter with the aileron authority split 60% manual/40% ride control, and the elevator authority split 80% manual/20% ride control. Figure 63 shows the potential effectiveness of this type of system. An aileron-only RCS could provide a 55% reduction in vertical g's in cruise. The addition of elevator RCS brings the total reduction in cruise gust response to 70%. For the climb and approach flight segments, the total ride quality improvements are 55% and 40% respectively.

The cost impact of Level 1 is minimal and results from sizing for high wing loadings with the higher cost flaps, rather than for minimum DOC. Level 2 includes this cost as well as the RCS avionics and mechanical hardware costs, which were fixed at $100,000 per airplane.

C-2

ORIGINAL PAGE IS
OF POOR QUALITY

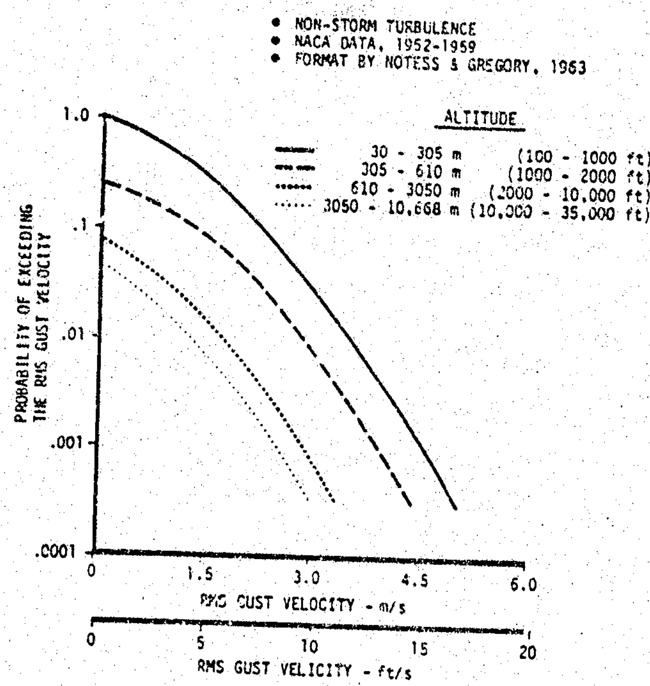

Figure 59. Turbulence Model

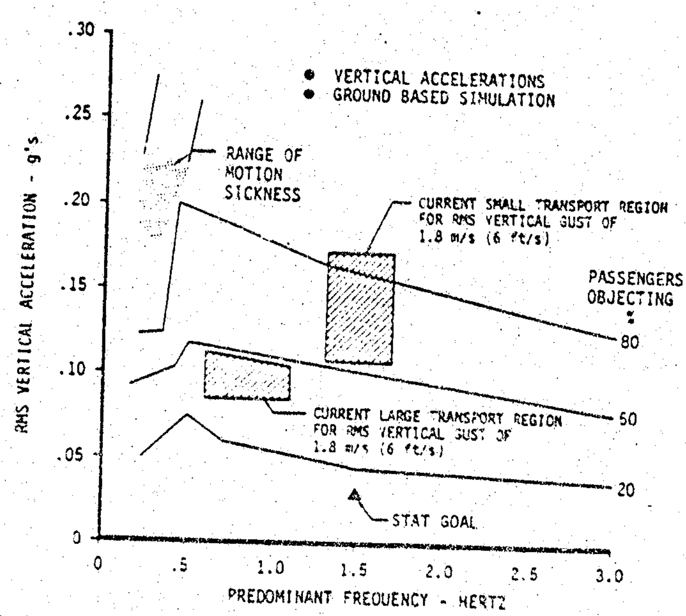

Figure 60. Response of Passengers and Airplanes to Vertical Gusts

ORIGINAL PAGE IS
OF POOR QUALITY

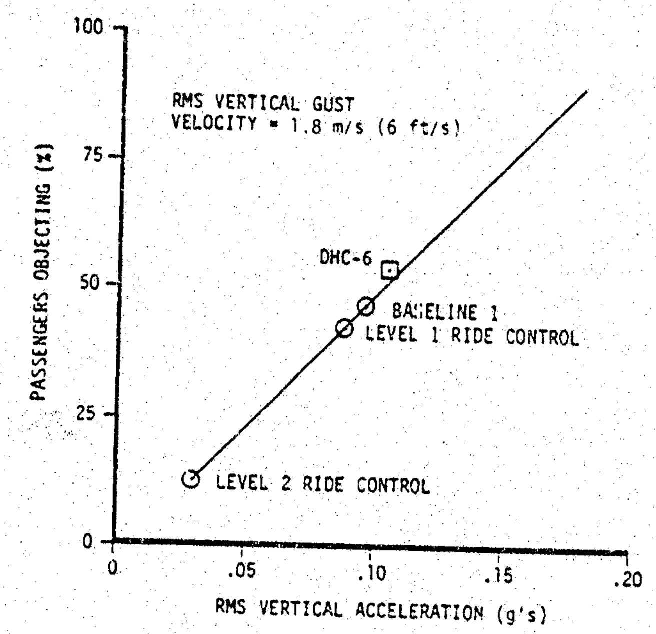

Figure 61. Effect of Vertical Acceleration on Perceived Ride Quality

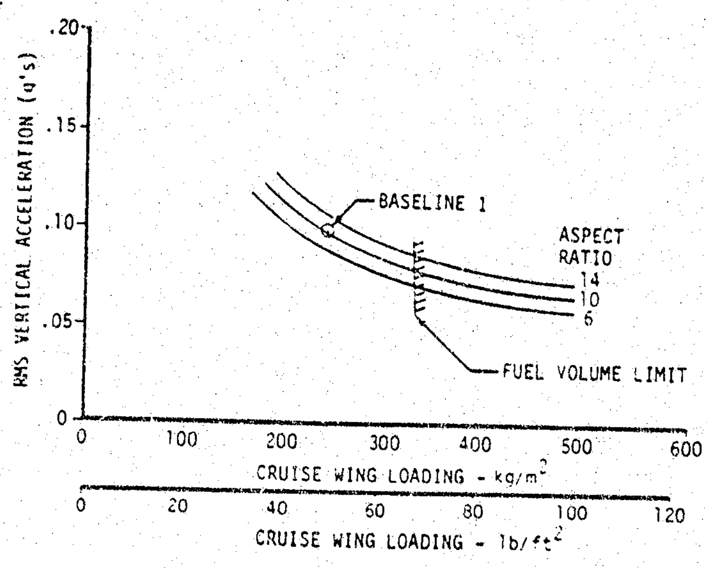

Figure 62. Level 1 Ride Quality Control

Table 15. Maximum Allowable Wing Loadings

AIRCRAFT	WING LOADING				LIMITING PARAMETER
	BASELINE		LEVEL 1 RIDE CONTROL		
	Kg/m²	(lb/ft²)	Kg/m²	(lb/ft²)	
19 PAX, 2-ABREAST	240	(49.1)	326	(66.8)	FUEL VOLUME
19 PAX, 3-ABREAST	250	(51.3)	340	(69.6)	FUEL VOLUME
30 PAX	259	(53.1)	380	(77.9)	APPROACH SPEED

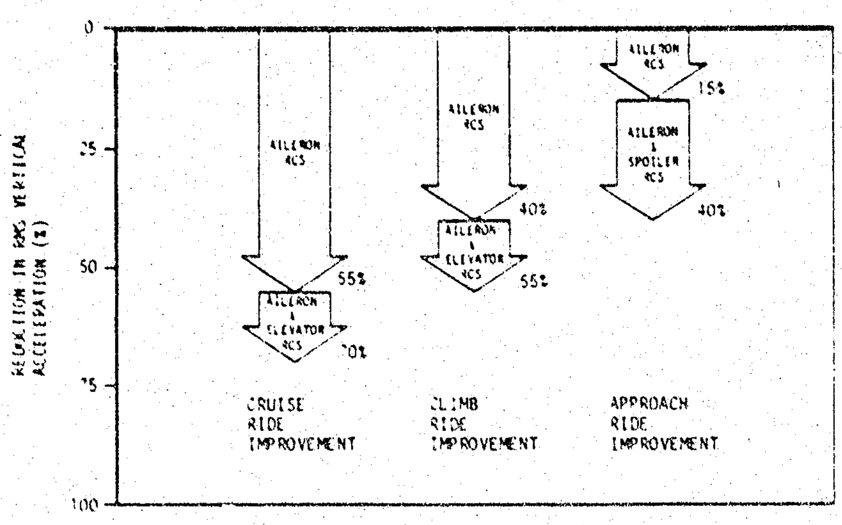

Figure 63. NASA-Boeing DHC-6 Study

7.0 ADVANCED TECHNOLOGY AIRCRAFT EVALUATION

The aerodynamic, propulsion and structural technologies were applied separately and in combination to the baseline airplanes. The ride control improvements were only applied separately, because ride control is intended for passenger comfort rather than improved costs or efficiencies.

A total of 28 advanced technology aircraft were sized and optimized, 14 each in Level 1 and Level 2. The principle characteristics of these aircraft are given in Tables 16 through 23. The application of the Level 1 and Level 2 technologies is shown to provide significant benefits in both operating costs and fuel efficiency. Tables 24 and 25 summarize these benefits for each aircraft, and average values for the combined technologies are also shown. Based on these averages, the combined aerodynamic, propulsion, and structural study technologies provide the following overall advantages.

	Level 1 Low Risk	Level 2 Moderate Risk
Reduction in DOC	13%	21%
Reduction in Fuel Consumption	24%	39%

The benefits for each aircraft fall within 1% of these average values as shown in Tables 24 and 25.

The ranking of the Level 2 applied technologies in reducing DOC and fuel consumption on small, short-haul transports is shown in Table 26.

These rankings represent the interaction of three effects:

- the sensitivities of the baseline airplanes to basic design parameters (drag, $C_{L\ MAX}$, weight, SFC, and cost), as discussed in Section 5.5.2,
- the effectiveness of each technology for improving these basic design parameters,
- the relative aggressiveness of the assumed Level 1 and Level 2 applications.

Advanced powerplant technology ranks highest because DOC and fuel efficiency are highly sensitive to SFC improvements, and the advanced engine technologies were extensively applied. Advanced flap systems rank second, even though the baselines showed the lowest technical sensitivity to improvements in maximum lift coefficient. The importance of high lift systems results from the very large gains in $C_{L\ MAX}$ available with advanced flaps.

Given the high sensitivity of DOC to airplane empty weight, as shown in Section 5.5.2. the low ranking of advanced structural technologies is surprising. Clearly, even the 43.8% composite airframe assumed for the Level 2 structure does not use enough composites to fully exploit the design sensitivity to weight. Another way to take better advantage of this sensitivity is to pursue weight savings for non-structural airframe components (i.e., systems and furnishings), which account for approximately 40% of airframe weight.

The effect of advanced structures technology on empty weight for Baseline 1, with and without resizing, is shown below. Unresized weight savings increased about 1% with resizing.

	Level 1 Advanced Structures	Level 2 Advanced Structures
Unresized Empty Weight Reduction	2.9%	7.5%
Resized Empty Weight Reduction	3.9%	8.3%

Advanced propellers rank fourth in DOC improvement and third in SFC improvement. The aircraft were very sensitive to propeller efficiency and weight improvements, but the available efficiency and weight gains were small compared to other technologies.

Advanced airfoils ranked low because the Level 1 and Level 2 applications were not aggressive. In particular, natural laminar flow was not included in the study because it has been difficult to achieve in practice (Section 6.1.1). However, very recent NASA work with natural laminar flow airfoils (Reference 34) shows the potential for significantly lower drag using practical design, manufacturing, and operating procedures.

The rankings of Level 1 and Level 2 applied technologies in improving DOC and block fuel are further illustrated in Figures 64 and 65. It should be noted that the Level 1 and Level 2 ride control technologies are based on Level 2 advanced airfoils and flaps, which accounts for the apparent improvement in DOC due to ride control technology. The active ride control system introduced in Level 2 adds cost to the aircraft, which reduces the DOC improvement.

Plan and perspective views of the four Level 2 advanced technology airplanes are presented in Figures 66 through 72. Table 27 summarizes configuration differences between the current and advanced technology airplanes. In general, the combined Level 2 technologies reduce TOGW 14%, power 24%, wing area 25%, wing span 3%, and increase aspect ratios 25%.

ORIGINAL PAGE IS
OF POOR QUALITY

Table 16. Characteristics of 19 Passenger, 2-Abreast Airplane Incorporating Level 1 Advanced Technologies

AIRCRAFT	CHARACTERISTICS		CURRENT TECHNOLOGY BASELINE	LEVEL 1 TECHNOLOGY				
				A	P	S	C	R/C
19 PAX 2 ABR	TOGW	kg (lb)	7239 (15960)	7121 (15699)	6930 (15278)	7054 (15552)	6696 (14763)	7170 (15807)
	POWER/ENGINE[1]	kw (SHP)	928 (1245)	842 (1129)	892 (1196)	909 (1219)	800 (1073)	888 (1190)
	PRICE	$M	1.49	1.45	1.49	1.45	1.43	1.49
	BLOCK FUEL[2]	kg (lb)	249 (550)	234 (515)	208 (458)	246 (543)	191 (422)	231 (509)
	DOC[2]	¢/SEAT-km (¢/SEAT-nm)	5.936 (10.993)	5.704 (10.564)	5.480 (10.149)	5.808 (10.756)	5.194 (9.619)	5.622 (10.412)
	RELATIVE DOC		1.000	0.961	0.923	0.978	0.875	0.947

1. THERMODYNAMIC
2. STAGE LENGTH 185 km (100 nm)

A - AERODYNAMICS
P - PROPULSION
S - STRUCTURES
C - COMBINED A,P,S
R/C - RIDE CONTROL

Table 17. Characteristics of Short Field, 19 Passenger, 2-Abreast Airplane Incorporating Level 1 Advanced Technologies

AIRCRAFT	CHARACTERISTICS		CURRENT TECHNOLOGY BASELINE	LEVEL 1 TECHNOLOGY			
				A	P	S	C
19 PAX 2 ABR SHORT FIELD	TOGW	kg (lb)	7468 (16465)	--	--	--	6835 (15069)
	POWER/ENGINE[1]	kw (SHP)	1041 (1399)	--	--	--	891 (1195)
	PRICE	$M	1.56	--	--	--	1.49
	BLOCK FUEL[2]	kg (lb)	272 (600)	--	--	--	207 (456)
	DOC[2]	¢/SEAT-km (¢/SEAT-nm)	6.278 (11.627)	--	--	--	5.435 (10.065)
	RELATIVE DOC		1.058	--	--	--	0.916

1. THERMODYNAMIC
2. STAGE LENGTH 185 km (100 nm)

A - AERODYNAMICS
P - PROPULSION
S - STRUCTURES
C - COMBINED A,P,S
R/C - RIDE CONTROL

ORIGINAL PAGE IS
OF POOR QUALITY

Table 18. Characteristics of 19 Passenger, 3-Abreast Airplane Incorporating Level 1 Advanced Technologies

AIRCRAFT	CHARACTERISTICS		CURRENT TECHNOLOGY BASELINE	LEVEL 1 TECHNOLOGY			
				A	P	S	C
19 PAX 3 ABR	TOGW	kg (lb)	8140 (17945)	7983 (17600)	7757 (17102)	7902 (17421)	7502 (16539)
	POWER/ENGINE[1]	kw (SHP)	1070 (1435)	974 (1306)	1031 (1382)	1050 (1408)	922 (1236)
	PRICE BLOCK FUEL[2]	$M kg (lb)	1.74 281 (620)	1.69 262 (578)	1.73 233 (514)	1.69 277 (610)	1.67 214 (472)
	DOC[2]	¢/SEAT-km (¢/SEAT-nm)	6.712 (12.430)	6.439 (11.925)	6.185 (11.455)	6.556 (12.141)	5.856 (10.845)
	RELATIVE DOC		1.131	1.085	1.042	1.104	0.987

1. THERMODYNAMIC
2. STAGE LENGTH 185 km (100 nm)

A - AERODYNAMICS
P - PROPULSION
S - STRUCTURES
C - COMBINED A,P,S
R/C - RIDE CONTROL

Table 19. Characteristics of 30 Passenger Airplane Incorporating Level 1 Advanced Technologies

AIRCRAFT	CHARACTERISTICS		CURRENT TECHNOLOGY BASELINE	LEVEL 1 TECHNOLOGY			
				A	P	S	C
30 PAX	TOGW	kg (lb)	10981 (24210)	10760 (23721)	10507 (23165)	10730 (23655)	10115 (22300)
	POWER/ENGINE[1]	kw (SHP)	1439 (1930)	1311 (1758)	1388 (1860)	1414 (1896)	1241 (1663)
	PRICE BLOCK FUEL[2]	$M kg (lb)	2.23 363 (800)	2.17 338 (745)	2.23 300 (662)	2.18 357 (788)	2.13 275 (607)
	DOC[2]	¢/SEAT-km (¢/SEAT-nm)	5.657 (10.476)	5.426 (10.049)	5.235 (9.696)	5.547 (10.273)	4.941 (9.151)
	RELATIVE DOC		0.953	0.914	0.882	0.935	0.832

1. THERMODYNAMIC
2. STAGE LENGTH 185 km (100 nm)

A - AERODYNAMICS
P - PROPULSION
S - STRUCTURES
C - COMBINED A,P,S
R/C - RIDE CONTROL

ORIGINAL PAGE IS OF POOR QUALITY

Table 20. Characteristics of 19 Passenger, 2-Abreast Airplane Incorporating Level 2 Advanced Technologies

AIRCRAFT	CHARACTERISTICS		CURRENT TECHNOLOGY BASELINE	LEVEL 2 TECHNOLOGY				
				A	P	S	C	R/C
19 PAX 2 ABR	TOGW	kg (lb)	7239 (15960)	7087 (15625)	6724 (14823)	6833 (15065)	6303 (13895)	7262 (16010)
	POWER/ENGINE[1]	kw (SHP)	928 (1245)	786 (1054)	873 (1170)	879 (1178)	711 (953)	899 (1205)
	PRICE	$M	(1.49)	(1.45)	(1.50)	(1.44)	(1.41)	(1.58)
	BLOCK FUEL[2]	kg (lb)	249 (550)	223 (491)	178 (393)	239 (527)	154 (339)	234 (516)
	DOC[2]	¢/SEAT-km (¢/SEAT-nm)	5.936 (10.993)	5.581 (10.336)	5.179 (9.591)	5.644 (10.452)	4.709 (8.721)	5.673 (10.507)
	RELATIVE DOC		1.000	0.940	0.872	0.951	0.793	0.956

1. THERMODYNAMIC
2. STAGE LENGTH 185 km (100 nm)

A - AERODYNAMICS
P - PROPULSION
S - STRUCTURES
C - COMBINED A,P,S
R/C - RIDE CONTROL

Table 21. Characteristics of Short Field, 19 Passenger, 2-Abreast Airplane Incorporating Level 2 Advanced Technologies

AIRCRAFT	CHARACTERISTICS		CURRENT TECHNOLOGY BASELINE	LEVEL 2 TECHNOLOGY			
				A	P	S	C
19 PAX 2 ABR SHORT FIELD	TOGW	kg (lb)	7468 (16465)	--	--	--	6418 (14149)
	POWER/ENGINE[1]	kw (SHP)	1040 (1395)	--	--	--	787 (1055)
	PRICE	$M	(1.56)	--	--	--	(1.47)
	BLOCK FUEL[2]	kg (lb)	272 (600)	--	--	--	165 (364)
	DOC[2]	¢/SEAT-km (¢/SEAT-nm)	6.278 (11.627)	--	--	--	4.898 (9.072)
	RELATIVE DOC		1.058	--	--	--	0.825

1. THERMODYNAMIC
2. STAGE LENGTH 185 km (100 nm)

A - AERODYNAMICS
P - PROPULSION
S - STRUCTURES
C - COMBINED A,P,S
R/C - RIDE CONTROL

Table 22. Characteristics of 19 Passenger, 3-Abreast Airplane Incorporating Level 2 Advanced Technologies

AIRCRAFT	CHARACTERISTICS		CURRENT TECHNOLOGY BASELINE	LEVEL 2 TECHNOLOGY			
				A	P	S	C
19 PAX 3 ABR-	TOGW	kg (lb)	8140 (17945)	7973 (17578)	7520 (16579)	7633 (16828)	7023 (15483)
	POWER/ENGINE[1]	kw (SHP)	1070 (1435)	906 (1214)	1009 (1352)	1012 (1357)	811 (1087)
	PRICE	SM	(1.74)	(1.69)	(1.74)	(1.67)	(1.64)
	BLOCK FUEL[2]	kg (lb)	281 (620)	249 (549)	200 (442)	268 (591)	171 (376)
	DOC[2]	¢/SEAT-km (¢/SEAT-lb)	6.712 (12.430)	6.303 (11.673)	5.847 (10.829)	6.353 (11.766)	5.278 (9.774)
	RELATIVE DOC		1.131	1.062	0.985	1.070	0.889

1. THERMODYNAMIC
2. STAGE LENGTH 185 km (100 nm)

A - AERODYNAMICS
P - PROPULSION
S - STRUCTURES
C - COMBINED A,P,S
R/C - RIDE CONTROL

Table 23. Characteristics of 30 Passenger Airplane Incorporating Level 2 Advanced Technologies

AIRCRAFT	CHARACTERISTICS		CURRENT TECHNOLOGY BASELINE	LEVEL 2 TECHNOLOGY			
				A	P	S	C
30 PAX	TOGW	kg (lb)	10981 (24210)	10723 (23640)	10181 (22445)	10354 (22826)	9496 (20936)
	POWER/ENGINE[1]	kw (SHP)	1439 (1930)	1214 (1627)	1352 (1813)	1367 (1833)	1091 (1462)
	PRICE	SM	(2.23)	(2.16)	(2.24)	(2.15)	(2.10)
	BLOCK FUEL[2]	kg (lb)	363 (800)	319 (703)	258 (568)	347 (765)	218 (481)
	DOC[2]	¢/SEAT-km (¢/SEAT-nm)	5.657 (10.476)	5.294 (9.805)	4.949 (9.165)	5.379 (9.962)	4.464 (8.267)
	RELATIVE DOC		0.953	0.892	0.834	0.906	0.752

1. THERMODYNAMIC
2. STAGE LENGTH 185 km (100 nm)

A - AERODYNAMICS
P - PROPULSION
S - STRUCTURES
C - COMBINED A,P,S
R/C - RIDE CONTROL

ORIGINAL PAGE IS
OF POOR QUALITY

Table 24. Percent Change in DOC Resulting From Advanced Technology Applications

100 nm STAGE LENGTH

AIRCRAFT	TECHNOLOGY									
	AERODYNAMICS		PROPULSION		STRUCTURES		COMBINED		RIDE CONTROL	
	LEVEL 1	LEVEL 2	LEVEL 1	LEVEL 2	LEVEL 1	LEVEL 2	LEVEL 1	LEVEL 2	LEVEL 1	LEVEL 2
19 PAX 2-ABREAST	-3.9	-6.0	-7.7	-12.8	-2.2	-4.9	-12.5	-20.7	-5.3	-4.4
19 PAX 2-ABREAST 2 SHORT FIELD	-	-	-	-	-	-	-13.4	-22.0	-	-
19 PAX 3-ABREAST	-4.1	-6.1	-7.9	-12.9	-2.3	-5.3	-12.8	-21.4	-	-
30 PAX	4.1	-6.4	-7.5	-12.5	-1.9	-4.9	-12.7	-21.1	-	-
AVERAGE	-	-	-	-	-	-	-12.9	-21.3	-	-

Table 25. Percent Change in Block Fuel Resulting From Advanced Technology Applications

100 nm STAGE LENGTH

AIRCRAFT	TECHNOLOGY									
	AERODYNAMICS		PROPULSION		STRUCTURES		COMBINED		RIDE CONTROL	
	LEVEL 1	LEVEL 2	LEVEL 1	LEVEL 2	LEVEL 1	LEVEL 2	LEVEL 1	LEVEL 2	LEVEL 1	LEVEL 2
19 PAX 2-ABREAST	-6.4	10.7	-16.7	-28.5	-1.3	-4.2	-23.3	-38.4	-7.5	-6.2
19 PAX 2-ABREAST SHORT FIELD	-	-	-	-	-	-	-24.0	-39.3	-	-
19 PAX 3-ABREAST	-6.8	-11.5	-17.1	-28.7	-1.6	-4.7	-23.9	-39.4	-	-
30 PAX	-6.9	-12.1	-17.3	-29.0	-1.5	-4.4	-24.1	-39.9	-	-
AVERAGE	-	-	-	-	-	-	-23.8	-39.3	-	-

Table 26. Average Effectiveness of Level 2 Study Technologies

100 nm STAGE LENGTH

TECHNOLOGY	PERCENT REDUCTION	
	DOC	BLOCK FUEL
ADVANCED POWERPLANT	10.2	23.0
ADVANCED HIGH LIFT SYSTEMS	5.5	10.2
ADVANCED STRUCTURES	5.0	4.4
ADVANCED PROPELLERS	2.5	5.7
ADVANCED AIRFOILS	0.7	1.2

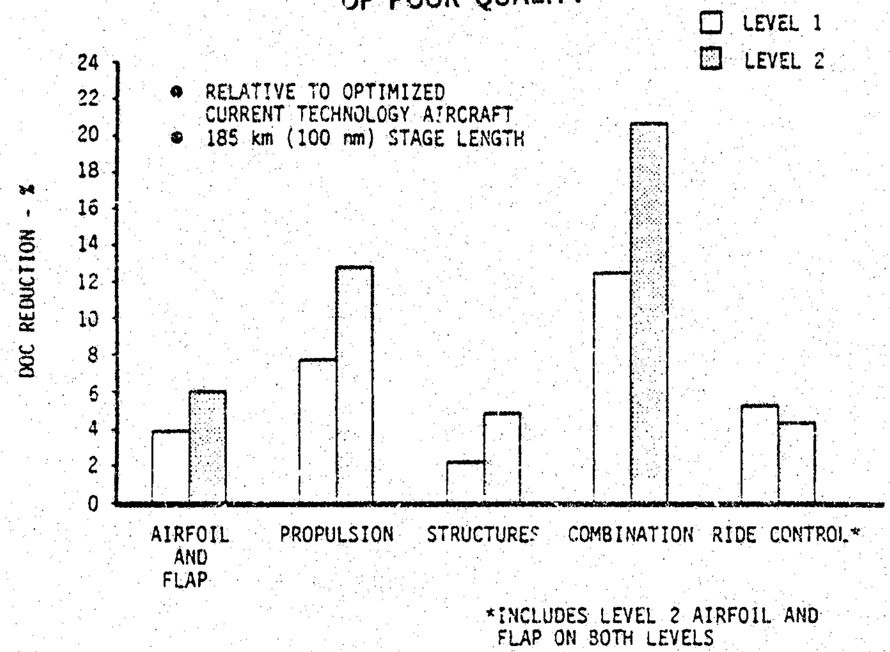

Figure 64. DOC Improvement Summary

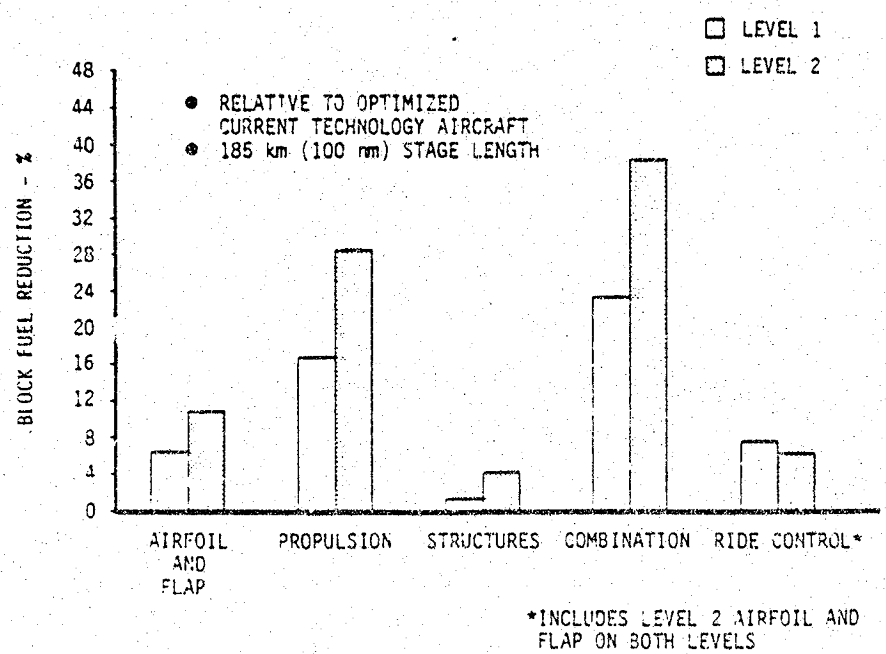

Figure 65. Block Fuel Improvement Summary

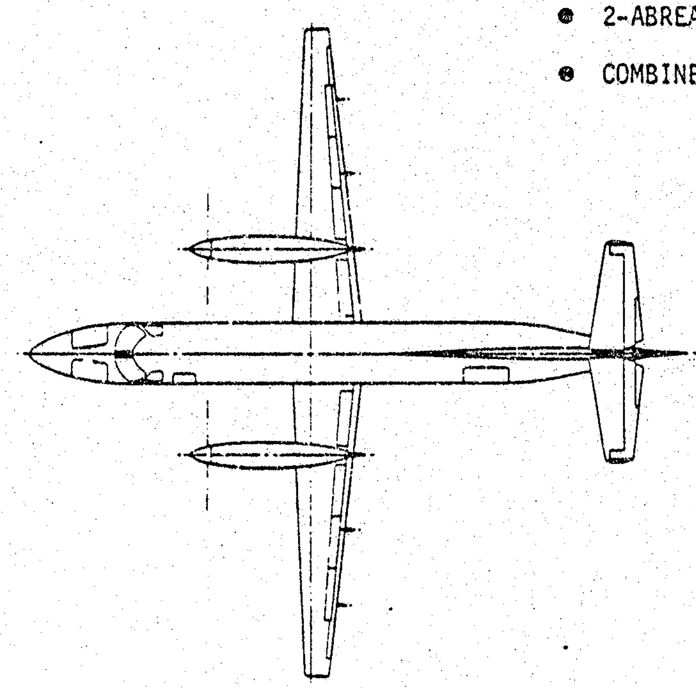

19 PASSENGERS

- 2-ABREAST SEATING
- COMBINED LEVEL 2 TECHNOLOGIES

TOGW	6303 kg	(13,895 lb)
POWER/ENGINE	711 kW	(953 shp)
PROPELLER DIAMETER	3.0 m	(10.0 ft)
WING AREA	22.9 m^2	(246 ft^2)
WING SPAN	17.5 m	(57.3 ft)
ASPECT RATIO	13.35	

Figure 66. Plan View of Level 2 Advanced Technology Aircraft -- 19 Passenger, 2-Abreast Seating

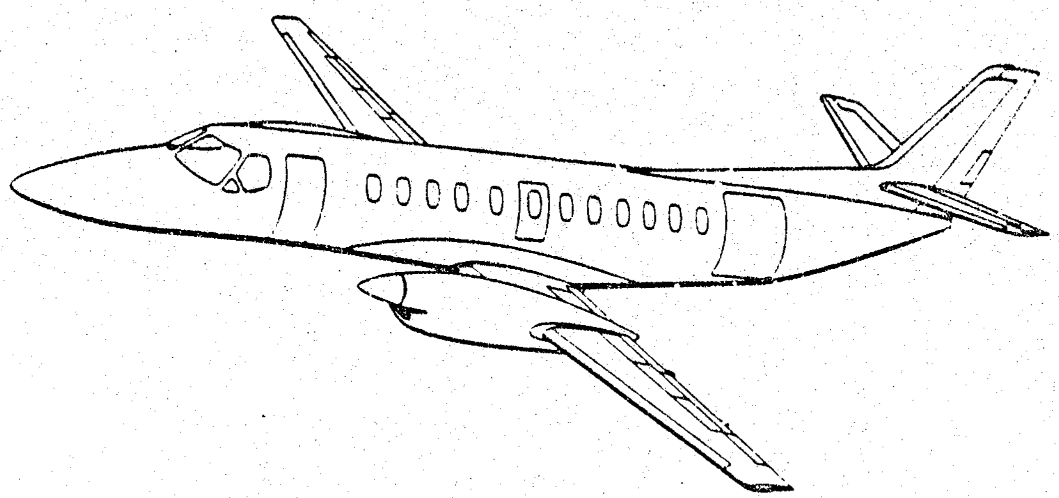

- 19 PASSENGERS
- 2-ABREAST SEATING
- COMBINED LEVEL 2 TECHNOLOGIES

Figure 67. Level 2 Advanced Technology Aircraft -- 19 Passenger, 2-Abreast Seating

ORIGINAL PAGE IS
OF POOR QUALITY

19 PASSENGERS

- 2-ABREAST SEATING
- 914 m (3000 ft) TOFL
- COMBINED LEVEL 2 TECHNOLOGIES

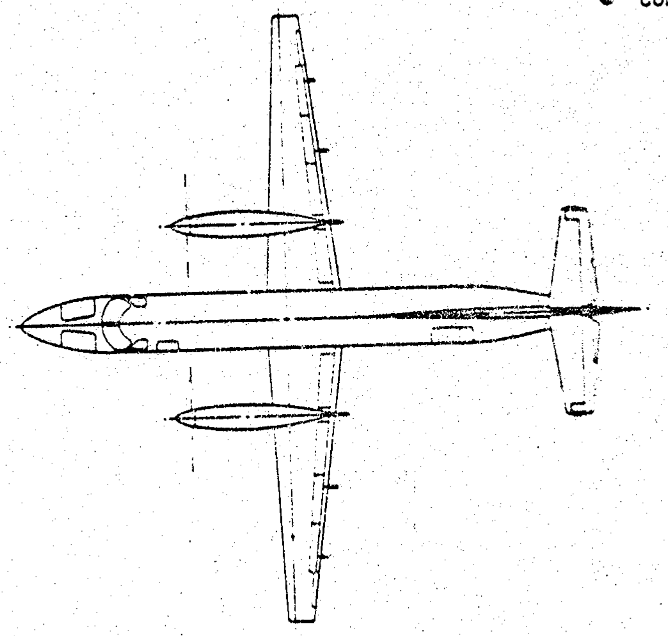

TOGW	6418 kg	(14,149 lb)
POWER/ENGINE	787 kW	(1055 shp)
PROPELLER DIAMETER	3.0 m	(10.0 ft)
WING AREA	25.9 m^2	(279 ft^2)
WING SPAN	17.3 m	(56.9 ft)
ASPECT RATIO	11.6	

Figure 68. Plan View of Level 2 Advanced Technology Aircraft -- 19 Passenger, 2-Abreast Seating, Short Field Capability

19 PASSENGERS

- 3-ABREAST SEATING
- COMBINED LEVEL 2 TECHNOLOGIES

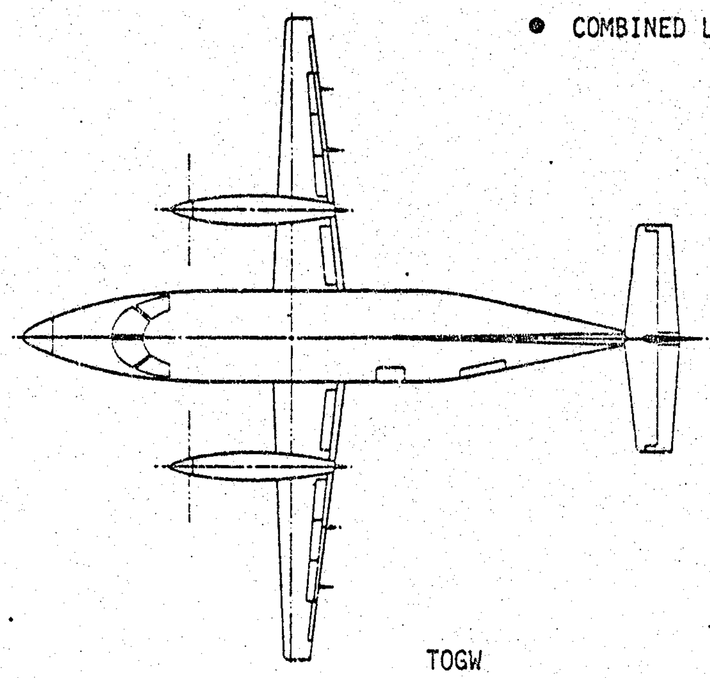

TOGW	7023 kg	(15,483 lb)
POWER/ENGINE	811 kW	(1087 shp)
PROPELLER DIAMETER	3.0 m	(10.0 ft)
WING AREA	24.2 m^2	(261 ft^2)
WING SPAN	17.3 m	(56.6 ft)
ASPECT RATIO	12.25	

Figure 69. Plan View of Level 2 Advanced Technology Aircraft -- 19 Passenger, 3-Abreast Seating

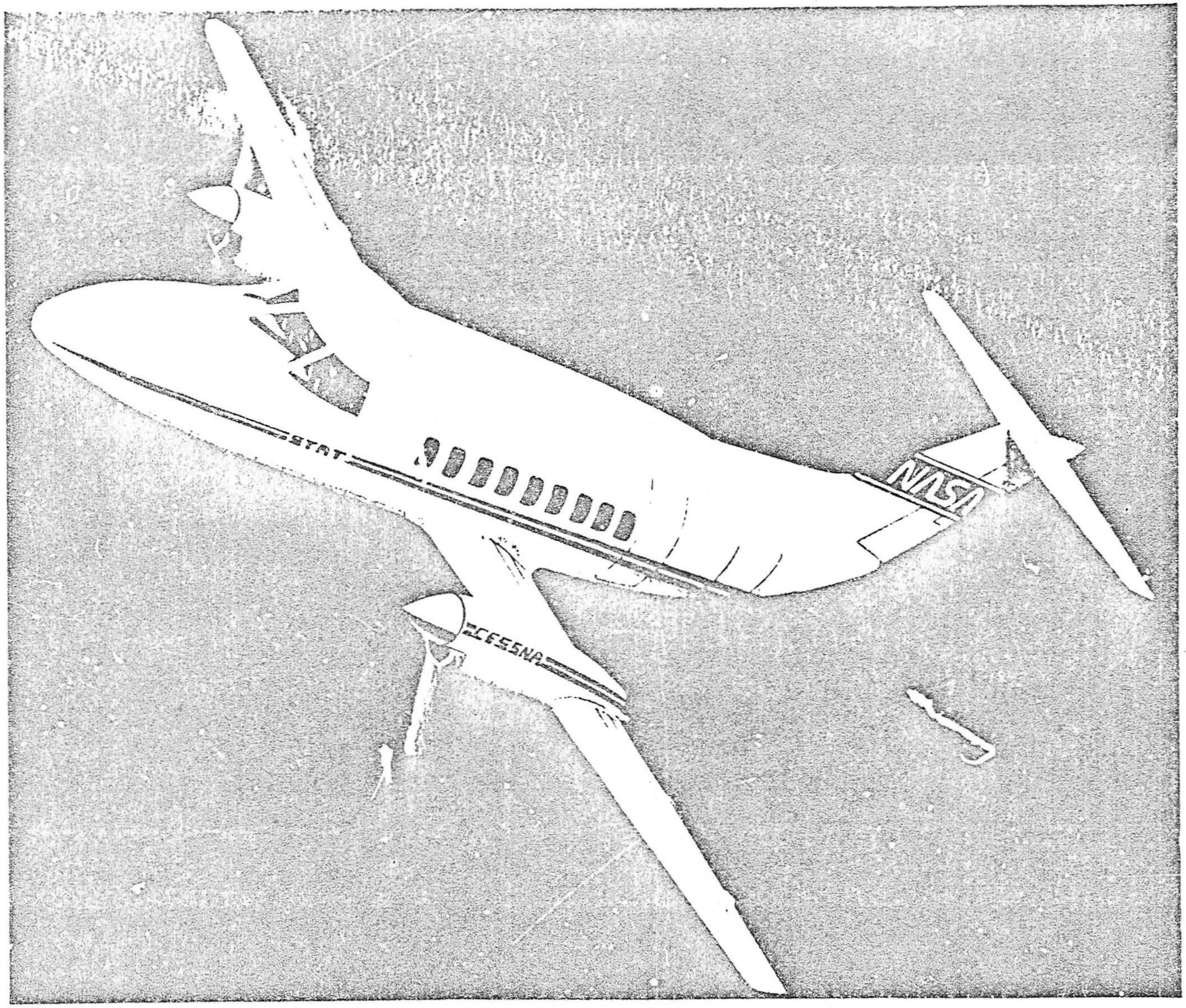

Figure 70. Level 2 Advanced Technology Aircraft
-- 19 Passenger, 3-Abreast Seating

30 PASSENGERS

- 3-ABREAST SEATING
- COMBINED LEVEL 2 TECHNOLOGIES

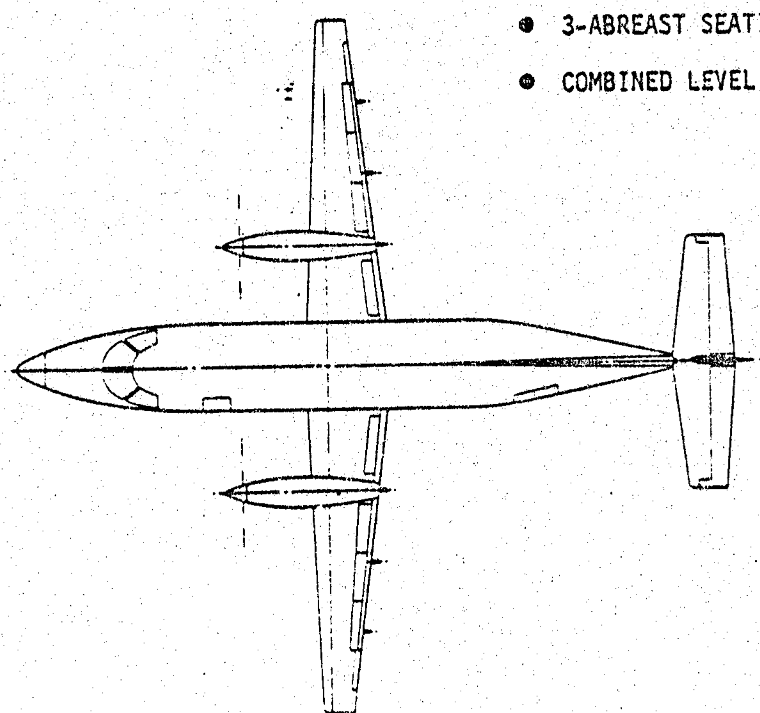

TOGW	9496 kg	(20,936 lb)
POWER/ENGINE	1090 kW	(1462 shp)
PROPELLER DIAMETER	3.0 m	(10.0 ft)
WING AREA	31.7 m^2	(341 ft^2)
WING SPAN	19.3 m	(63.4 ft)
ASPECT RATIO	11.8	

Figure 71. Plan View of Level 2 Advanced Technology Aircraft -- 30 Passenger

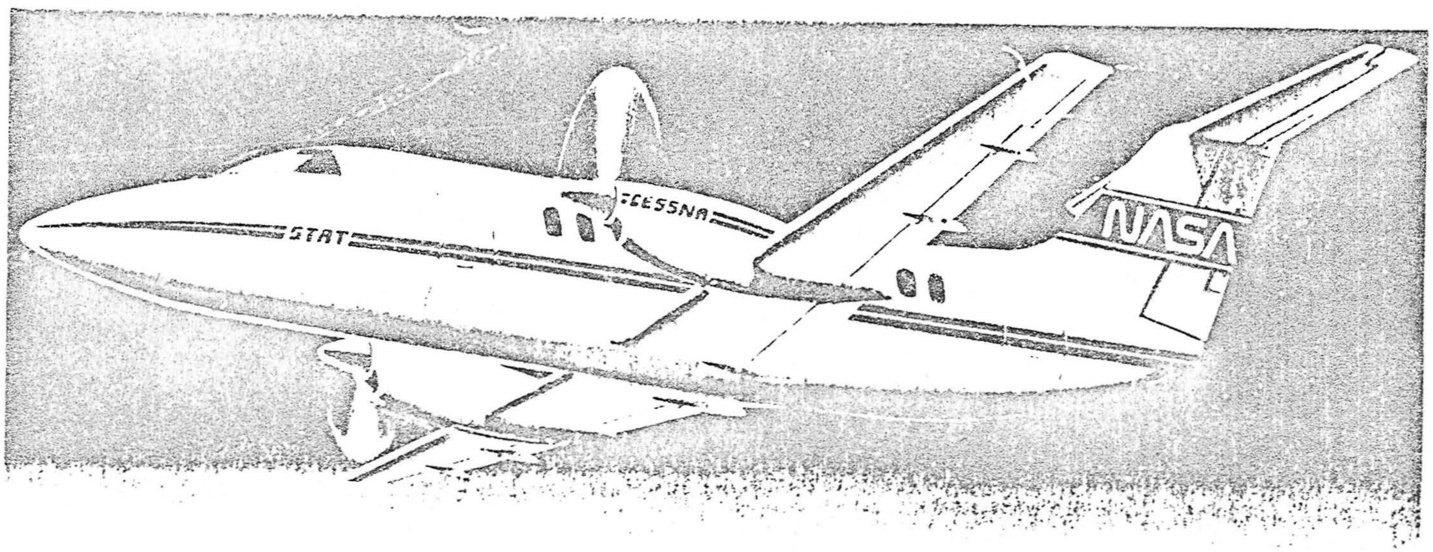

Figure 72. Level 2 Advanced Technology Aircraft
-- 30 Passenger, 3-Abreast Seating

Table 27. Effect of Combined Advanced Technologies on Optimum Aircraft Configuration

CONFIGURATION ITEM	AIRCRAFT	CURRENT TECHNOLOGY	LEVEL 1	Δ %	LEVEL 2	Δ %
TOGW (LB)	1. 19 PAX, 2 ABR	15,960	14,763	-7.5	13,895	-12.9
	2. 19 PAX, 2 ABR, SHORT FIELD	16,465	15,069	-8.5	14,149	-14.1
	3. 19 PAX, 3 ABR	17,945	16,539	-7.8	15,483	-13.7
	4. 30 PAX	24,210	22,300	-7.9	20,936	-13.5
POWER PER ENGINE (SHP)	1. 19 PAX, 2 ABR	1245	1073	-13.8	953	-23.5
	2. 19 PAX, 2 ABR, SHORT FIELD	1395	1195	-14.3	1055	-24.4
	3. 19 PAX, 3 ABR	1435	1236	-13.9	1087	-24.3
	4. 30 PAX	1930	1663	-13.8	1462	-24.2
WING AREA (FT^2)	1. 19 PAX, 2 ABR	325	283	-12.9	246	-24.3
	2. 19 PAX, 2 ABR, SHORT FIELD	373	324	-13.1	279	-25.2
	3. 19 PAX, 3 ABR	350	304	-13.1	261	-25.4
	4. 30 PAX	456	397	-12.9	341	-25.2
WING SPAN (FT)	1. 19 PAX, 2 ABR	57.7	56.8	-1.6	57.3	-0.7
	2. 19 PAX, 2 ABR, SHORT FIELD	58.7	55.5	-5.5	56.9	-3.1
	3. 19 PAX, 3 ABR	58.4	56.5	-3.3	56.6	-3.1
	4. 30 PAX	65.8	63.0	-4.3	63.4	-3.6
WING ASPECT RATIO	1. 19 PAX, 2 ABR	10.25	11.40	+11.2	13.35	+30.2
	2. 19 PAX, 2 ABR, SHORT FIELD	9.25	9.50	+ 2.7	11.60	+25.4
	3. 19 PAX, 3 ABR	9.75	10.60	+ 8.7	12.25	+25.6
	4. 30 PAX	9.50	10.0	+ 5.3	11.80	+24.2

8.0 RECOMMENDATIONS

Further research and technology efforts are required in several areas to assure the incorporation of promising technologies in future small, short-haul aircraft. The goal of these efforts is to reduce direct operating costs and fuel consumption by improvements in aerodynamics, propulsion, structures, and systems.

Aerodynamics

- Conduct powered model tests with full-span trailing edge flaps for developing high values of approach L/D along with high takeoff $C_{L\ MAX}$. Analytical 3-D prediction methods should be developed to reliably predict flap characteristics. The analytical methods could be verified by the flap model tests. A broad 3-D data bank is required for Reynolds numbers in the neighborhood of 6×10^6.

- Continue investigation of NLF airfoils, with specific tailoring to minimize transition due to insect contamination.

- Develop a non-steady theory for predicting transition and drag for NLF airfoils in the wake of highly loaded propellers.

- Continue investigations of airframe/propulsion integration. Wing/fuselage and wing/nacelle analyses for conventional and unconventional configurations should be included. Theory should be verified by experiment. This should include high angle-of-attack and high yaw angle tests to assure satisfactory stability characteristics.

Propulsion

- Continue development of high work stages, advanced diffusers, high temperature turbine materials, variable internal geometry, high modulus shafts, and more efficient cooling.

- Emphasize development of broad range cycles that include the capability for low idle power settings along with high bleed airflow and pressures. Idle bleed air performance is the deciding factor in providing realistic air conditioning with light weight air cycle machines. Idle-to-full power acceleration times should remain as short as for current engines.

- Improve engine durability in the severe short-haul duty cycle. Better hot section analysis methods are needed and continued development of digital controllers is encouraged.

- Develop analytical methods for optimizing propeller/hub/nacelle integration. Conduct powered model tests to confirm predictions.

- Continue development of propeller noise prediction methods.

- Develop advanced structural concepts for hubs and multiple low activity factor blades, making fuller use of advanced composites. This will require development of more precise aerolastic analysis techniques, including both structural modeling and unsteady aerodynamics.

Structures

- Continue development of higher strength matrix materials with better fiber bond strengths. Graphite fibers are available with filament strengths of 600,000 psi. The limiting factor is the matrix and matrix/fiber bond. Research to improve fiber wetting is also required.

- Expand research on the durability and damage tolerance of composite structures. Establish a data base for current materials and assembly techniques, and develop materials with better impact/fatigue/crack growth characteristics.

- Continue research in lightning protection for composite wings with integral fuel tanks.

- Continue tests of environmental effects on bonded and composite structure. Accelerated environmental tests should be complemented with tests of in-service components.

- Expand development of automated composite manufacturing methods, including component layups and windings.

- Continue development of inspection techniques for bonded and composite components and assemblies.

Systems

- Develop lighter weight systems, including digital avionics, flat panel displays, fiber optic data channels, and use of composites in mechanical systems.

- Test the use of fluid-wetted porous leading edges for both insect and ice protection on NLF wings.

- Develop ride control system technologies, including sensor design, system response rates, and effective aerodynamic devices for use in combination with advanced high lift system, ailerons, and elevators. System design studies should be continued, and promising concepts could be tested at the NASA-Ames 7 x 10 ft wind tunnel facility.

9.0 REFERENCES

1. The Aerospace Corporation: Light Transport Market Forecast. Report ATR-79(4857-03)-2ND, July 1979.

2. Douglas Aircraft Company: Study of Operational Requirements for Medium Density Air Transportation. Volume I, NASA CR-137603; Volume II, NASA CR-137604; Volume III, NASA CR-137605; March 1975.

3. Boeing Commercial Airplane Company: Application of Advanced Technologies to Small, Short-Haul Aircraft. NASA CR-152089, March 1978.

4. Foody, James J. and Colwell, Samuel C.: Role of the Turboprop in the Air Transportation System for the 1980's and Onward. SAE Paper 801197, October 1980.

5. Williams, Louis J. and Galloway, Thomas L.: Design for Supercommuters. Aeronautics and Astronautics, February 1981, pp 20-30.

6. Douglas Aircraft Company: Study of Short-Haul Aircraft Operating Economics. September 1975.

7. Summerfield Associates: A Study of Commuter Airline Economics. NASA CR-152069, November 1977.

8. Summerfield Associates: Determination of the Flight Equipment Maintenance Costs of Commuter Airlines. NASA CR-152069, November 1977.

9. The Aerospace Corporation: A Direct Operating Cost Model for Commuter and Local Service Airlines. Report ATR-79(4811)-2ND, November 1979.

10. Civil Aeronautics Board: Small Aircraft Costing System, October 1979.

11. Civil Aeronautics Board: Costing Inputs for the 12 Months Ended June 30, 1979. October 1979.

12. Civil Aeronautics Board: Costing Inputs for the 12 Months Ended September 30, 1979. January 1980.

13. Air Transport Association of America: Standard Method of Estimating Comparative Direct Operating Costs of Turbine Powered Transport Airplanes. December 1967.

14. Walters, R.A.: Small Transport Aircraft Technology Propeller Data Package for Current Technology Commuter Aircraft Propellers. Prepared under Contract No. NAS3-22039 (STAT Study) by Hamilton Standard Division of United Technologies Corporation, December 1979.

15. Giulianetta, Demo J. and Williams, Louis J.: Toward New Small Transports for Commuter Airlines. Aeronautics and Astronautics, February 1980.

16. Szelazek, C.A. and Hicks, Raymond M.: Upper-Surface Modifications for $C_{L\ MAX}$ Improvements of Selected NASA 6-Series Airfoils. NASA TM78603, August 1979.

17. Narramore, J.C.: The Use of Small Computers in a Subsonic Airfoil Design Application. NASA Conference Publication 2046, March 1978.

18. Carmichael, B.H.: Summary of Past Experience in Natural Laminar Flow and Experimental Program for Resilient Leading Edge. NASA CR-152276, May 1979.

19. Cahill, Jones F.: Summary of Section Data on Trailing-Edge High-Lift Devices. NACA TR-938, 1949.

20. Callaghan, J.G. and Beatty, T.D.: A Theoretical Method for the Analysis and Design of Multi-Element Airfoils. Journal of Aircraft, Volume 9, No. 12, December 1972, pp 844-848.

21. Callaghan, J.G.: Aerodynamic Prediction Methods for Aircraft at Low Speeds With Mechanical High-Lift Devices. Agard Lecture Series No. 67, May 13-17, 1974.

22. Sanders, Karl L.: High Lift Devices, A Weight and Performance Trade-Off Methodology. Technical Paper No. 761, The Society of Aeronautical Weight Engineers, May 1969.

23. Gill, J.C., Earle, R.V., Staton, D.V., Stolp, P.C., Huelster, D.S. and Zolezzi, B.A.: Propulsion Study for Small Transport Aircraft Technology (STAT). Detroit Diesel Allison, NASA CR-165499, December 1980.

24. Baerst, C.F., Heldenbrand, R.W. and Rowse, J.H.: Study of Advanced Propulsion Systems for Small Transport Aircraft Technology (STAT). Garrett Turbine Engine Company, NASA CR-165610, March 1981.

25. Smith, C.E., Hirshkron, R. and Warren, R.E.: Propulsion System Study for Small Transport Aircraft Technology (STAT). General Electric Company, NASA CR-165330, May 1981.

26. Keiter, Ira D.: Impact of Advanced Propeller Technology on Aircraft Mission Characterisitics of Several General Aviation Aircraft. SAE Paper 810584, April 1981.

27. Reneau, Verlyn L.: Composite Design Allowables. Cessna Aircraft Company Report S-650-702, June 1978.

28. Smillie, D.G. and Purdy, D.M.: Advanced Material Applications to Subsonic Transport Aviation. Douglas Aircraft Company Paper 6186, August 1974.

29. Stauffer, Warren A. and James, Arthur M.: Development of Advanced Composite Structures for Lockheed Aircraft. N78-27062, reprinted in NASA CP-2036. CTOL Transport Technology-1978, Part 1, June 1978.

30. Notess, Charles B. and Gregory, Philip C.: Requirements for the Flight Control System of a Supersonic Transport. SAE 679C, April 1963.

31. Holloway, Richard B. and Brumaghim, Stanley H.: Tests and Analyses Applicable to Passenger Ride Quality of Large Transport Aircraft. Symposium on Vehicle Ride Quality, NASA TMX-2620, October 1972.

32. Andrews, D.G. et al.: Application of Advanced Technologies to Small, Short-Haul Aircraft. Boeing Commerical Airplane Co., NASA CR-152089, March 1978.

33. Gordon, C.K. and Dodson, R.O.: STOL Ride Control Feasibility Study. NASA CR-2276, July 1973.

34. Holmes, Bruce J. and Obara, Clifford J.: Observations and Implications of Natural Laminar Flow on Practical Airplane Surfaces. ICAS-82-5.1.1, presented at the 13th Congress of the International Council of the Aeronautical Sciences/AIAA Aircraft Systems and Technology Conference, Seattle, August 22-27, 1982.

END

DATE

FILMED

JAN 31 1983